

URANIUM DEPOSITS OF THE GRANTS,
NEW MEXICO, MINERAL BELT

Douglas G. Brookins

University of New Mexico
Department of Geology
Albuquerque, New Mexico 87131

December 31, 1975

USA

MASTER

DISTRIBUTION OF THIS DOCUMENT IS UNLIMITED

PREPARED FOR THE U.S. ENERGY RESEARCH AND DEVELOPMENT ADMINISTRATION,
GRAND JUNCTION OFFICE, UNDER CONTRACT NO. AT(05-1)-1636-1.

DISCLAIMER

This report was prepared as an account of work sponsored by an agency of the United States Government. Neither the United States Government nor any agency thereof, nor any of their employees, makes any warranty, express or implied, or assumes any legal liability or responsibility for the accuracy, completeness, or usefulness of any information, apparatus, product, or process disclosed, or represents that its use would not infringe privately owned rights. Reference herein to any specific commercial product, process, or service by trade name, trademark, manufacturer, or otherwise does not necessarily constitute or imply its endorsement, recommendation, or favoring by the United States Government or any agency thereof. The views and opinions of authors expressed herein do not necessarily state or reflect those of the United States Government or any agency thereof.

DISCLAIMER

Portions of this document may be illegible in electronic image products. Images are produced from the best available original document.

URANIUM DEPOSITS OF THE GRANTS, NEW MEXICO MINERAL BELT

Douglas G. Brookins

University of New Mexico

Department of Geology

Albuquerque, New Mexico 87131

December 31, 1975

PREPARED FOR THE U. S. ENERGY RESEARCH AND DEVELOPMENT ADMINISTRATION

GRAND JUNCTION OFFICE

UNDER CONTRACT NO. AT(05-1)-1636-1

DISTRIBUTION OF THIS DOCUMENT IS UNLIMITED

TABLE OF CONTENTS

Topic	Page
Geology of the Grants Mineral Belt	1
Stratigraphy	1
Morrison Formation	3
Local Stratigraphic Relations of the Morrison Formation	8
Laguna District	8
Ambrosia Lake District	9
Smith Lake District	10
Churchrock District	11
Structure	12
Pre-Dakota Structures	14
Post-Dakota Structures	15
Historical Geology and Tectonic History	16
Description of the Ore Deposits	17
Ambrosia Lake District	19
Smith Lake District	20
Laguna District	21
Churchrock District	21
Mineralogy of the Ore Deposits	22
Authigenic Minerals	22
Coffinite	22
Other Uranium Minerals	25
Vanadium Minerals	25
Molybdenum Minerals	26
Selenium Minerals	26
Organic Carbonaceous Matter (OCM)	27
Calcite and Iron Oxides	29
Other Authigenic Minerals	31
Detrital Minerals	31
Quartz and Feldspars	31
Heavy Minerals	32
Rock and Wood Fragments	33
Detrital Clay Minerals	34

TABLE OF CONTENTS (continued)

Topic	Page
Geochronologic Studies	35
Introduction	35
U-Pb Dates from the Grants Mineral Belt	36
K-Ar Ages from the Grants Mineral Belt	37
Rb-Sr Geochronology	40
Ambrosia Lake District	40
Smith Lake District	43
Jackpile-Paguate District	45
K-Feldspar Detrital Grains	49
Clay Mineralogy	50
Introduction	50
Analytical Procedures	50
Identification of Phyllosilicates	51
Kaolinite	52
Montmorillonite	52
Illite-Montmorillonite	53
Chlorite	53
Mixed-layer Chlorite	54
Identification of Polytypes	54
Distribution of Clay Minerals	56
Outcrops	56
Ore Zones	62
Remote Bleached Sandstone	65
Polytypism of Clay Minerals	65
Activity Relations	67
Scanning Electron Microscopy	72
Organo-Clay Mineral Reactions	73
Discussion	74
Preliminary Study of Drill Core Samples from Northeast of the Ambrosia Lake District	81
Trace Element Analysis	88
Uranium Content of Various Rocks from the Grants Mineral Belt and Other Selected Areas	119

TABLE OF CONTENTS (continued)

Topic	Page
Plates	125
References Cited	135
Appendices	145
A. Laboratory Procedures for Clay Mineral Analysis	145
B. Rb-Sr Data	147

Preface

The report which follows is 'final' per contractual agreement; yet it should be emphasized that the results contained herein more realistically fall in the 'progress' category. Many of our initial objectives have been realized from research conducted to date and, of those not yet realized (i.e., trace element analysis in particular), we anticipate completion in the near future.

Of the various projects undertaken in this research, those involving sampling in the Grants Mineral Belt and/or analytical and other work undertaken solely at the University of New Mexico are complete; although we have, under separate cover, proposed more related research to complement the clay mineral-logic, Rb-Sr geochronologic and trace element studies.

Those projects which involve use of the facilities at the Los Alamos Scientific Laboratory (i.e., trace element analyses by neutron activation analysis on whole rocks and clay mineral separates plus delayed neutron activation analysis for uranium determination in the same and related materials) are in progress. The samples were prepared on schedule but the results are being obtained at a slower pace than anticipated. This is understandable as this work is being done gratis at LASL as part of joint UNM-LASL research and the reactor backlog is considerable. We are optimistic, as outlined in the report, that the NAA and DNAA data, in conjunction with other work, will justify subsequent work.

The personnel involved in this study who have received U. S. E. R. D. A. funding include: Dr. B. Mukhopadhyay, Research Associate (9/74 - 6/75); Mr. M. J. Lee, Research Assistant (9/74 - 12/75); Mr. R. S. Della Valle, Research Assistant (6/75 - 12/75); Ms. C. Perea, Student Helper (part-time, 1974-75) in addition to Dr. D. G. Brookins, Project Supervisor. Finally, Mr. S. L. Bolivar has worked on the project for one month (12/75) and two other graduate students, Messrs. S. R. Hafefeld and W. E. Riese, Jr. have collaborated with us on some phases of the research.

The publications acknowledging U. S. E. R. D. A. support are appended to the report; I wish only to mention here that much of the research report has been excerpted from the Ph. D. Dissertation in progress by M. J. Lee following earlier writings by D. G. Brookins and with input from B. Mukhopadhyay and R. S. Della Valle.

D. G. Brookins
December 31, 1975

Acknowledgments

While the bulk of the financial support for this study has come from U. S. E. R. D. A. (Contract AT(05-1)-1636-1) I wish also to acknowledge partial financial support from the University of New Mexico. In addition, this study would have been impossible without the cooperation of Industry. Special thanks are due The Anaconda Company, United Nuclear, Inc., United Nuclear-Homestake Partners, Kerr-McGee Nuclear Corporation, CONOCO, and Gulf Minerals, Inc. Personnel from these companies allowed visitation of their properties for sampling, advised us on various phases of the research and cooperated in many other ways. Numerous individuals from the U. S. E. R. D. A.- Grand Junction and Albuquerque Offices, and the U. S. Geological Survey discussed many facets of the study with us; special thanks are due S. R. Austin, William Chenoweth, Ben Bowyer, Eugene Grutt, Jr., Donald Curry, Roger Malan, Hans Adler, Luther Smith, Wayne Roberts, Harry Granger, C. Gerry Warren, Ken Ludwig and others.

Special acknowledgment is due to many personnel of the Los Alamos Scientific Laboratory for their willingness to conduct experiments for our project and to provide invaluable discussions. I wish to specifically mention J. P. Balagna and S. Helmick, CNC-11 Division, for DNAA and NAA studies (in progress); G. R. Keepin, A. Evans, R. Walton, H. Menlove, A-Division, for preliminary work on use of Van De Graaff and 252-Cf Shuffler for uranium analyses; R. R. Sharp and C. E. Olsen, J-5 Division; for valuable discussions.

GEOLOGY OF THE GRANTS MINERAL BELT

The Grants Mineral Belt (GMB) forms a southeasterly trending linear belt of uranium deposits at the southern margin of the San Juan Basin. According to the tectonic subdivisions of Kelley (1955) the belt lies between the northern limit of the Zuni Uplift and the Chaco Slope and is bounded by the Rio Grande Trough on the east and the Gallup Sag on the west (Fig. 1 and 3).

Within the Belt four major uranium districts are recognized. They are, from east to west, the Laguna, Ambrosia Lake (including San Mateo area), Smith Lake and the Churchrock districts. Sporadic deposits have also been found farther north in the Shiprock and Chuska districts. Present exploration and mining activities are mostly confined to the deposits in the Westwater Canyon Member and the Jackpile Sandstone of the Morrison Formation and subsequent discussion will be concentrated on the regional stratigraphic variations of these units.

Stratigraphy

Some six thousand feet of sedimentary rocks are present in the general area of the GMB and range in age from Pennsylvanian to Cretaceous; these are overlain on the crystalline Precambrian rocks of the Zuni Uplift. The sedimentary rocks generally dip north to northeastward into the San Juan Basin except in the Laguna district where northwestward dips are common. Of the sedimentary rocks continental varieties are most common in the Cretaceous rocks. Late Cretaceous and Tertiary sediments of both marine and continental origin are exposed in the interior of the San Juan Basin to the northeast of the GMB.

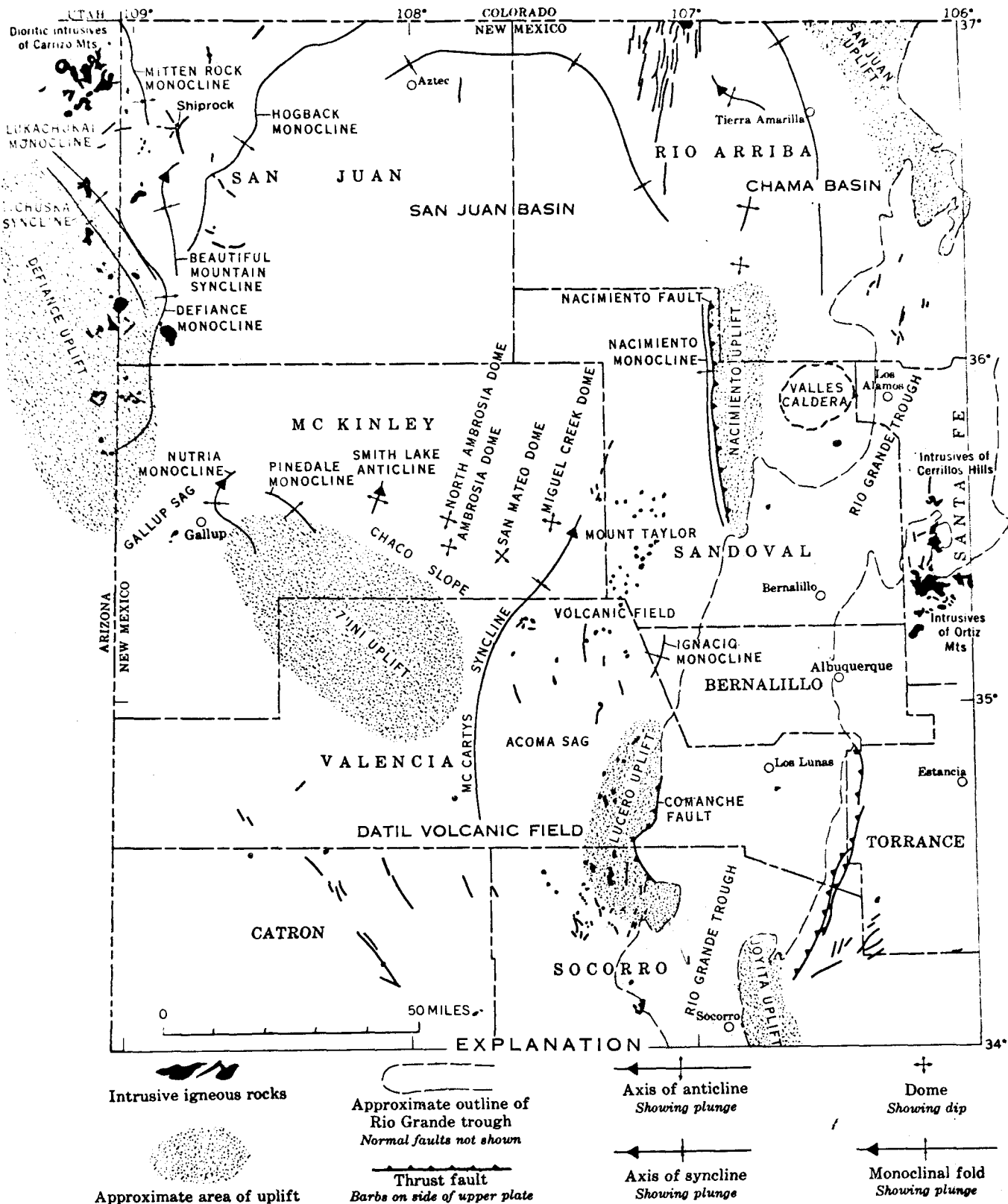


FIGURE 1. "Principal Structural Elements in Northwestern New Mexico and Adjoining Areas" (from Hilpert, 1969)

The outcropping Precambrian rocks in the Zuni Uplift are composed mostly of leucocratic granite, aplite, granite gneiss, metarhyolite and schists. The absolute isotopic ages of these rocks have not been reported. These rocks will be analyzed for Rb-Sr ages and reported at a later time.

The area between the Laguna and the Ambrosia Lake districts is extensively covered with the volcanic rocks of the Mt. Taylor volcanic field. These rocks range in age from Miocene to Recent with a wide range in composition. Potassium-argon age determinations on obsidian, perlite and sanidine from the Mt. Taylor rocks yield ages ranging from 1.5 to 3.0 m.y. (Bassett and others, 1963a; b).

Morrison Formation. The Morrison Formation was first defined by Emmons and others (1896) for the beds of variegated shale and sandstone near Morrison, Colorado in the Front Range. These beds were later correlated with similar strata in New Mexico and southwestern Colorado by Lee (1902; 1917), but have been shown to include Lower Cretaceous beds. This resulted in much controversy on the question whether the Morrison is Jurassic or Cretaceous in age. Later work by Baker and others (1936), and by Renick (1931), have resulted in the Morrison being assigned to the Upper Jurassic although the age of its upper limits is questionable (Imlay, 1952).

Literatures pertaining to the stratigraphic and petrologic descriptions on the Morrison Formation of the Colorado Plateau are numerous; detailed information relevant to the Morrison in the Grants Mineral Belt can be found in Craig and others (1955; 1959), Freeman and Hilpert (1956), Hilpert (1963), Moench and Schlee (1967), Cadigan (1967) and Santos (1970).

In the Grants Mineral Belt and vicinity the Morrison can be divided into four members. These are, in ascending order; the Salt Wash, Recapture, Westwater Canyon, Brushy Basin members from lower to upper Morrison. In

addition, two sandstone bodies located in the upper part of the Brushy Basin member, of economic usage, are recognized; the Poison Canyon sandstone of the Ambrosia Lake district and the Jackpile sandstone of the Laguna district.

In the Four Corners region, the Salt Wash Member extensively intertongues with the Recapture Member and contains many groups of uranium deposits in the Shiprock district (Hilpert, 1969). Unlike the other deposits in the Morrison Formation of the Grants Mineral Belt, they are high in vanadium content, with an average U:V ratio of 1:7. The Salt Wash Member in this region ranges in thickness from a featheredge to about 220 feet near the Carrizo Mountains (Strobell, 1956). To the south in northeastern Arizona and northwestern New Mexico, the Salt Wash Member pinches out by grading into and intertonguing with the Recapture Member. In some localities the Salt Wash Member grades into the Cow Springs Sandstone (See Fig. 2). To the north over a large part of eastern Utah and western Colorado, the Salt Wash Member replaces the Recapture Member and constitutes the lower half of the Morrison Formation. In northwestern New Mexico the Salt Wash Member is generally a reddish-brown to gray, medium-grained sandstone interbedded with some mudstone. Orientations of the cross stratifications in the sandstone indicate a general eastward trend (Craig and others, 1955), suggesting that the major source area was southeastern California and western Arizona.

The Recapture Member conformably overlies the Bluff Sandstone in the Grants Mineral Belt; to the southwest it intertongues with and grades into the Cow Springs Sandstone. Throughout northwestern New Mexico and northeastern Arizona it is about 200-300 feet thick, attaining a maximum thickness of more than 600 feet. The Recapture Member generally consists of interstratified pale-red to dusky red, silty to sandy mudstone and light-brown,

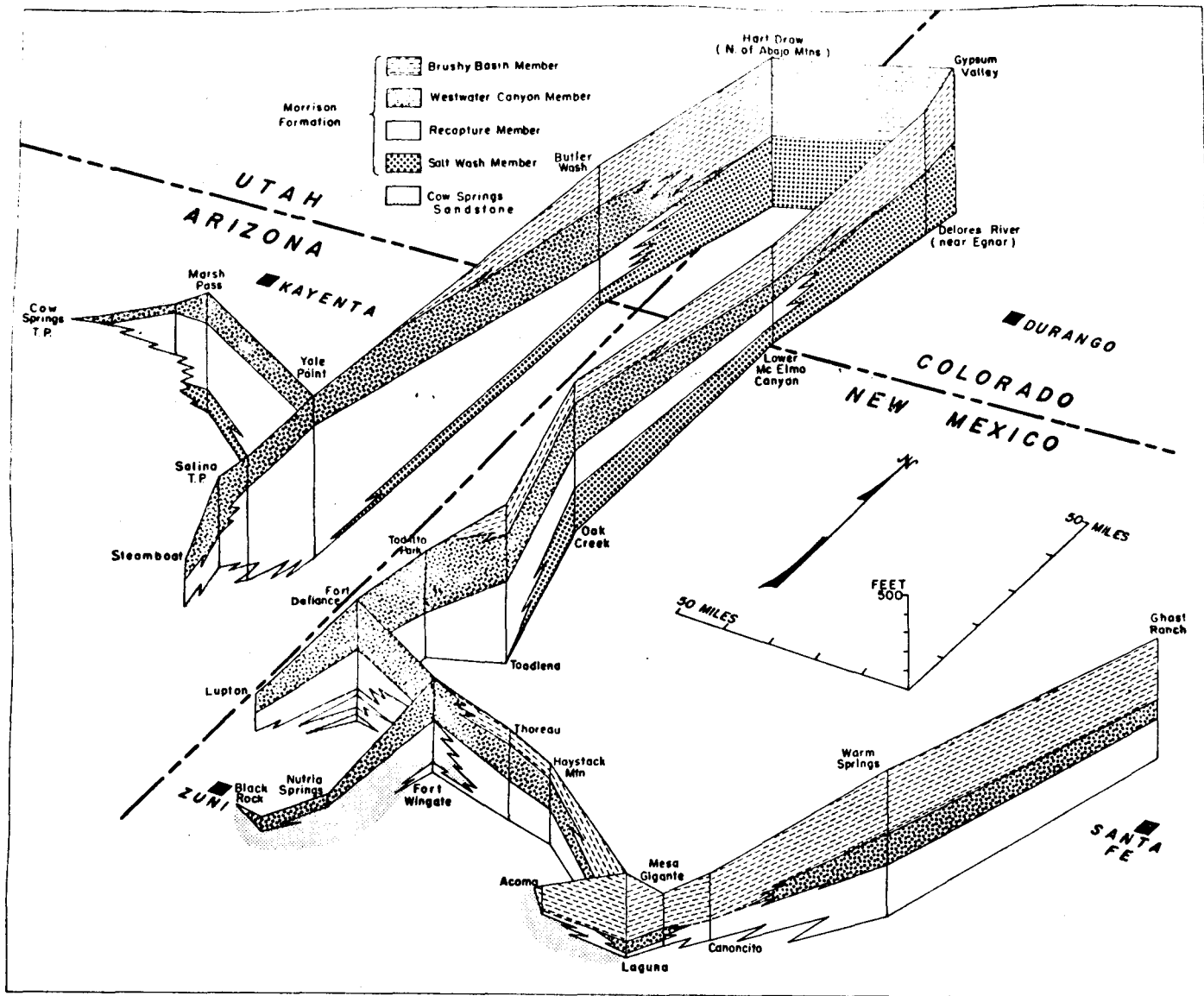


FIGURE 2. Fence diagram of Morrison Formation in parts of Arizona, New Mexico and adjacent areas. Datum is top of fence. Sections at Black Rock and Nutria Springs from Harshbarger, Repenning and Irwin (1957, pl. 3); sections at Acoma and Canoncito from Freeman and Hilpert (1956, p. 322, 328). Remainder measured by Craig and others (1959). (from O'Sullivan and Craig, 1973)

fine-to-medium-grained sandstone. No significant uranium deposits have been found in the Recapture Member in the Grants Mineral Belt. Limited studies of the cross-bedding from a few localities along the south and west margins of the San Juan Basin indicate a southwestern source for the Recapture Member sediments (Hilpert, 1969). The Recapture and Salt Wash Members have been interpreted as an alluvial fan deposit consisting of two partially coalescing alluvial facies (Craig and others, 1955).

The Westwater Canyon Member generally overlies the Recapture Member and has about the same distribution pattern in New Mexico. In some places the contact forms a scour surface, or is gradational or intertonguing. The Westwater Canyon Member attains a maximum thickness of more than 300 feet near the New Mexico-Arizona state line, from where it grades northward into the Brushy Basin Member in southwestern Colorado. Eastward into the San Juan Basin it thins somewhat and ranges from 100 to 250 feet thick on the eastern margin of the Basin. To the south the member thins rapidly to a featheredge that passes near Cow Springs Trading Post, Arizona and along the southern margin of the San Juan Basin. This is interpreted as combined depositional thinning and pre-Dakota erosion.

The Westwater Canyon Member in New Mexico is mostly a gray or reddish-brown, medium-to-coarse grained, arkosic sandstone interbedded with mudstones. Locally it contains stringers and layers of pebbles of quartz, feldspar, granite, quartzite and darker gray and black chert. The conglomerate sandstone facies occupy a wide lobate area near Gallup. Craig and others (1955) interpreted a broad fan-shaped alluvial plain or fan, formed by a complex system of braided channels as the depositional environment. Deposition of the Westwater Canyon Member may represent a continuous process from Recapture Member deposition with a rejuvenation of the source area as seen

by the coarser material in the Westwater Member plus a greater abundance of fossil plants, logs, and dinosaur bones. Green (1975), however, has argued for an unconformity between the Westwater Canyon and Recapture Members.

Studies on cross-stratification dips, heavy mineral and pebble-size distributions (Craig and others, 1955; Cadigan, 1967; Dodge, 1973; Flesch, 1974) in the Westwater Canyon Member generally indicate a source area to the south and southwest, probably from the ancient Mogollon highland. In the Grants Mineral Belt and eastern San Juan Basin dip azimuth measurements generally show an easterly or southeasterly trend, compared to a northward trend south of Gallup.

The Brushy Basin Member conformably overlies the Westwater Canyon Member and is unconformably overlain by the Dakota Sandstone of Cretaceous age. The contact of the Brushy Basin Member with the Westwater Canyon Member is gradational and intertonguing so that the selection of the contact in many places is arbitrary. In New Mexico, the Brushy Basin Member has about the same distribution patterns as the Recapture and Westwater Canyon Members. It generally thickens to the northeast to the Four Corners Region and westward from eastern San Juan Basin, ranging in thickness from 250 to 300 feet. Near Todilto Park and east of Gallup the member becomes a northwest-trending feather edge that is largely the result of post-Morrison and pre-Dakota erosion. The Brushy Basin Member in New Mexico consists primarily of greenish, variegated silty and sandy mudstone. The mudstone contains an abundance of montmorillonite and is interbedded with sandstone lenses which are similar to the sandstones of the Westwater Canyon Member. The source area and depositional environment of the Brushy Basin Member are believed to be essentially the same as those of the Westwater Canyon Member. Much of the mudstones of the Brushy Basin accumulated from volcanic ash falls.

Local Stratigraphic Relations of the Morrison Formation

Laguna District. The most important uranium host rock in the Laguna district is the Jackpile Sandstone of local usage (Hilpert and Freeman, 1956), which lies unconformably beneath the Dakota Sandstone, forming a northeastward belt across the district. The Jackpile Sandstone and its uranium deposits have been studied in great detail and the results can be found in Schlee and Moench (1961) and Moench and Schlee (1967). The sandstone body is as much as 13 miles wide, more than 30 miles long, and locally 200 feet thick. It tapers to its margins, broadens and splits into two trough-shaped fingers about 20 miles northeast of Laguna. The Jackpile Sandstone is recognized as far north as Cuba, New Mexico (Santos, 1975) although some question remains on whether this represents the Cretaceous Burro Canyon Sandstone instead (Saucier, 1974). The Jackpile Sandstone presumably represent deposition in a northeast-trending pre-Dakota structural depression developed in the upper Morrison Formation (Schlee and Moench, 1961).

The Jackpile Sandstone is generally a yellowish-gray to white, friable, fine-to-coarse-grained fluvial sandstone with minor conglomerate, clay pebbles and galls. Commonly it grades from coarser grained subarkosic material at the base to finer material at the top. Near the unconformity with the Dakota Sandstone the interstices of the sandstone are filled with white kaolinite which is a most conspicuous feature of the Jackpile Sandstone in many outcrops.

In the Laguna district, the Morrison Formation is composed mostly of the relatively thick Brushy Basin Member (avg. 300 feet) and the markedly thinner Westwater Canyon (avg. 50 feet) and Recapture Members. Locally, in the southwestern part of the district, the Recapture Member is absent where the

overlying Westwater Canyon Member has filled channel scours formed in the underlying Bluff Sandstone. The Morrison Formation attains its maximum thickness of about 600 feet in the central part of the district and then thins laterally; to the west it is deeply buried in the McCartys syncline. Southward it is leveled under the pre-Dakota erosion surface.

Ambrosia Lake District. Throughout most of the Ambrosia Lake district the Morrison Formation is about 500 feet thick but it tends to thicken northward attaining a maximum known thickness of about 800 feet in the western part (Hilpert, 1969).

The basal Recapture Member has an average thickness of about 150 feet and is composed of alternating beds of red and gray siltstone, mudstone, and sandstone, which range in thickness from a foot to about 20 feet. The contact with the underlying Bluff Sandstone is generally sharp and conformable.

The Westwater Canyon Member, the major uranium host rock in the Grants Mineral Belt, ranges in thickness from about 125 to 270 feet in the main part of the Ambrosia Lake District and thins to as little as 50 feet at the outcrop. The lower contact with the Recapture Member is generally conformable, but in places it forms scour surfaces, is gradational, or the two members intertongue. The Recapture Member in the district is principally a light-yellow-brown to gray, fine-to-coarse-grained, poorly-sorted, cross-bedded subarkosic sandstone interstratified with green or yellow mudstone. Throughout the district the sandstone:mudstone ratios range from about 2:1 to 10:1 and the ratio decreases toward the top of the Member. The mudstone layers range in thickness from less than 1 foot to 40 feet and are laterally discontinuous. In the major part of the district, numerous overlapping stream channels were developed as can be seen from an isopach and lithofacies map (Santos, 1970). The uranium deposits are generally enclosed in or parallel to the southeast-

trending channels.

At the top of the Westwater Canyon Member, separated by a 15 foot to 25 foot thick mudstone unit, is the Poison Canyon Sandstone of economic usage (Hilpert and Freeman, 1956). The unit is well exposed along the outcrop near the Poison Canyon Mine, where it is about 50 feet thick, and extends several miles north and eastward until it pinches out into the Brushy Basin Member. The thickness of the sandstone ranges from 30 to 80 feet. In the main part of the district the Poison Canyon Sandstone cannot be defined precisely in the subsurface. The Poison Canyon Sandstone is texturally and lithologically similar to the sandstone in the Westwater Canyon Member. In the outcrop west of Highway 53 the Poison Canyon shows limonitic-yellow colors against hematitic-red colors of the Westwater Canyon Member.

The Brushy Basin Member in the district is mostly greenish-gray sandstone interbedded with thin sandstone layers which are similar in color and lithology to the Westwater Canyon Sandstones. The contact with the Westwater Canyon Member is gradational. With the overlying Dakota Sandstone, the top of the Member forms an unconformable erosion surface of small local relief, generally less than a few feet. The Brushy Basin Member is 60 to 200 feet thick in the district.

Smith Lake District. Relatively little is known about the subsurface Morrison Formation in this district. The following information is obtained from MacRae (1963) and Hoskins (1963), plus some electric logs from exploratory drill holes in the district.

The Brushy Basin Member ranges from 80 to 160 feet in thickness and is fairly consistent in thickness and lithology in most parts of the district. In the central part of the district the Brushy Basin is divided into two layers by a sandstone lense ranging in thickness from about 20 to 60 feet.

This sandstone tongue has been referred to as Poison Canyon Sandstone but correlation with the Poison Canyon Sandstone of the Ambrosia Lake District is very difficult. It may be more properly included with the underlying Westwater Canyon Member.

The Westwater Canyon Sandstone in this area is about 200 feet thick. It abruptly thickens to the north and becomes as thick as 280 feet about 10 miles north of the district. The Member can be roughly divided into two parts by a laterally continuous reddish brown mudstone layer which varies from 15 to 35 feet in thickness. Furthermore, the mudstone layer thickens and tends to rise higher in stratigraphic position within the Westwater Canyon Member. Similar lithologies and textural features compare to those noted at Ambrosia Lake except the color of the member in the mining area is limonitic-brown to hematitic-red.

Churchrock District. In this district the Morrison Formation crops out to the west and north flanks of the Zuni Uplift from where it thickens in all directions except to the south. The Morrison Formation in this region represents conglomeratic facies (Craig and others, 1955) and all members, except the Salt Wash Member, are present.

In the western and southern part of the district the Recapture Member grades and intertongues with the light-gray Cow Springs Sandstone and recognition of this member is difficult. It varies in thickness from 150 to 300 feet and thickens markedly to the west from the district.

The Westwater Canyon Member in the district is rather uniform in thickness and lithologic character. It ranges in thickness from 170 to 350 feet. At the outcrop near Kit Carson's Cave and westward, intense kaolinization occurred and the sandstones show typical white color. Here the Westwater Canyon Member is directly under the Morrison-Dakota unconformity, a feature

similar to the Jackpile Sandstone of the Laguna District. Compared to other districts, the Westwater Canyon in the main part of the district lacks mudstone layers and, if present, have only limited lateral continuity.

The Brushy Basin Member varies in thickness from a featheredge to about 120 feet; this is caused by extensive pre-Dakota erosion to the south and southwest plus intertonguing with the underlying Westwater Canyon Member. Lenticular sandstone bodies are usually present in the middle part of the Brushy Basin.

Structure

The Grants Mineral Belt is on the northern flank of the Zuni Uplift on a monocline referred to as the Chaco Slope, whereas the Laguna district is on the east limb of the McCarty's syncline which dips northwestward into the San Juan Basin. The stratified rocks in most of the belt dip gently to the north to northeastward on to westward as in the Laguna district. These rocks have been deformed by a few periods of deformation from Morrison time to the present which have formed faults, gentle folds, domal and collapse structures and uplifts. The first deformation is thought to have occurred in the Late Jurassic followed by the major deformation of the region during the Laramide (Late Cretaceous - Early Tertiary) Orogeny which involved the development of Zuni Uplifts, further subsidence and northward tilting of the San Juan Basin. The third period of deformation of the region, which probably happened during Late Tertiary to Quaternary, developed the Rio Grande Trough and involved the volcanic eruptions in the Mt. Taylor area. For convenience, these features are divided into pre-Dakota and post-Dakota structures. Some of these features are shown in Fig. 3.

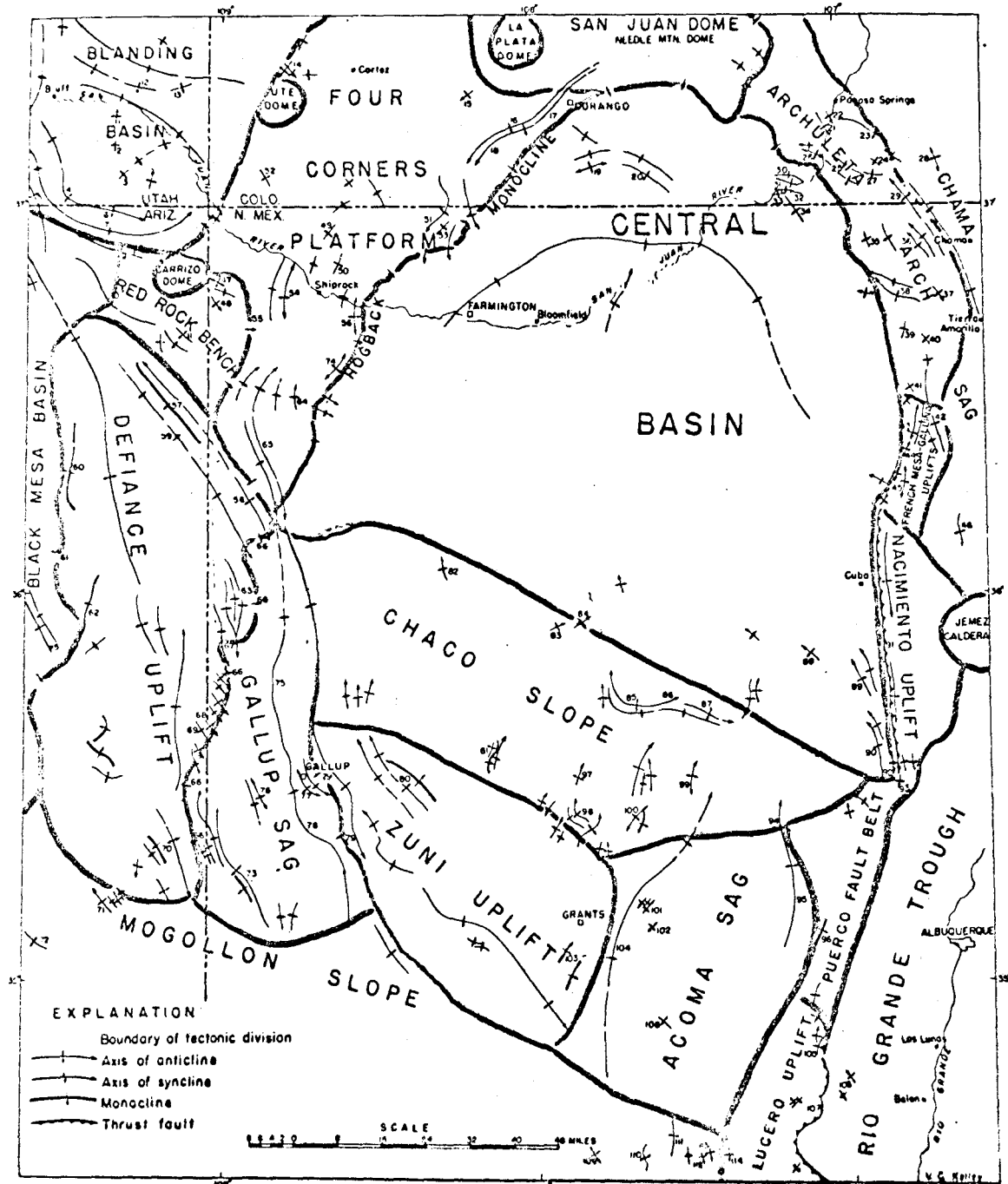


FIGURE 3. "Tectonic Map of San Juan Basin and Adjacent Areas" (from Kelley, 1963)

Pre-Dakota Structures

The depositional thinning and truncation of the Morrison Formation and older Jurassic rocks to the south indicate an uplift during and after Morrison deposition. The uplift probably existed in the Mogollon Highland (Harshbargar and others, 1957) and its affect on sedimentation can be seen southward in the Entrada Sandstone, the pinching of the Todilto Limestone and the thinning of the Summerville Formation.

Related to the uplift, two sets of low amplitude folds were developed in the Laguna District (Hilpert and Moench, 1960; Moench, 1963; Moench and Schlee, 1967) during or shortly after Morrison time; one trending east to northeast in the central and southern part, and the other trending north to northeast in the southeastern portion of the district. These folds have amplitudes ranging from near 100 to several hundred feet and lateral dimensions ranging from a few thousand feet to possibly several miles in width. The northeast trending fold in the central part of the district in particular appears to have provided stream channels in which the fluvial Jackpile Sandstone was deposited. Contemporaneous with the folding, Moench and Schlee (1967) describe numerous pipe-like collapse structures formed in the Summerville, Bluff and Morrison Formations. They suggest that the pipes were formed by injection of sand into spring vents created during folding.

The pre-Dakota folding is believed to be less conspicuous in the other parts of the Grants Mineral Belt, although Hilpert and Corey (1957) and Hilpert and Moench (1960) described a set of rather shallow, eastward trending folds in the Ambrosia Lake District which may have an amplitude of 100 feet or more and lateral dimensions varying from a mile to several miles. They suggested that the deposition of the eastward-trending Westwater

channels may have been controlled by these folds. Santos (1970), however, rejected this idea based on his isopachous maps and cross-sections of the Jurassic rocks in this area. Hazlett and Kreek (1963) reported a possible northward-trending pre-Dakota fold in the central part of the district. Collapse structures, similar to those in the Laguna District, are also found in the Morrison Formation of the Ambrosia Lake District (Granger and Santos, 1963; Clark and Havenstrite, 1963). These structures appear to be pre-Dakota in age as seen by their stratigraphic relations but it is not clearly shown whether they were formed by fold or fault controlled process.

Post-Dakota Structures

The major deformation of the region appears to have occurred during Laramide time. Initial development of the Zuni Uplifts and the deepening of the San Juan Basin probably accompanied horizontally directed compressive forces and these formed numerous strike-slip and normal faults, anticlinal folds and monoclines. These structures were later modified during the deformation which extended from middle to later Tertiary and possibly extended into Quaternary time. This involved the regional uplift of the Colorado Plateau, the formation of the Rio Grande Trough and the volcanic eruption of the Mt. Taylor volcanic pile. However, lack of sedimentary strata younger than late Cretaceous in the Grants Mineral Belt makes it difficult to assign relative ages for the post-Dakota structures. Pronounced structural features formed during this time include the McCarty's syncline, the Ambrosia and San Mateo Domes, the San Rafael, Big San Mateo and the Ambrosia Fault Zones in the Ambrosia Lake District; the Madera anticline and the San Ignacio faulted monocline in the eastern part of the Laguna District; the Mariano anticline of the Smith Lake District; the Pinedale and Nutria monoclines near the Churchrock District.

Domal structures are mostly asymmetrical with closures of a few hundred feet. Most faults trend northeast and are steeply dipping with displacements of a few tens of feet to several hundred feet. A few faults, such as San Rafael faults, show horizontal movements of up to 20,000 feet (Thaden and others, 1967).

Historical Geology and Tectonic History

After erosion of the Precambrian rocks, the area under study was probably a stable shelf for most of the Paleozoic era (Kelley, 1955) bounded by the Uncompahgre Uplift to the north and the ancient Zuni and Defiance Uplifts to the south and west which formed a broad upwarp. Throughout much of the Mesozoic Era, however, the Mogollon Highland in central Arizona and west-central New Mexico was a predominant, east-trending positive area contributing sediments to the north (Stewart and others, 1972; Repenning and others, 1969; Cooley and Davidson, 1963; Harshbarger and others, 1957). In late Jurassic time the Highland was probably rejuvenated and a broad shallow basin and flood plain was formed to the north while the Jurassic sediments were being deposited. The differential movement of the basin and highland caused broad folding along the southern margin of the Jurassic basin (Hilpert and Moench, 1960). These folds appear to have played partial control in determining the course of the early Morrison streams as seen by the east-trending channel sandstones of the lower Westwater Canyon Member. The folds along with the change in drainage patterns to the northeast during late Morrison time may also account for formation of local sandstone bodies such as the Jackpile and the Poison Canyon Sandstones. Some volcanic activity appears to have occurred in the Highland and the ashes were incorporated in the Morrison sediments. The Zuni Mountains during this time seemed

to have been a low lying area (Smith, 1959), although some uplifting with local folding may have occurred during late Jurassic time as evidenced by thinning and by truncation of the Morrison beds along some of the folds near the uplift (Kelley and Clinton, 1958).

The presence of a local, positive area is quite possible if one considers the shift in paleocurrent patterns within the Morrison; streams depositing the Westwater Canyon Member flowed north to northeast near Gallup. However, in the Ambrosia Lake District and adjacent area, the cross-bedding shows a general easterly trend (Rapaport and others, 1952; Dodge, 1973; Flesch, 1974).

In late Jurassic or early Cretaceous time the southern highland area and basin margin were tilted upward and leveled (Hilpert, 1969), followed by gradual subsidence of the basin and transgression of sea way from the north and northeast (Young, 1960). Cretaceous deposition occurred during several transgressions and regressions until Laramide time during which the Zuni, Defiance and Nacimiento Uplifts emerged and the San Juan Basin shaped.

The Epeirogenic Uplift of the Colorado Plateau as a whole took place in late Tertiary time and by the middle-Pliocene the present topography of the San Juan Basin was essentially developed (Hunt, 1956). Tension developed during this time probably produced numerous normal-faults and joints in the Grants Mineral Belt (Santos, 1970). During the uplift volcanic activity continued and the newly-formed Rio Grande Trough received several thousand feet of sediments from adjacent uplifts and volcanic centers.

Description of the Ore Deposits

Most of the uranium deposits in the Morrison Formation of the Grants Mineral Belt occur in the sandstone of the Westwater Canyon Member, the Poison Canyon Sandstone and the Jackpile Sandstone as pore fillings or

coatings of a mixture of organic material, various uranium minerals, iron oxides and sulfides. The color of the ore body ranges from gray to vitreous black and the higher grade deposits are generally darker. Any individual ore body is typically layered, parallel or subparallel to the bedding, with a thickness ranging from a few inches to a few feet. Its lateral extension may go to several hundred feet wide and a few thousand feet long.

Two types of ore deposits have been recognized in the region; most distinctive and of greatest economic importance are the primary (also called trend or pre-fault) deposits which show no apparent genetic relation to but are replaced by the Laramide, faults, and the redistributed (also called stack or post-fault) ore bodies which have been controlled by and concentrated near the fracture systems. They differ mainly in shape, age, and structural relations (and in some trace element contents). The two are closely associated and redistributed ore is rarely found more than a several hundred feet apart from the primary ore.

The primary ore bodies are tabular elongate or lensoid masses with their long dimensions generally parallel to the depositional trends or belts a few miles to several miles long with widths ranging from a few hundred feet to more than a thousand feet. Individual primary ore bodies range in thickness from a few inches to about 15 feet and are composed of flat-lying elongated pods or rolls which occur singly, side by side, or stacked, having a variety of shapes. All the primary ore is intimately mixed with organic carbonaceous residue that impregnates the sandstones.

The redistributed ore bodies are closely associated with the primary deposits. Compared to the latter they are thicker, ranging from several tens of feet to locally as much as 100 feet, with reduced lateral extent. Their distribution and shape are mostly controlled by fractures or some stratigraphic features such as thick mudstone beds.

Roll-type ore bodies are more common in the redistributed deposit bounded by oxidized and unaltered sandstones on opposite sides. The redistributed ore is generally lower grade, contains less organic carbonaceous matter and more vanadium than the unaltered primary ore.

Ambrosia Lake District

Deposits in sandstone in the Morrison Formation in the Ambrosia Lake district occur mainly in the Westwater Canyon Member and the Poison Canyon Sandstone. The primary ore deposits known in this district occur in four easterly or southeasterly trending belts which are roughly parallel to the paleochannel directions; the first three are referred to as the Ambrosia Lake trend and the last as the Poison Canyon trend.

Although ore deposits occur at all stratigraphic levels of the Westwater, the deposits show a general tendency to rise stratigraphically northward in the Ambrosia Lake trend (Santos, 1963; Hazlett and Kreek, 1963). In the southern ore trend they occur throughout the host sandstone whereas in the middle and in the northern margin they are mostly in the upper part. Furthermore, although somewhat arbitrarily defined, the deposits in the Ambrosia Lake trend occur in an area where the Westwater Canyon Member is 200 feet or more in thickness (Santos, 1963; 1970). The northward rise of the ore deposits may indicate renewed uplift of the source area to the south at the time of either channel deposition or ore formation.

Deposits in the Poison Canyon trend, on the other hand, do not appear to be related to the thickness of the host sandstone; as the ore trend itself transects the thickest part of the channel in many places (Rapaport, 1963).

Both oxidized and unoxidized redistributed ore deposits are abundant; particularly in the western portion of the district. These deposits lack

typical southeasterly elongation characteristic of primary ore bodies. Some of the redistributed ore bodies in the district occur at a margin of oxidized and unaltered sandstones, resembling the primary roll-type deposits of Wyoming (Harshman, 1972; Rubin, 1970).

The ore deposits in the district contain lower vanadium when compared with other districts; primary ore generally has a U:V ratio ranging from 2:1 to 10:1 depending on ore grade. Redistributed ore is richer in vanadium and typically the U:V ratio is 1:1 or less.

Smith Lake District

At least two ore trends occur in the Smith Lake district; the southern trend near the Smith Lake and the other several miles north. All known deposits occur in the Westwater Canyon Member.

The deposits near the Smith Lake area were described by MacRae (1963), Hoskins (1963) and Fitch (1961). The uranium ore bodies in the area occur near the Mariano Lake Anticline which plunges southeasterly and the ore is limited to the middle and upper part of the Westwater Canyon Member. The primary ore bodies show either easterly or northeasterly trends whereas the redistributed deposits are formed in areas of fracture zones along normal dip-slip and strike-slip faults. In this area the ore bodies are surrounded by both a lateral and vertical color halo that changes from a hematitic-red to limonitic-yellow. The ore, on the other hand, is generally confined to the bleached, gray sandstone suggesting that the deposits represent remnant pods that have been redistributed.

Furthermore, another southeasterly ore trend is currently being explored. No details are available on this trend except that both primary and redistributed ore are present and that ore bodies tend to rise to stratigraphically higher positions northward.

Laguna District

Most of the deposits in the district are in the northeasterly trending Jackpile Sandstone and are generally concentrated within the thicker part of the channel where it ranges from 100 to 200 feet thick. In addition several pipe-like structures in the Morrison Formation have yielded considerable amounts of ore.

Among others, the Jackpile and adjacent Paguate Mines have been the most productive. Generally the uranium mineralization in the Jackpile Mine occurs throughout the section with some tendency of concentration in the lower half. In the Paguate deposit, however, the ore bodies are confined to the upper one third of the host rock and some of them appear to have been truncated by the pre-Dakota unconformity (Kittel, 1963; Nash, 1968).

Compared to other districts, the ore body in this district is somewhat thicker, ranging from 20 to 50 feet in thickness. No redistributed ores similar to those found in the Ambrosia Lake district have been recognized in the Laguna district, although small scale redistribution can be found along joint faces and in the borders of diabasic intrusives.

The U:V ratio of the primary ore in the district appears to be somewhat lower than other parts of the Grants Mineral Belt ranging from 3:1 to 1:2.

Churchrock District

In the Churchrock district the uranium deposits have been found throughout the Westwater Canyon and Brushy Basin Members plus a few deposits in the lower part of the Dakota Sandstone. The mineralization in the Dakota and Brushy Basin, found in the old Churchrock mine near the Pipeline Fault zone, appears to be unusual in that it occurs in Dakota channel scour formed within the underlying Brushy Basin. Some geologists refer to this as redistributed Westwater deposit (Hilpert, 1969), while others as primary

mineralization based on the presence of fossil logs and other carbonaceous material.

Deposits in the Westwater Canyon are widely scattered throughout the member and it appears that much of the mineralization in this district has been controlled by fracture zones developed along the northeast trending Pipeline Fault. Redistributed ore bodies up to 20 feet or more have been commonly found. These primary deposits, although mostly discontinuous, show a south-easterly trend normal to the Pipeline Fault in the southern part of T17N, R16W. The northwestern limit of this trend is not known.

Mineralogy of the Ore Deposits

For convenience, the minerals identified in the ore deposits of the Morrison Formation will be divided into two categories; the authigenic mineral occurring within or close to the ore bodies and the detrital minerals. Substances other than minerals, such as fossil logs and organic carbonaceous material which are closely associated with the deposits, are also discussed. Phyllosilicates found in the ore and barren grounds will be discussed in a separate section of this report.

Authigenic Minerals

Coffinite, $(U(SiO_4)_{1-X}(OH)_{4X})$. X-ray diffraction of approximately one hundred ore grade samples indicate that coffinite is the major uranium-bearing phase in the Grants Mineral Belt. Diagnostic x-ray peaks (Cu $K\alpha$) for coffinite are 4.66° \AA (011), 3.47° \AA (200), and 2.64° \AA (112). The mineral is extremely fine-grained and cannot be recognized in thin section. From the line broadening in the x-ray diffractograms, Stieff and others (1956) estimate the crystal size of coffinites to be 10^{-5} to 10^{-6} cm.

The coffinite is always closely associated with organic carbonaceous material in the deposits and is especially abundant in the black, vitreous, primary ore bodies. Granger (1963a) reported that the coffinite found in the redistributed ore can be resolved optically and can be separated. Unlike in primary ore where it fills the interstices, coffinite in redistributed ore forms aggregates that coat sand grains with a thin film.

Coffinite has been synthesized in the laboratory (Hoekstra and Fuchs, 1956; Fuchs and Hoekstra, 1959) in the pH range 7.5 to 10.7; below pH 7.5 only uraninite was produced in their experiments. The synthetic coffinite approached stoichiometric U_4SiO_4 without any hydroxyl component, but possessed physical properties similar to natural coffinite.

Recently, the stability field of coffinite in Eh-pH has been estimated by Brookins (1975) using free energy data obtained by an indirect method. The silicates of U, Th, and Zr have identical crystal structures, and the oxides for Th, U and Zr are somewhat similar (i.e., UO_2 and ThO_2 isometric; but ZrO_2 is monoclinic) and because U-Th exhibit near ideal diadochic relations, the differences in ΔG_f° values of oxide-silicate pairs of Zr, Th and U compounds may be used to obtain a ΔG_f° value for coffinite. The relation is shown in Table 1.

The differences for the Zr and Th pairs are 210.0 ± 7.2 kcal and 210.1 ± 1.1 kcal, respectively. By adding the average difference of 210 kcal to the ΔG_f° value for uraninite, one obtains an approximate value for coffinite, of -456.0 ± 2.6 kcal per gram formula weight. The validity of the calculation is limited, but in the absence of any experimental data, this ΔG_f° value for the coffinite is used for subsequent discussions.

Of particular interest is the stability relation of coffinite and uraninite with regard to uranium-bearing dissolved species such as the uranyl dicarbonate

TABLE 1

Free Energies of Formation: Zr, Th, and U Species

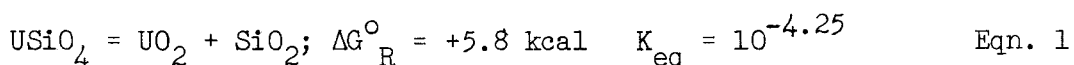
Element	ΔG_f° _{MO₂} (1)	ΔG_f° _{MSiO₄} (2)	Differences in ΔG_f°
Zr	-248.7 (248.5)	-458.7	-210
Th	-279.4	-489.5	-210.1
U	246.6	(-456.0; {3})	-210.0 (assumed)

(1) Source of ΔG_f° : Robie and Waldbaum (1968)

(2) " " " : Vergouen (1974; written comm. to D. G. Brookins)

(3) " " " : Calculated by Brookins (1975)

and the uranyl tricarbonate ions. Both coffinite and uraninite have been identified from most deposits; the former in far greater abundance than the latter. However, it is not known if coffinite was formed simultaneously with uraninite, earlier or later than uraninite. Gruner and others (1955) indicated that uraninite is predominant in deposits of high vanadium content, but the high vanadium deposits in the Salt Wash Member and the sandstones do not show this (Weeks and others, 1959). The ΔG_R° of the following reaction:



may indicate that coffinite should be favored over uraninite, although, in view of (OH⁻) substitution in tetrahedral sites in coffinite the ΔG_R° may well be negative for eqn. 1. This is suspect as a function of geologic aging as coffinite is far less abundant in Precambrian uranium deposits than uraninite (Brookins; unpublished data). Brookins (1973; 1975) has shown that the Eh-pH stability field of coffinite is, as predicted by Hostetler and Garrels (1962) very close to that for uraninite. The controlling factor for coffinite versus uraninite may, then, be availability of dissolved silica.

For quartz saturation the activity of dissolved silica = $10^{-3.5}$ at 25°C and the ion activity product (IAP) for equation 1 is $10^{-3.5}$ which is greater than K_{eq} hence coffinite should be formed under these assumed ideal conditions.

This matter is being pursued by Brookins and others at the University of New Mexico.

Other Uranium Minerals. As explained in the previous section, uraninite is very rare in the Grants Mineral Belt and only a few occurrences have been reported (See Granger, 1963). A variety of uranium bearing minerals, both pre- and post-mine have been identified. Most frequently found are the uranium carbonates and sulfates all of them in the hexavalent state.

Andersonite $\text{Na}_2\text{Ca}(\text{UO}_2)(\text{CO}_3)_3 \cdot 6\text{H}_2\text{O}$ is very common in all districts and is found on mine walls forming light green crystals. It is commonly associated with gypsum and schroekingerite $\{\text{NaCa}_3(\text{UO}_2)(\text{CO}_3)_3(\text{SO}_4) \cdot 10\text{H}_2\text{O}\}$. Bayleyite $\{\text{Mg}_2(\text{UO}_2)(\text{CO}_3)_3 \cdot 18\text{H}_2\text{O}\}$ and zippeite-like minerals are also frequently found in many mines as minute crystals with yellow or orange colors. These minerals are more commonly associated with high-grade primary ore bodies. Other oxidized minerals identified during the course of this study include uranophane $\{\text{Ca}(\text{UO}_2)_2\text{Si}_2\text{O}_7 \cdot 6\text{H}_2\text{O}\}$, Tyuyamunite $\{\text{Ca}(\text{UO}_2)_2(\text{UO}_4)_2 \cdot 5-8\text{H}_2\text{O}\}$ and carnotite $\{\text{K}_2(\text{UO}_2)_2(\text{UO}_4)_2 \cdot 1-3\text{H}_2\text{O}\}$.

Vanadium Minerals. No low-valence vanadium minerals, other than the clay minerals, have been detected optically or from x-ray patterns in this study although their occurrence has been reported in some unoxidized, redistributed ore bodies.

According to Granger (1963), montroseite $\{\text{V}_2\text{O}_3 \cdot \text{H}_2\text{O}\}$, paramontroseite $\{\text{V}_2\text{O}_4\}$ and haggite $\{\text{V}_2\text{O}_3 \cdot \text{V}_2\text{O}_4 \cdot 3\text{H}_2\text{O}\}$ occur as fracture fillings commonly with radiobarite and native selenium, as crusts and felted layers of crystals, and as interstitial fillings in sand grains associated with coffinite, pyrite, calcite and kaolinite.

Molybdenum Minerals. Amorphous black jordisite, MoS_2 , is commonly present in association with primary ore bodies, coating sand grains and mudstone and siltstone layers. No appreciable amount of molybdenum is found in the redistributed ore.

The jordisite-rich sandstone layers generally occur around the periphery of the ore bodies separated by a few feet of barren sandstone. Commonly the layers form feathery edges or lenticular masses which are crudely parallel to the ore boundaries. The jordisite-rich sandstone samples also have high selenium content, although the Se:Mo ratios are variable (Granger, 1963). Generally the jordisite shows indistinguishable x-ray peaks, but Granger and Ingram (1966), and Kendall (1971) report a few samples having a diffuse peak corresponding to the major basal molybdenite diffraction.

Selenium Minerals. Ferroselite $\{\text{FeSe}_2\}$ and native selenium, though not detected during this study, have been reported in a few mines. The ferroselite has been found both in primary and redistributed ores (Granger, 1963) and in the roll-type deposits of Wyoming (Granger, 1966). Due to limited occurrence, the distribution of Se phases is not well understood.

Native Se sometimes occurs as red coatings on mine walls near primary ore bodies. More commonly it occurs as acicular crystals or gray foil-like flakes in mudstone clasts along the surfaces of small fractures or perched on sand grains. According to Squyres (1969), the acicular native selenium occurs largely in redistributed ore whereas the foil-like native selenium is mostly associated with the primary ore. The selenium content in the ore samples are quite variable, ranging from 0.02 to 0.07% (Squyres, 1969) and it is doubtful whether it can be used for the differentiation of ore types. Undoubtedly some selenium could also be present in jordisite and pyrite due to S-Se diadochy.

Ferroselite has been synthesized at temperatures from 25°*C* to 80°*C* (Warren, 1968). The synthesis produced ferroselite only at slightly alkaline conditions, similar to the case of coffinite.

Organic Carbonaceous Matter (OCM). Organic carbonaceous matter of probable lignin-derived parent origin is noted everywhere in the uranium deposits, usually in direct association with the ore. Humic and fulvic acids and their derivatives are abundant in the OCM. It is asphaltic material that commonly possess dark gray to vitreous black colors, or brown color in low grade ore. The OCM has been aged and altered by radioactivity and is insoluble in common inorganic acids and bases (Jacobs and others, 1970), so that it is difficult to characterize the original substance although it is now generally believed that the OCM in the Grants Mineral Belt is plant-derived, based on extensive laboratory and field observations (Vine, 1962; Moench and Schlee, 1967; Haji-Vassiliou and Kerr, 1973).

The humic acid, hitherto defined as the mobile organic matter extracted by alkaline solutions from decaying plant material, possess several properties which may have been important for the uranium mineralization:

(1) Humic acids have high ion-exchange capacity in the form of reversible sorption so that uranium and other metals can be easily adsorbed and concentrated from dilute solutions (Szalay, 1964; Szalay and Szilagyi, 1968). For most peat extracts, the enrichment factor (U per gm. peat/U per ml H_2O) is about 10^4 , and the maximum adsorption occurs in the pH range 5 to 6. Further, uranium can be fixed in the humic acid by chelation which is not removable (Schmidt-Collerus, 1969).

(2) The natural humic acids have high reducing capacity. Organic materials such as wood, lignite, peat and kerogen, in contact with a solution, can reduce hexavalent uranium and pentavalent vanadium (Pommer, 1957; Garrels

and Pommer, 1959; Swain, 1963; Andreyev and Chumachenko, 1964). It has been shown by experiments that about 0.5 wt. % of lignite is sufficient to form a typical Colorado Plateau uranium vanadium ore by reduction (Garrels and Pommer, 1959).

(3) The humic acids commonly form colloids. The coffinite-organic mixtures frequently show colloform habit (Nash, 1969; Kendall, 1971), suggesting a possible colloidal deposition.

(4) Natural humic acids dissolve (or reprecipitate) rock-forming silicates, especially clay minerals. Laboratory experiments by Huang and Keller (1970, 1971 and 1972 a, b) have shown that strongly complexing organic acids, such as tartaric or tannic acid, are effective reagents in the dissolution of major types of clay minerals.

(5) Solubility of the humic substances is strongly dependent on pH. They are readily dissolved in alkaline solutions and precipitate in acidic solutions (Stevenson and Butler, 1969).

The source(s) of the OCM in the ore deposits has been a subject of much debate. Part of the dispute arises from the doubt that vegetable matter within the Westwater Canyon and Jackpile sediments could not have contained enough OCM for that now present in the deposits, although small scale trash piles, enough for individual ore bodies, are present (See Weege, 1963; for example). Granger and others (1961) listed three possible sources: (1) an extrinsic epigenetic source from highly vegetated swamps that covered upper Morrison prior to Dakota deposition, (2) an extrinsic penecontemporaneous source from the streams that transported dissolved humic acids from vegetated source areas, and (3) an intrinsic diagenetic source from the plant debris deposited with the Morrison sands. They consider the first-listed to be the most probable source. Squyres (1969), on the other hand, favors the

third possibility based on the close spatial association between fossil plant material and humic substances.

Another possible source of the OCM, that has been entirely overlooked, is the organic compounds present in the interlayer site of the expandable clay minerals. It is known that soils derived from volcanic ashes have high retention capacities for organic matter (Zunino and others, 1974). Experiments have shown that by eliminating the Al ions, the organic matter can be separated into two different fractions, humic and fulvic acids, according to their solubility in alkaline or acidic mediums. In addition, the well-known inorganic-organic cation exchange phenomena for montmorillonite suggest that the humic compounds could have been present in the clay structure. For example, Demolin and Barbier (1929) showed a definite fixation of humic acid and protein by the clay minerals in soils and, as far as uranium deposits are concerned, even humate-clay mineral solid-solution phenomena has been suggested. This subject needs further inquiry and will be discussed later in this report.

Calcite. Two types of calcite found near the ore bodies bear probable genetic relationships to the chemical processes responsible for the ore formation. Layers of dense, calcite-cemented sandstone are particularly common a few to several feet below and above the lenticular ore pods. The calcite in this case completely replaced interstitial material and is opaque or translucent. Although firm evidence is lacking the calcite-cemented sandstones appear to have formed a crude discontinuous halo around the ore pods. The other type of calcite is the so-called buckshot calcite which forms conspicuous spherules or shells near the edge of and within the primary ore bodies. At the Sandstone Mine, the calcite shells occur as complete spheres or ovals a few feet in diameter enclosing high-grade ore, and in turn enclosed by ore (Squyres, 1969) whereas in some other localities smaller buckshot calcite encloses sand grains which are not coated with coffinite-bearing OCM (Kendall, 1971).

The overall distribution pattern of the two calcites indicate that they are the product of probable buffering reactions associated with primary mineralization. Calcite is an effective buffering agent to maintain a constant pH in sea water. Any pH shift during the ore formation could have been buffered by the preexisting calcite in the sediment and may have been reprecipitated outside of the ore boundaries.

Iron Oxides. Goethite and hematite coatings on sand grains cause yellow and red colors in the sandstones of the Westwater Canyon Member both on the subsurface and on outcrops. Opinions regarding the original color of the Morrison sediments in the Grants Mineral Belt are still controversial. It has been suggested that all sandstone of the Morrison were red-bed deposits and that the white or gray to green ore bearing sandstones were the result of bleaching of the organic environment after deposition (Konigsmark, 1955; Sharp, 1955; Squyres, 1969). A similar view was expressed by Shawe and others (1959) for the deposits of Salt Wash Member in the Slick Rock district, Colorado.

Granger and others (1961) and Granger (1968) doubt the presence of original red beds and argue that much of the present red sandstone represents recent oxidation of pyrite-bearing favorable sandstone. They, however, agree to a certain degree that "original drab-colored sandstones" were diagenetically bleached in a reducing environment.

According to our observations, extensive red-bed type deposits were not present. This postulation is largely based on the presence of abundant detrital titanomagnetite grains in some of the sandstone core samples from north of Ambrosia Lake district. Here the magnetite content exceeds 10 wt. % in a few samples and, although rounded, fresh grains are abundant. In another location, near Laguna, thin layers of magnetite are present in the goethite-

yellow Westwater Canyon Member rather than hematitic sandstones. It is our opinion that much of the original Westwater Canyon Member was associated with the goethite-yellow colors commonly seen in many Morrison sections at the margin of the San Juan Basin.

Most of the primary deposits are present in non-iron oxide bearing sandstones. In some cases, such as in the Sec. 23, Black Jack, and Cliffside Mines, the ore pods are in direct contact with the hematitic sandstones. These probably represent partial retention of the primary ore after redistribution. The redistributed ore bodies are commonly present near the boundary between the hematitic sandstone and pyrite-bearing bleached host rock. The interface commonly shows a narrow zone of goethite-yellow sandstone resembling somewhat the roll-type deposits of Wyoming.

Other Authigenic Minerals. Radiobarite and gypsum have been found near the ore deposits. The barite is mostly present in fracture zones associated with redistributed ore. According to Granger (1961) the radiobarite was formed by radium-bearing solutions in the presence of Ba^{2+} and SO_4^{2-} and this precipitated in the outer zones of the crystals. Minor amounts of gypsum have been identified below the pre-mine water table associated with zippeite and andersonite on mine walls.

Detrital Minerals

Quartz. Quartz constitutes the bulk of the detrital grains both in the Westwater Canyon and Jackpile sandstones. Using Folk's (1968) classification the predominate types are the volcanic quartz with straight extinction, and the plutonic quartz with vacuoles and slightly undulose extinction. Thin layers of sandstone containing rounded smoky quartz are common throughout the entire Grants Mineral Belt.

The quartz grains are markedly etched in the OCM-bearing sandstones. In some vitreous high-grade ore-haloes around clay galls, as much as 40 to 60% detrital quartz is dissolved. The fate of the dissolved silica is unclear. Presumably much of it was incorporated into newly formed coffinite and reprecipitated as an overgrowth around other quartz grains in the ore body. However, the distribution of the overgrowth-bearing quartz is very erratic and, further, a few generations of overgrowths are present in the Westwater Canyon sediments.

Both Squyres (1969) and Kendall (1971) note total absence of amorphous silica precipitation. However, in one outcrop section near Thoreau, we noted an abundant opaline silica which shows well-developed colloform texture. Evidently the activity of dissolved silica was higher near the deposits as well as in the other parts of the Westwater Canyon Member.

Feldspars. Microcline and sodic plagioclase are the most common feldspars in the Westwater Canyon Member. The pink microcline grains are coarser grained than other detrital minerals and some pebble-sized fractions are common. Within the ore deposits and elsewhere, the potassium feldspar is relatively fresh, although some degree of kaolinization and sericitization are observed. Orthoclase and hollow sanidine grains, as observed by Austin (1963), are much less common. The overall alteration pattern of the feldspars probably represent several cycles of depositional history which are difficult to relate to uranium mineralization.

Heavy Minerals. The general absence of detrital heavy minerals, especially magnetite and ilmenite in the Westwater Canyon Member, have been previously noted. However, we find this is not completely true. In a few locations, abundant titanomagnetite has been found both in oxidized and bleached sandstones. In one representative sample, the magnetite content is well over 10 percent. The magnetites in these samples are visibly rounded, and associated

with detrital zircon and epidote. Many grains have a hollow inside where authigenic titanium oxides formed.

Because the magnetite and ilmenite are relatively resistant to weathering one should be able to find these minerals, in immature, subarkosic sediments. Austin (1963) presumed these minerals were originally present in the Westwater Canyon Member but have been destroyed by dissolution or by alteration to pyrite and titanium oxides. In the Slick Rock district Colorado, Shawe and others (1959) postulated that the destruction of the opaque detrital opaques provided a source of the ore-related elements, such as vanadium, titanium and iron.

Rock and Wood Fragments. Red and green clay galls and clasts are common in the sandstones of Westwater Canyon Member area. Clay galls of more than a foot in diameter are abundant. One of the most conspicuous features in many ore deposits is the presence of high-grade ore haloes around these green clay galls. Red clay galls are seldom found and, when found, no such ore haloes are present. Mineralogically, the red and green clay galls and clasts do not show any difference, they are all montmorillonitic. Squyres (1969) indicates that many of these halos have southeasterly trending tails, and suggest this is the direction of movement of the solutions which deposited the ore substances. According to our observations, however such tail development is very rare and erratic, and no systematic pattern could be found. It is the belief of one of us (M. J. L.) that the halo was formed by adsorption in relatively stagnant solution. The clay galls, being montmorillonitic, built up a significant negative charge on the surface, and simple adsorption of the positively charged humate particles formed the halo.

Volcanic, granitic and metamorphic rock fragments are also present.

The matrix of the volcanic fragments are highly altered, and light green chloritic clay minerals developed as patch-like coatings. Granitic rock fragments are mostly fresh aggregates of microcline and quartz. Polycrystalline quartz grains are dominant in metamorphic fragments.

Fossil trunks and other woody material, as well as fossil bones, are locally abundant in paleochannels. These materials are often highly uraniferous. Some of the silicified and calcified materials show a mineralization only at the surface.

Detrital Clay Minerals

Distinction between detrital and authigenic clay minerals is often difficult. In thin section some kaolinite, chlorite and illite-montmorillonite appear to be detrital. Detrital kaolinite generally forms rounded aggregates with faint oxidation coating whereas illite-montmorillonite coats sand grains as thin films. Detrital chlorite shows higher birefringence than the authigenic variety and can be differentiated by textural relationship and size. It is our belief that the overall proportion of the detrital clay minerals in the upper Morrison is very low.

GEOCHRONOLOGIC STUDIES

Introduction

In this report we focus our efforts on the Rb-Sr geochronologic method although we also report on some previously unreported K-Ar data from some samples used for Rb-Sr study. Our attempts at dating the source area(s), allogenic and authigenic constituents of the ore-bearing strata, etc. by the Rb-Sr method are based on the following assumptions and/or observations:

- (1) U-Pb dates (Note: No Th-Pb dates have been attempted for the ores of the Grants Mineral Belt) are largely discordant (See discussion below) and interpreted by most workers as possibly representing minimum ages only.
- (2) K-Ar dates have been reported in oral presentations (Adams, 1975) but they, too, are extremely scattered. (3) We note the presence of K-bearing, authigenic, clay minerals intimately associated with uranium mineralization.
- (4) We further note that much of the montmorillonite in the barren, reduced sandstones is apparently authigenic as well. (5) As Rb and Sr are presumably incorporated into the K-bearing and montmorillonitic clays (3, 4 above) then these minerals, if unperturbed, may be suitable for Rb-Sr age work.

In brief the advantage of the Rb-Sr method relative to the other methods is that daughter loss (i.e., either from intermediate radioactive daughters formed from ^{235}U or from ^{238}U or due to loss of stable daughter ^{40}Ar from parent ^{40}K) is not likely as ^{87}Sr , the daughter product of ^{87}Rb , is stable in the environment of ore deposition and clay mineral formation. Further, in the U-Pb and K-Ar methods one sample is analyzed at a time whereas for the Rb-Sr method many samples must be analyzed for the isochron (i.e., line along which all coeval samples lie) to be calculated. If points exhibit wide scatter about the isochron then either open system conditions (i.e., gain or loss of either parent or daughter) have existed after mineral (or rock)

formation or else detrital minerals with different pre-histories (i.e., different source areas) account for the scatter. Alternately, if a linear array of points is noted about the isochron then the slope of the isochron (i.e., λt where λ = decay constant of the parent isotope = $1.39 \times 10^{-11}/y$ and t = age) yields an age of homogenization---presumably due to events at time of mineral or rock formation. There always exists the possibility, albeit small, that allogenic material from different sources and with different prehistories (i.e., some metamorphosed, etc.) could conceivably yield such a linear array but we feel this is unlikely. Further, if this unlikely event was more common then drastic discordance of Rb-Sr isochron ages with K-Ar and/or U, Th-Pb ages from unaltered igneous systems might be noted and this is not the case.

U-Pb Dates from the Grants Mineral Belt

There exist few U-Pb dates worth mention from the Grants Mineral Belt. The reason for this, as stated briefly above, is apparently due to loss of some of the intermediate daughters from the ^{235}U and ^{238}U decay chains. For a U-Pb age to be considered most reliable the ^{238}U - ^{206}Pb , ^{235}U - ^{207}Pb and ^{207}Pb / ^{206}Pb would have to be concordant. The usual case is for greater loss of intermediate daughters from the ^{238}U decay scheme relative to loss(es) from the ^{235}U decay scheme resulting in the ^{207}Pb / ^{206}Pb age being greater than either the ^{238}U / ^{206}Pb or ^{235}U / ^{207}Pb ages. In turn, the ^{235}U - ^{207}Pb age is then interpreted as a minimum age of formation for the particular ore mineral (or mineral "assemblage" in the case of very fine ore; see, for example, Ludwig, 1975). For the Jackpile-Paguate area Nash and Kerr (1966) and Nash (1968) cite ^{235}U - ^{207}Pb dates for coffinite of 94 ± 3 m.y. and 90 ± 3 m.y., respectively; Miller and Kulp (1963) cite a ^{235}U - ^{207}Pb

date of 107 ± 6 m.y. for ore from Section 33 Mine, Ambrosia Lake district.

For all three samples the ^{238}U - ^{206}Pb dates are lower such that the ^{207}Pb - ^{206}Pb dates are anomalously high. Unfortunately crude 'chemical-lead' apparent dates reported by Granger (1963) average about 100 m.y. and this "date" is commonly referred to in discussing the age of mineralization. This is completely unwarranted and only the ^{235}U - ^{207}Pb dates (of U-Pb dates) should be cited.

The reader is also reminded that based on geologic grounds Moench and Schlee (1967) have argued for ore emplacement before any Cretaceous sedimentation which would infer an approximate age of about 135 m.y. (error uncertain) for ore in the Grants Mineral Belt. Their arguments are not refuted, in fact they are given due attention, by Dooley and other (1966) in discussing loss of radon, radium, etc. in conjunction with ^{234}U / ^{238}U disequilibrium studies at Ambrosia Lake.

K-Ar Ages from the Grants Mineral Belt

Although not part of the research funded by the present contract we felt it necessary to investigate the K-Ar systematics of several samples used for Rb-Sr study. The results are given in Table 2. It is perhaps significant that the two samples containing detrital K-feldspar (nos. Al-35-201 and Al-35-205) yield the oldest age; one falling in excess of 240 m.y. This is to be expected and, in view of the abundance of K-Ar ages below 100 m.y. (7 of 9 clay size samples), daughter ^{40}Ar loss is suspect. Mixed layer clay minerals are usually not well suited for accurate age assessment and the data in Table 2 confirm this statement. Possible diagenetic and/or epigenetic K-absorption is another factor which could effectively cause age lowering (i.e., as opposed to ^{40}Ar loss) but we do not feel this to be the

case because of the Rb-Sr data. Rb^+ is a larger ion than K^+ and would be even more preferentially absorbed on the clay surfaces hence one might expect very low Rb-Sr ages as well. As discussed below, this is not the case hence we feel ${}^{40}\text{Ar}$ loss to be the cause of the age lowering.

TABLE 2

K-Ar DATA ON PROBABLE AUTHIGENIC CLAYS FROM
 URANIUM-RICH (MORRISON FM.) SAMPLES
 AMBROSIA LAKE AND JACKPILE-PAGUATE AREAS
 UNIV. NEW MEXICO COOPERATIVE RESEARCH PROJECT WITH PROF. D. G. BROOKINS

Description and Location	Age in m.y.
AMBROSIA LAKE AREA	
Clay (mixture of chlorite, illite and kaolinite) with organic materials. #AL-35-209.	104.3 <u>±</u> 2.5
Clay (mixture of chlorite, illite, and kaolinite) with organic material. #AL-35-306.	138.9 <u>±</u> 3.0
Whole rock, clay and silt-sized fraction with detrital K-feldspar. #AL-35-201.	141.7 <u>±</u> 2.9
Whole rock, clay and silt-sized fraction with detrital feldspar. #AL-35-205.	244.3 <u>±</u> 5.2
Whole rock, clay-sized fraction, volcanic ash derived clays---montmorillonite and mixed-layer illite with very little organic material. #AL-35-207.	68.7 <u>±</u> 1.5
Whole rock, clay-sized fraction, volcanic ash-derived clays (montmorillonite and mixed layer illite) with very little organic material. #AL-35-305.	85.5 <u>±</u> 1.8
Clay (illite-chlorite-kaolinite mixture) rich in organic matter. #AL-23-303.	59.1 <u>±</u> 1.6
Clay (chlorite-kaolinite-illite mixture) rich in organic matter. Difficult to clean up and contains unusually high atmospheric argon and low K. #AL-23-313.	62.9 <u>±</u> 4.1
Clay (chlorite-illite-kaolinite mixture) rich in organic matter and associated with uranium ore. #AL-23-302.	63.9 <u>±</u> 1.6
JACKPILE-PAGUATE AREA	
Clay (mixed layer illite-montmorillonite, 1Md illite, minor kaolinite) with organic matter. #CS-1.	58.7 <u>±</u> 1.4
Clay (1Md illite, illite-montmorillonite, some kaolinite). #FS-1.	45.4 <u>±</u> 1.0

Note: The data in Table 2 are in press (Brookins and others).

Rb-Sr Geochronology

For some time the Principal Investigator and the other co-workers of this research effort have been involved with study of clay minerals by the Rb-Sr method to study problems of provenance, age of sedimentation, etc. That we should employ this technique to study of the ore deposits of the Grants Mineral Belt is a logical outgrowth of several years work in this area. We have mentioned elsewhere in this report that authigenic clay minerals of two types are noted: (1) montmorillonites presumably formed at the time of sedimentation and (2) authigenic chlorite, chlorite-illite, illite-montmorillonite in the ore zones which has formed at the expense of the authigenic montmorillonite (See Plate III). This latter group of clay minerals is assumed to have formed at the time of mineralization as the clay minerals are intimately mixed with coffinite, pyrite, organic matter, etc. in such a fashion as to indicate penecontemporaneous formation of the ore minerals as the clay minerals were forming---both types of formation presumably linked to alteration of pre-existing silicates (including authigenic montmorillonite) influenced if not directly due to organic acid attack. For the sake of clarity the Rb-Sr studies will be divided into those from the Ambrosia Lake district relative to those from the Jackpile-Paguate and Smith Lake districts. Finally, the isochrons were calculated using York's (1966) least squares regression method.

Ambrosia Lake District

Studies of three suites of samples were conducted in the Ambrosia Lake District (from the Section 23 and 35 Mines): (1) The minus-two micron fraction of montmorillonite-rich samples from barren, reduced ground (Fig. 4). (2) The minus-two micron fraction from chlorite-(and related K-bearing

mixed-layer clay minerals) rich material from U:OCM ore pods (Fig. 5).

(3) The two to sixty two micron fraction from reduced ground (Fig. 6).

These are interpreted as follows.

Ten samples of minus-two micron montmorillonite (from barren, oxidized and barren, reduced ground) are presumed from scanning electron microscopic (SEM) evidence to be authigenic. The Rb-Sr isochron in Figure 4 indicates an age of formation of 149 ± 17 m.y. with initial $^{87}\text{Sr}/^{86}\text{Sr} = 0.7056 \pm 0.0021$. There is no good reason to indicate that this age is other than that accompanying the age of montmorillonite formation; viz., the age of sedimentation and we interpret it accordingly. The scatter in data is somewhat to be expected and accounts for the relatively large error, but the spread in both $^{87}\text{Sr}/^{86}\text{Sr}$ and $^{87}\text{Rb}/^{86}\text{Sr}$ is sufficient such that the age is statistically significant within the stated limits of error. This age, 149 ± 17 m.y. is within the limits of uncertainty for the Jurassic - Cretaceous boundary and may be used to confirm that the Westwater Canyon Member of the Morrison Formation is indeed late Jurassic.

Nine minus-two micron samples of chlorite-rich clay mineral(s) from ore pods are plotted in Figure 5. The 139 ± 10 m.y. age with initial $^{87}\text{Sr}/^{86}\text{Sr} = 0.7091 \pm 0.0020$ is within the limits of error for the age and initial $^{87}\text{Sr}/^{86}\text{Sr}$ ratio of Figure 4 but the petrographic and SEM data clearly show that the chlorite-rich material has formed at the expense of the montmorillonite. As the chloritic material is evidently formed penecontemporaneously with the uranium mineralization then 139 ± 10 m.y. may be taken as the age of mineralization for the samples from the Section 23 and 35 Mines. This suggested age of mineralization agrees with the interpretation of Moench and Schlee (1967) but is in disagreement with the 100 or so m.y. age of mineralization advocated by many (after Granger, 1963).

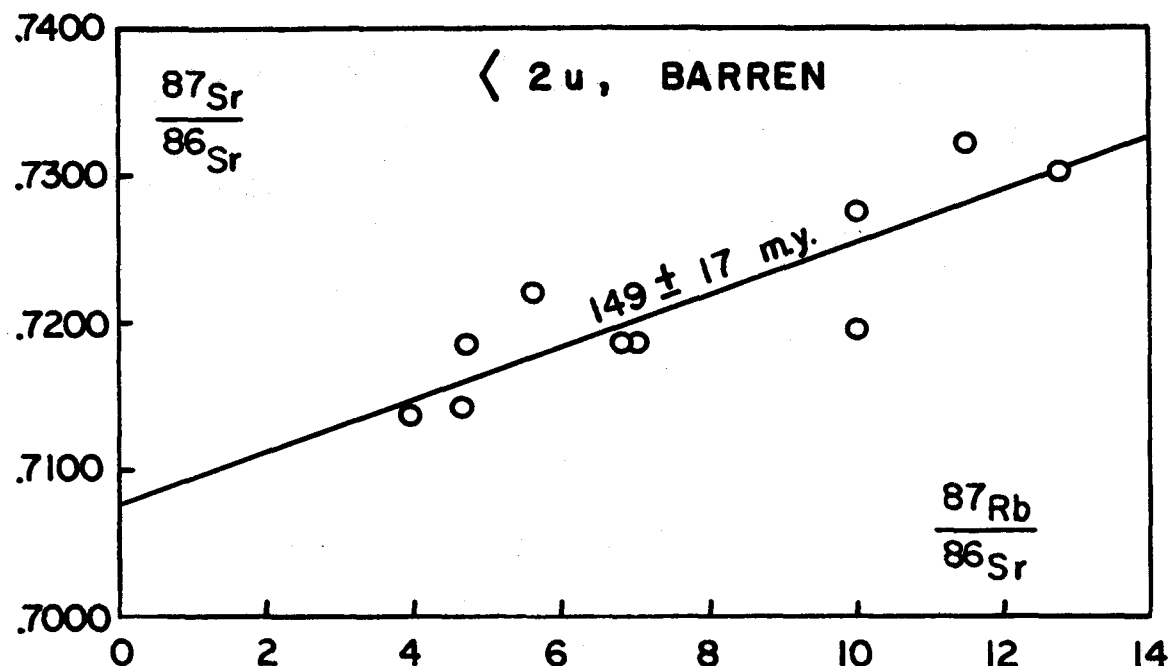


FIGURE 4. Rb-Sr Isochron for Minus-Two Micron Montmorillonite from Barren Ground, Section 23 and 35 Mines, Ambrosia Lake District

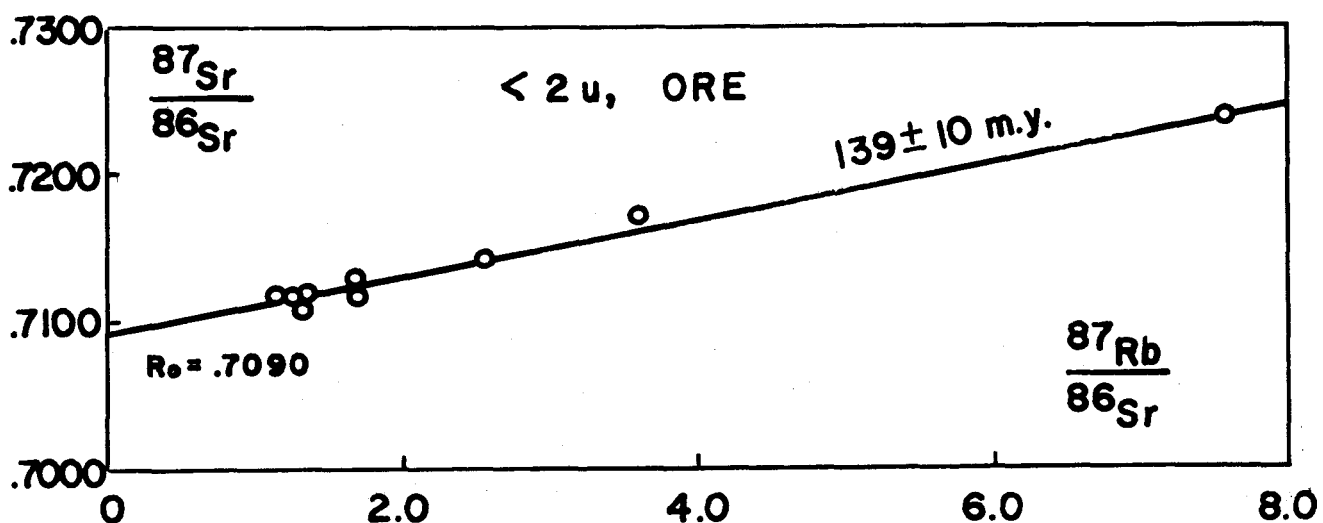


FIGURE 5. Rb-Sr Isochron for Minus-Two Micron Chlorite-Rich Clay Minerals from Ore Pods, Section 23 and 35 Mines, Ambrosia Lake District

Nine two to sixty two micron size fractions from oxidized, barren and reduced, barren ground from Sec. 23 and 35 Mines were studied and the results shown in Figure 6. Two linear arrays are apparent; a steep isochron of an apparent 774 ± 27 m.y. with initial $^{87}\text{Sr}/^{86}\text{Sr} = 0.703 \pm 0.002$ and a less steep apparent 273 ± 5 m.y. isochron with initial $^{87}\text{Sr}/^{86}\text{Sr} = 0.7051 \pm 0.0038$. The spread in $^{87}\text{Rb}/^{86}\text{Sr}$ is narrow for the former and all one can say with confidence is that this isochron is weighted by Precambrian material; in fact these points may actually fall on the K-feldspar pebble isochron of Figure 11 (discussed below). Of more interest is the 273 ± 5 m.y. isochron as this apparent Permian date may be of more significance. In thin section volcanic shards are commonly noted which are less corroded than presumed Precambrian quartz-feldspar detrital grains. Further, volcanic activity in the general area occurred during Permian time to the west and southwest of the San Juan Basin. Consequently, pending more data, we interpret Figure 6 to indicate (a) the presence of Precambrian detritus plus (b) possible Permian detritus. Unfortunately, due to paleogeographic uncertainties, the question of which direction provided more detritus cannot be resolved. That the two lines are clearly resolvable, however, indicates that this question may be answered by subsequent study.

Smith Lake District

Core samples from the CONOCO property in the Smith Lake District were made available for study. Nine minus-two micron, chlorite-rich clay mineral assemblages were separated from relatively high grade ore. The resultant isochron shown in Figure 7 yields 139 ± 13 m.y. with initial $^{87}\text{Sr}/^{86}\text{Sr} = 0.7102 \pm 0.0013$. This age is indistinguishable from that for the same size fraction from Ambrosia Lake samples (Fig. 5) and, as both the Smith Lake and Ambrosia Lake samples are from the same approximate stratigraphic position

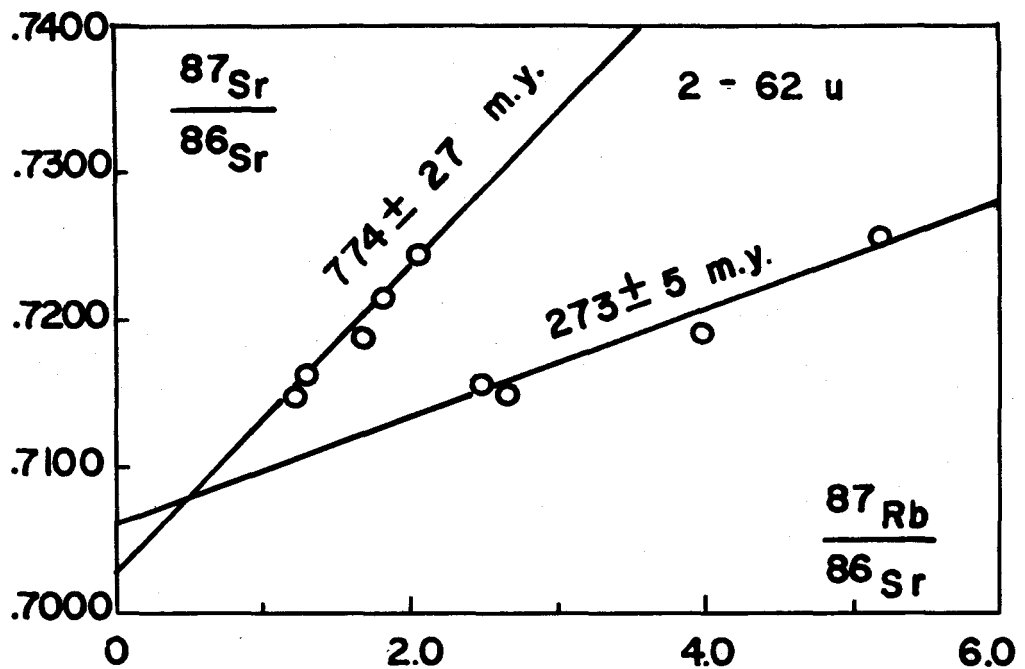


FIGURE 6. Rb-Sr Isochron for Plus-Two: Minus-Sixty Two Micron (Silt Size) Detrital Material from Barren, Reduced Ground, Section 35 Mine, Ambrosia Lake District

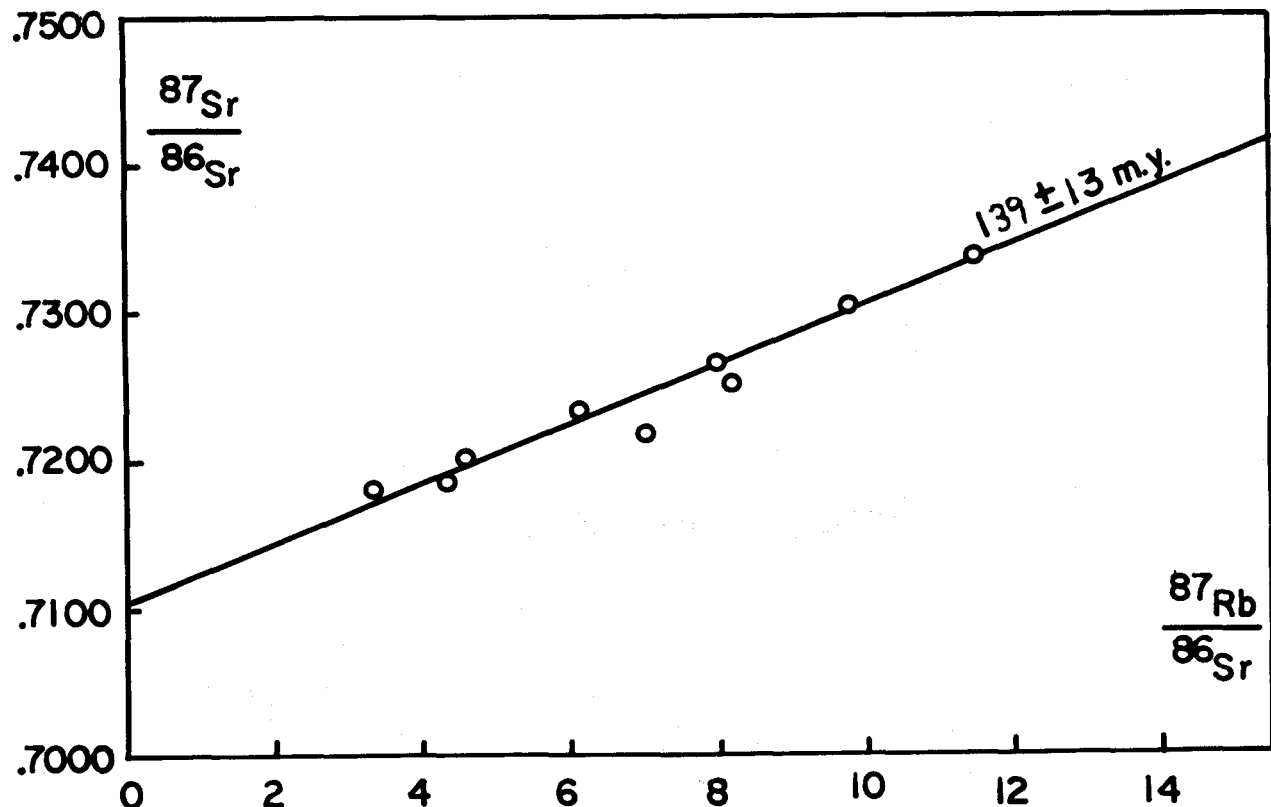


FIGURE 7. Rb-Sr Isochron for Minus-Two Micron Chlorite-Rich Clay Minerals from Ore-Bearing Core Samples, Smith Lake District

in the Westwater Canyon Member, then this lends support to an age of mineralization at about 139 ± 10 m.y. which, while within the error limits for the authigenic montmorillonite (i.e., 149 ± 17 m.y.; Fig. 4), again indicates mineralization in this part of the Grants Mineral Belt in late Jurassic time. Again, the reader is reminded that SEM and other work clearly shows the ore and associated chlorite-rich clay minerals to be epigenetic---but the data also show the epigenetic events to have occurred not too long after sedimentation.

Laguna District

Nine minus-two micron fractions samples from barren, reduced ground from the Jackpile Mine have been analyzed and the results shown in Figure 8.

The isochron age is 146 ± 5 m.y. with initial $^{87}\text{Sr}/^{86}\text{Sr} = 0.7100 \pm 0.0001$. This age is almost exact agreement with the 149 ± 17 m.y. age (Fig. 4) for the same material from Ambrosia Lake and, if the two are averaged, an approximate age of sedimentation of 147 ± 8 m.y. may be inferred for Westwater Canyon - Jackpile sedimentation.

For ore samples from the Jackpile Mine both minus-two micron and minus-0.5 micron size fractions were separated. The results are shown in Figures 9 and 10. For fourteen minus-two micron samples (Fig. 9) an isochron age of 115 ± 9 m.y. with initial $^{87}\text{Sr}/^{86}\text{Sr} = 0.7112 \pm 0.0016$ is obtained and for eight minus 0.5 micron size samples (Fig. 10) an isochron age of 110 ± 10 m.y. with initial $^{87}\text{Sr}/^{86}\text{Sr} = 0.7088 \pm 0.0016$ is obtained. These two ages are identical within limits of error and significantly younger than the suggested age of mineralization for minus-two micron material from ore-bearing material in the Ambrosia Lake and Smith Lake districts. Interpretations that may be made include: (a) A truly younger period of mineralization for the Jackpile-Paguate ore than for that in the Westwater Canyon Member in the Ambrosia Lake-Smith Lake districts or (b) Some type of resetting of the isochrons

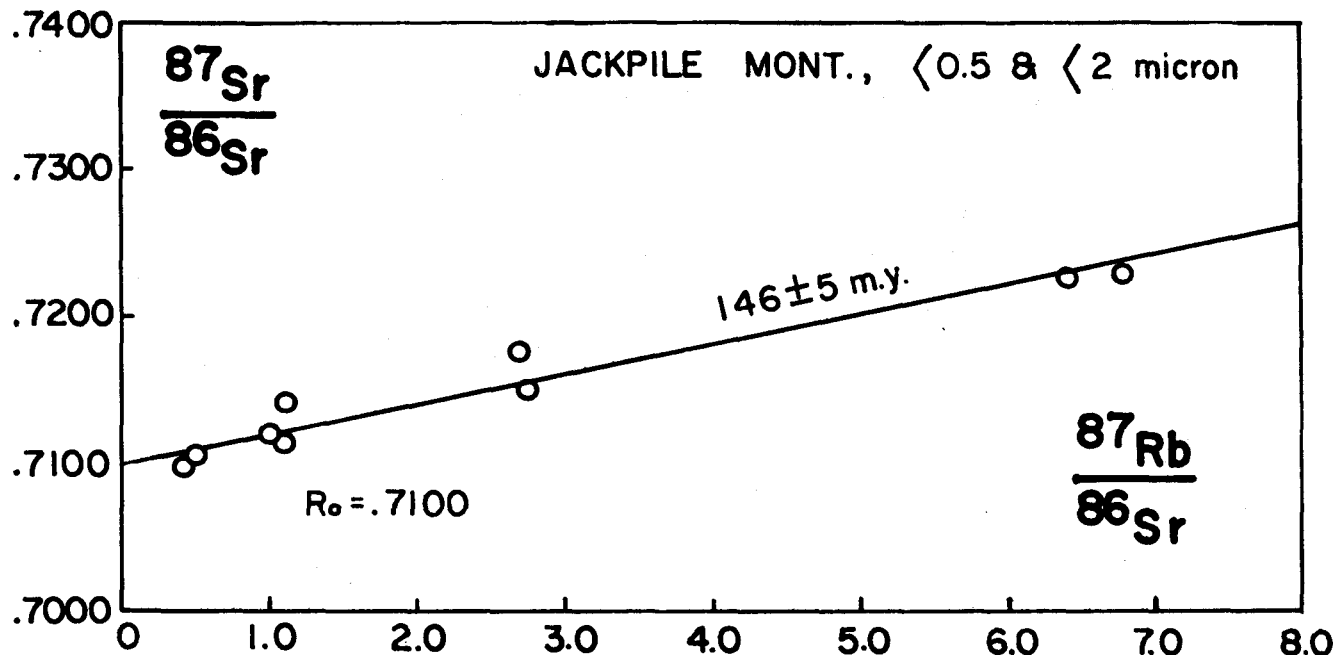


FIGURE 8. Rb-Sr Isochron for Minus-0.5 and Minus-Two Micron Montmorillonite from Barren, Reduced Ground, Laguna District.

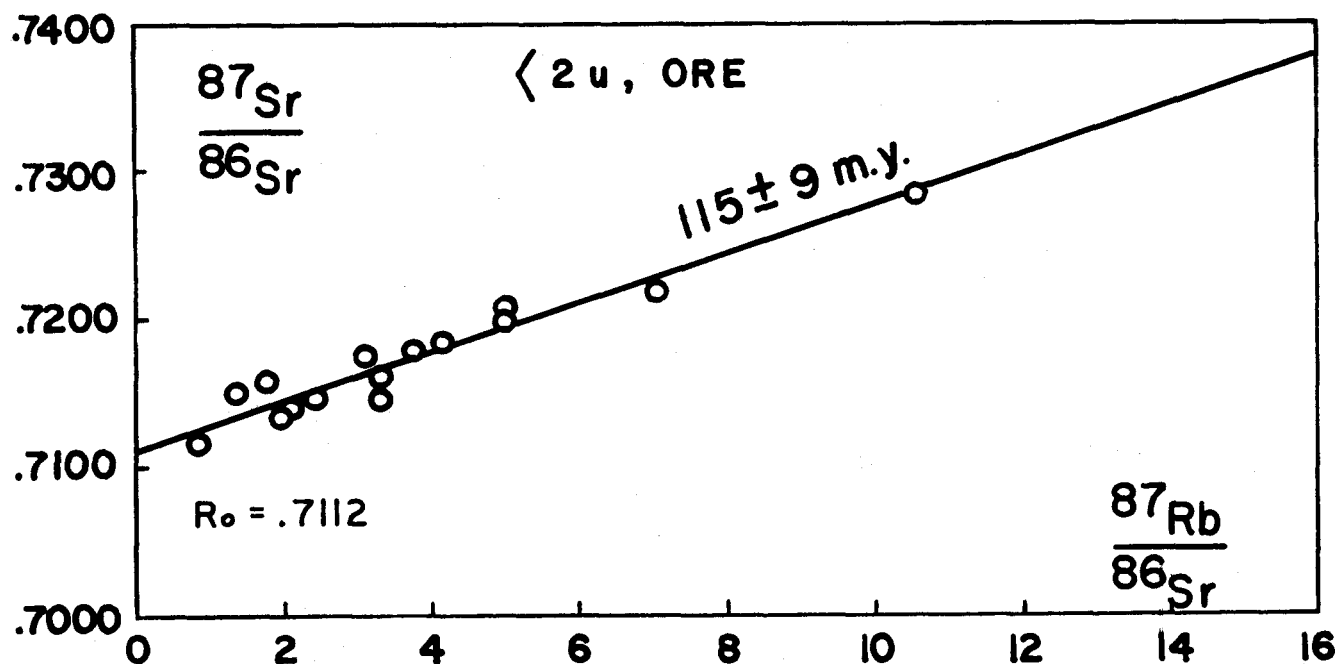


FIGURE 9. Rb-Sr Isochron for Minus-Two Micron K-Enriched Clay Minerals from Ore Pods, Jackpile Mine

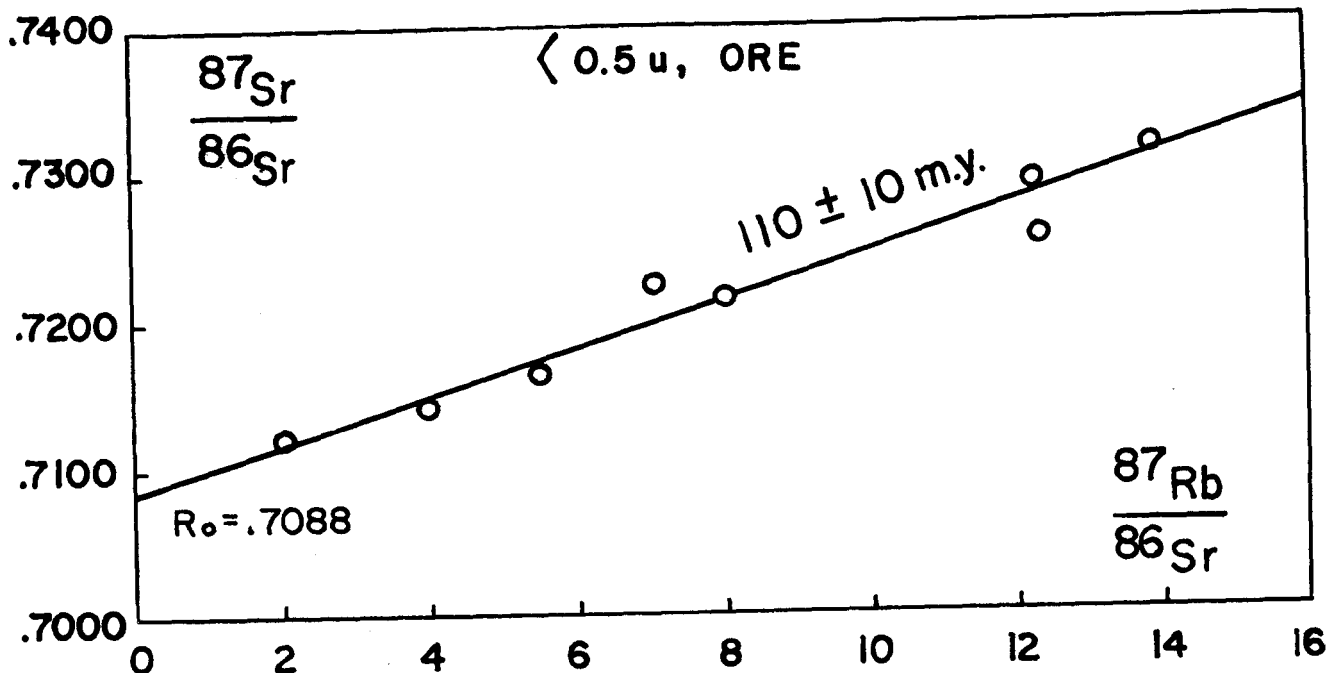


FIGURE 10. Rb-Sr Isochron for Minus-0.5 Micron K-Enriched Clay Minerals from Ore Pods, Jackpile Mine

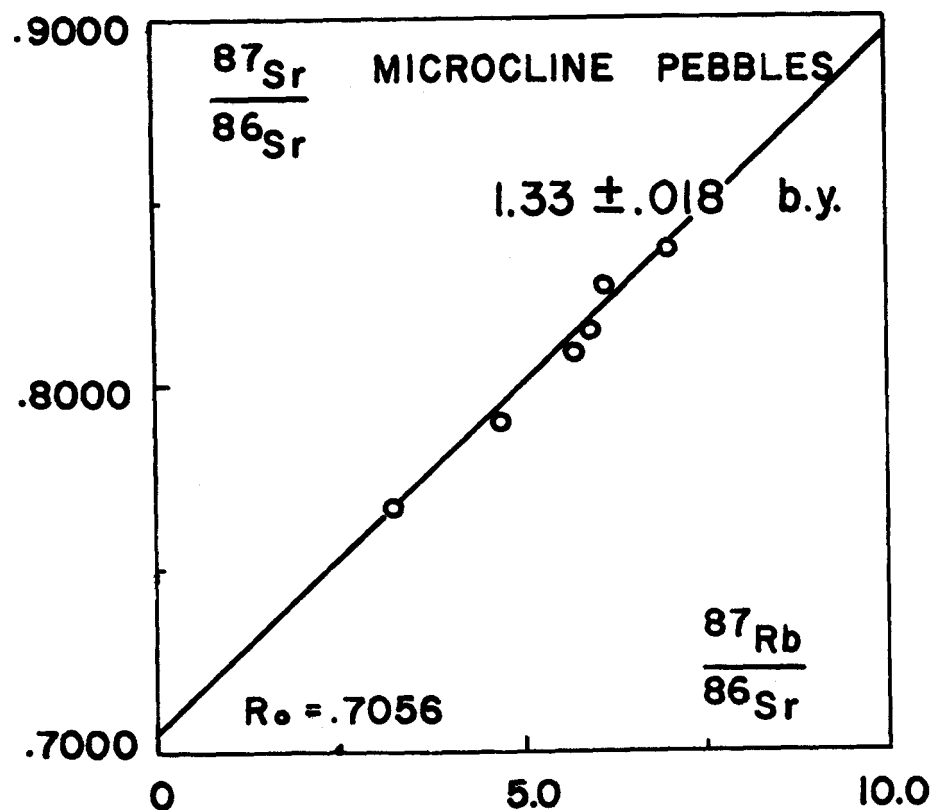


FIGURE 11. Rb-Sr Isochron for K-Feldspar (i.e. Microcline-Rich) Pebbles, Grants Mineral Belt, near Ambrosia Lake District

either at one, but not both, locations. We prefer the former interpretation and note that the sedimentological evidence suggests significantly younger paleochannel development (and in a different direction) in the Jackpile Sandstone relative to the Westwater Canyon Member Sandstone.

An outgrowth of the isochron assessment is that we suspect, but do not necessarily advocate, that the ore in the Ambrosia Lake district may well be the result of leaching of volcanogenic detritus from the overlying Brushy Basin Member. If so, then a different source would have to be proposed for the stratigraphically higher Jackpile-Paguate ores. In other words the sedimentation history may have been rapid enough for authigenic montmorillonite of essentially identical ages to be present in both the Westwater Canyon Member and Jackpile Sandstone but that uranium sources were temporally different by at least ten-twenty m.y. It is thus also perhaps noteworthy that, in addition to the paleochannel and other sedimentological evidence that there is a pronounced difference in U/V ratios between the two areas, difference in detrital assemblages, etc. A possible way to test this hypothesis, if applicable over the distance between the Laguna-Jackpile area and Ambrosia Lake area, would be to date the authigenic chloritic-clay minerals from ore zones in the Poison Canyon Sandstone in the Ambrosia Lake district. If they should yield ages in the 110 to 115 m.y. bracket as opposed to the 139 ± 10 m.y. range then this difference is real. Alternately, should the Poison Canyon clay minerals yield an age near 140 m.y. then the Ambrosia Lake district has been affected by only one pronounced period of primary mineralization or, alternately, the Jackpile area material has been rehomogenized in some fashion resulting in age lowering. This last possibility is difficult to envisage without some effect on the authigenic minus-two micron montmorillonite (i.e., 146 m.y.; Fig. 8) also being affected.

As a further outgrowth of this should the Jackpile age of 110-115 m.y. be verified relative to the Ambrosia Lake (Westwater Canyon Member ore) age then the ^{235}U - ^{207}Pb date of 94 m.y. for Jackpile coffinite (Nash and Kerr, 1966) may indicate more favorable possibilities for U-Pb dating throughout the entire Grants Mineral Belt.

K-Feldspar Detrital Grains

In order to examine some aspects of provenance for the Grants Mineral Belt we have examined the Rb-Sr systematics of six K-feldspar rich grains obtained by hand picking from outcrops and from underground workings. The results are shown in Figure 11. An isochron age of 1.33 ± 0.02 b.y. with initial $^{87}\text{Sr}/^{86}\text{Sr} = 0.7056 \pm 0.0007$ is obtained. This confirms the suspected Precambrian age of these grains but we cannot as yet trace them to any definite source. Work is underway to examine outcrops of similar appearing material from the core of the Zuni Mountains to the southwest of the Grants Mineral Belt. In way of a 'progress' comment we have preliminary data for some granitic phases of the Zuni core rocks of 1.4 b.y.

Clay Mineralogy

Introduction

The clay minerals of the Morrison Formation in the Grants Mineral Belt have been extensively studied by Keller (1962), Granger, (1962), Nash (1968), and Kendall (1971) among others. These studies have been generally limited to local aspects of clay mineralogy, and, although attempts have been made to establish clay mineral:uranium mineralization relationships in the region, no clear-cut mechanisms have been previously noted. Keller (1962) has pointed out earlier that apparently no specific clay minerals can be used as guides to uranium ore, although he does comment on the need for more work, especially on polytypism and trace element studies.

A broad regional assemblage of clay minerals is considered in this study which will be divided into three groups: outcrops, mine and core samples (ore grade), and bleached, barren core samples from reduced ground remote from the ore. Emphasis will be given to the clay minerals of the Westwater Canyon Member and the Jackpile Sandstone.

For comparative purposes, a semi-quantitative estimation has been made from the glycolated x-ray diffractograms. First-order peak intensities obtained from the x-ray patterns were corrected by absorption coefficients given by Carroll (1970). Although compositional variation is neglected, the estimation is considered to be sufficient for a statistical purpose. It was shown by Pierce and Siegel (1969) that, whatever method is used, internally consistent results can be obtained for comparative purposes if the same laboratory techniques and the same diffraction methods are used.

Analytical Procedures

Several varieties of sample suites were involved in this study. Most

of them are sandstones and mudstones from oxidized outcrops, underground and open-pit mine workings (ore-grade, and barren), and core samples. For comparative purposes, several volcanic rocks from the Jemez Mtn. were also included.

A general flow pattern is shown in the appendix. Many sandstone samples are very friable and great care was needed for subsequent study. Undisturbed whole-rock samples were used for the following purposes;

1. Standard thin-section petrography
2. Scanning electron microscopy by JEOL SEM JSM-2 equipped with x-ray energy spectrometer.
3. Electron microprobe x-ray photos with polished-section mount.
4. Whole-rock trace element analysis by neutron activation analysis.
5. Organic acid leaching experiments with tartaric and acetic acids.
6. Rb-Sr geochronology for the microcline pebbles separated from the sandstones.

For the mineralogical study of the silt and clay-sized fractions, a Norelco wide range x-ray diffractometer was extensively used. Sample treatment for the x-ray and mass spectrometric analyses are also given below.

Identification of Phyllosilicates

Routine schemes for x-ray identification of clay minerals were based on analyses of oriented samples for enhanced intensity. X-ray diffractograms were obtained from air-dried, glycolated, heated and acid-treated samples (refer to appendix). Random powders were x-rayed mainly for the differentiation of polytypes and identification of non-clay minerals. Basic criteria

for the identification are discussed below.

Kaolinite. Diffractograms of many untreated sandstone samples showed strong and sharp 001 and 002 reflections at $7-15^{\circ}\text{A}$ and 3.58°A . The intensity of higher order reflections, 003 and 004, was less than one-tenth of the 001 reflection. The peak positions were not shifted upon glycolation, and heating at 450°C caused some decrease in the peak intensity. Upon heating to 600°C all basal reflections disappeared, indicating complete structural decomposition. Warm acid treatment did not affect the kaolinite structure.

Differentiations of kaolinite in the presence of chloritic minerals were obtained by the 003 chlorite peak at about 4.7°A . Where the third order chlorite peak was absent or weak, as in iron-rich chlorite, acid treatment and slow scanning ($1/4^{\circ}$ 2 theta/min.) near the 3.5°A region were sufficient for identification.

The presence of dickite, although not found in this study, was checked by random powder diffraction. A peak near 3.74°A indicate kaolinite whereas 3.79°A corresponds to 022 reflection of dickite.

Montmorillonite. Montmorillonite was identified by its characteristic structural expansion upon saturation with organic liquid vapor. The strong 001 reflection at 14.9°A or at 12°A was readily expanded to 17°A ; higher order reflections were either weak or absent.

When heated to 450°C the first order spacing contracted to near 10°A by losing absorbed water layers. Upon potassium treatment, $d(001)$ decreased to 12°A , possibly due to the low layer charge of the montmorillonite. The contracted spacing of the K-treated sample was further expandable upon glycolation, suggesting a volcanic origin (Weaver, 1958). A broad peak at about 11.6°A after acid treatment suggests irregular interstratification of highly aluminous montmorillonite with only hydrogen ions remaining in the

interlayer sites after treatment with hydrochloric acid (MacEwan, 1961).

At room temperatures, montmorillonite having monovalent cations in exchangeable position has one water molecule with a basal spacing of about 12 \AA , whereas Mg or Ca in exchange sites have two water molecules, resulting in a d spacing of 15 \AA (Grim, 1968). Similarities between Mg-saturated and untreated patterns indicate that the exchangeable cations were mostly Mg in the samples analyzed.

Illite-Montmorillonite. Mixed-layer illite-montmorillonite was indicated in many samples showing a diffuse and broad peak near the $10-12 \text{ \AA}$ region. In some cases, a prominent reflection with an 11 \AA basal spacing appeared on the untreated diffractometer patterns. Glycolation shifted the peak to near 14 \AA , the exact spacing depending upon the relative amount of montmorillonite in the interstratification. Most of the interstratifications were of the random-type judging from the absence of higher order reflections and by the diffuse reflections. Some of the mixed-layer found in the reduced ground showed 1:1 type regular interstratification.

Both heating at 450°C and potassium treatment caused structural contraction to near 10 \AA . Ca- and Mg-treated samples showed broad and diffuse peaks in the 11 \AA region which indicate disorder in stacking sequences along the C-axes of the random interstratifications with a different magnitude of cation exchange capacity in each unit layer. The relative abundance of each component could not be determined because of the diffuse nature of the reflections and small amounts of the mixed-layers present.

Chlorite. Untreated slides showed reflections near 14 \AA , 7 \AA , 4.7 \AA and 3.5 \AA which could be attributed to either chlorite, vermiculite or interstratification between them. Glycolation usually revealed unexpandable 001 and 003 chlorite reflections at 14 \AA and 4.7 \AA . When heated to 450°C , the

001 and 002 intensities decreased, but at 600°C the 14°\AA intensity was sharply increased with the higher orders destroyed.

Both iron-rich and magnesian chlorites are observed. Iron-rich chlorites gave weak 001 and 003 basal reflections but strong 2nd and 4th order reflections. In many cases first order reflection at 14°\AA decreased to 13.5°\AA upon initial heating at 450°C , but no higher orders were observed. This probably indicates a presence of minor expandable layers in these samples.

Mixed-layer Chlorite. Some of the montmorillonite-rich samples showed a broad reflection near 29°\AA with somewhat enhanced 002, 004, 001, and 006 reflections. Odd-numbered higher order reflections are very weak or absent. Upon glycolation and heating, a slight expansion and contraction were observed. This may indicate some regular alternation between predominate chlorite and minor amounts of montmorillonite layers in the clay mineral. The relative proportion of the end members could not be determined satisfactorily due partly to poor reflections and to the presence of discrete montmorillonite in most of these samples.

Identification of Polytypes

One-dimensional polytypism in layer silicates occurs because the atomic arrangement in the subcell has monoclinic or triclinic symmetry, whereas symmetry of the surface of the subcell is hexagonal or pseudohexagonal formed by basal oxygens in the tetrahedral sheet (Smith and Yoder, 1956).

Brown and Bailey (1962) have shown that four structural polytypes of chlorite occur depending on different arrangements of the brucite sheet relative to the initial 2:1 layer. Hayes (1970) further indicated that the chlorite polytypes represent equilibrium conditions in the environment of their formation. More than 80 percent of the chlorites are the IIb polytype in which the structure is a monoclinic unit cell. This species is the most

stable and can be formed in normal metamorphism and as detrital components in sedimentary rocks. The IIb polytypes can be identified by the 2.59°A (20 $\overline{2}$) and the 2.54°A (201) peaks. Authigenic chlorites in the low-temperature environment are the monoclinic Ib or the orthohexagonal Ib polytypes. The Ib polytype can be found in marine sediments formed by halmyrolysis or in continental deposits due to alteration of ferromagnesian minerals. The conversion of Ib to the IIb polytype occurs through low-grade metamorphism or by deep burial. Characteristic x-ray peaks are 2.61°A (20 $\overline{2}$) and 2.33°A (203) for the monoclinic Ib and 2.50°A (202) for the orthohexagonal Ib. Two other polytypes, Ia and IIa, based on a monoclinic and an orthohexagonal unit cell, respectively, are very rare and limited to certain hydrothermal deposits.

Smith and Yoder (1956) configurated six possible polymorphs of mica on the basis of different ways of stacking two adjacent layers. Only the 1Md, 1M, 2M₁, 2M₂ and 3T polytypes are observed in nature. Earlier, Yoder and Eugster (1955) synthesized one-layer, monoclinic disordered (1Md), one-layer monoclinic (1M), and two-layer monoclinic (2M) muscovite polytypes from the $\text{K}_2\text{O}-\text{Al}_2\text{O}_3-\text{SiO}_2-\text{H}_2\text{O}$ system and found the conversion of 1Md \rightarrow 1M \rightarrow 2M during progressive increase of temperature. They believed that 1Md and 1M polymorphs are metastable or stable only at low temperatures (below 250°C) and transformation to 2M polymorph occurs at higher temperature. This mechanism has drawn much interests among sedimentary petrologists and mineralogists in determining the polymorphic forms of micaceous minerals as a basis for the differentiation of low-temperature, diagenetic and high-temperature, detrital minerals (Weaver, 1958; Velde and Hower, 1963; Hower and Mowatt, 1966). However, the temperature range in which the polytypes are metastable or stable, are so wide that their use as a geothermometer

is questionable.

Nevertheless, this concept can be used for the genetic differentiation of illitic clay minerals found in sedimentary rocks. Although many overlaps in peak positions commonly occur among the polymorphs, characteristic 2M peaks with no other interfering reflections occur at 4.29°A (111), 3.89°A (113), 3.74°A (023) and 3.50°A (114); 1M has 3.66°A (112) and 3.07°A (112 ?); and all 1Md peaks interfere with other reflections.

Distribution of Clay Minerals

Outcrops. The oxidized and barren outcrop samples appear to have a rather uniform clay mineral distribution. In all outcrop sections studied, the sandstones and siltstones of the Recapture Member are characterized by abundant montmorillonite followed by subordinate kaolinite, minor amounts of illite and illite-montmorillonite. Likewise in the Brushy Basin Member, montmorillonite is frequently the only clay mineral present with occasionally abundant kaolinite. A carbonaceous shale bed, persistent throughout the region at the Dakota-Morrison unconformity, contains only kaolinite which may be taken to indicate an acidic, swampy environment as postulated by Granger (1968).

Montmorillonite and kaolinite are the predominant species in the Westwater Canyon Member. At a section near Laguna, Na-montmorillonite is found in the middle part of the Westwater Canyon Member and is distinguishable from Mg-montmorillonite found in all other sections. In all sections studied the Westwater Canyon Member contains minor amount of chloritic clay minerals in the middle part. The Laguna section, however, contains expandable mixed-layer chlorite-montmorillonite. The distribution of minor illitic minerals is very erratic and appears to have no persistent pattern.

Much of the montmorillonite in the entire Morrison is believed to be authigenic formed by devitrification and hydrolysis of volcanic ashes (See Plate IV). Some may be detrital, but the well-crystalline nature of the mineral suggests no extensive multicycle deposition. Potassium treated montmorillonite contracts to 11 \AA but fully expands to near 17 \AA indicative of volcanic origin (Weaver, 1958). The analytical data of a typical Brushy Basin montmorillonite is shown in Table 3. The high potassium content suggests some development of mixed-layers in the structure and Mn and V contents are variable.

It is also noted that ferric iron occurs in the octahedral position and may be responsible for the prevalent green colors in the Brushy Basin Member.

Kaolinite in the Westwater Canyon Member typically occurs as "nests" that fill pore spaces and enclose several sand grains. The nest itself shows no oxidation coatings and its size appears to be proportional to grain size and permeability. The "nest-type" kaolinite is less abundant in the Jackpile Sandstone; here kaolinite is interstitial throughout the sand grains and gives typical white color to the host-rock in many localities. In both units potassium feldspar grains within the nests are generally fresh, and no sign of kaolinitization is evident.

The chloritic material in the outcrops is difficult to assess due to its very small amount and intense oxidation of the samples. Keller (1962) also reported sparse occurrence of the chlorite in many locations in the Colorado Plateau but presumed no relation to the ore deposits.

TABLE 3

Analytical Data of a Green Montmorillonite
 from the Brushy Basin Member
 (DLQ Jmb-4, $< 2\mu$)

SiO ₂	57.03 %
Al ₂ O ₃	19.39
FeO	0.31
Fe ₂ O ₃	5.84
MgO	3.03
CaO	0.40
Na ₂ O	0.14
K ₂ O	3.27
TiO ₂	0.62
MnO	0.012
S	< 0.01
SrO	0.012
V ₂ O ₄	0.022
H ₂ O ⁻	3.74
H ₂ O ⁺ + CO ₂	6.70
P ₂ O ₅	0.115
TOTAL	100.63 %

Structural Formula:

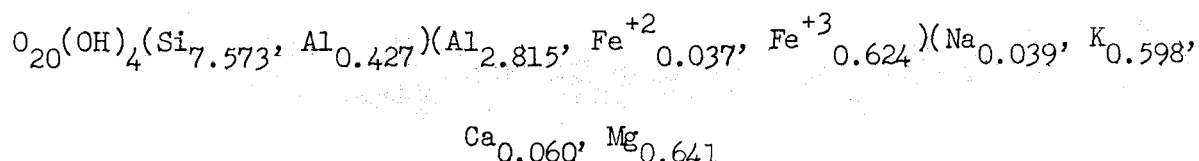


TABLE 4
Clay Mineral Distribution in Thoreau Section, NM
(Sec. 8, T14N, R12W)

Member	K	Ch	M	Ch-M	I	I-M	Remarks
Brushy Basin							
1	42	-	58	-	-	-	Carbonaceous shale, Dakota sandstone
2	5	-	85	-	5	5	Green mudstone
3	6	-	51	-	tr	43	Limonitic mudstone
Westwater Canyon							
1	61	-	12	27	-	-	Hematitic sandstone
2	5	-	26	-	tr	73	Green mudstone (Na-montmorillonite)
3	45	28	tr	tr	7	20	Hematitic sandstone + green mudstone pellets
4	56	35	9	-	-	tr	Hematitic sandstone
5	50	36	tr	-	-	14	Hematitic, silty mudstone
6	tr	13	87	-	-	-	Unoxidized calcitic sandstone
Recapture							
1	19	-	62	-	tr	19	Gray, silty mudstone
2	24	19	43	-	5	9	Green mudstone
3	35	-	65	-	-	-	Dark brown siltstone

Notes: K = kaolin, Ch = chlorite, M = montmorillonite, I = illite, I-M = illite-montmorillonite, Ch-M = chlorite-montmorillonite.

TABLE 5

Clay Mineral Distribution in Dos Lomas Section, NM
(Sec. 19, T13N, R9W)

Member (Unit)	K	Ch	M	Ch-M	I	I-M	Remarks
Brushy Basin							
1	94	-	6	-	-	tr	Carbonaceous shale, Dakota sandstone
2	5	-	95	-	tr	tr	Green silty mudstone
3	18	-	82	-	-	tr	Limonitic sandstone
4	-	-	95	-	-	5	Limonitic sandstone, mudstone
Poison Canyon Sandstone							
1	62	-	32	-	-	6	Hematitic sandstone
2	-	-	65	-	-	35	Gray sandstone
Westwater Canyon							
1	5	5	50	-	-	40	Limonitic sandstone with mudstone pellets
2	69	-	10	-	-	21	Hematitic sandstone
3	-	7	26	-	5	62	Green mudstone
4	8	10	23	-	5	54	Limonitic sandstone
Recapture							
1	-	-	95	-	5	-	Dark brown silty mudstone
2	5	-	70	-	5	20	Dark green silty mudstone

Notes: K = kaolin, Ch = chlorite, M = montmorillonite, I = illite, I-M = illite-montmorillonite, Ch-M = chlorite-montmorillonite.

TABLE 6
Clay Mineral Distribution in Laguna and Mesita Sections, NM

Member (Unit)	K	Ch	M	Ch-M	I	I-M	Remarks
Jackpile Sandstone							
1	95	-	5	-	tr	tr	Carbonaceous shale, Dakota sandstone
2	85	5	10	-	-	tr	Dark gray sandstone
3	5	-	5	-	26	64	Limonitic sandstone
4	32	-	13	55	tr	tr	Gray sandstone
5	24	5	-	tr	20	51	Gray sandstone
6	67	tr	-	-	33	tr	White coarse sandstone
Brushy Basin							
1	-	-	>95	-	-	-	Green silty mudstone
2	-	-	90	-	tr	10	Green silty mudstone
Westwater Canyon							
1	-	-	>95	-	tr	-	Limonitic sandstone and mudstone (Na-mont.)
2	67	-	24	9	tr	-	Limonitic sandstone and mudstone (Na-mont.)
3	50	-	40	10	-	-	Hematitic sandstone (Na-montmorillonite)
4	5	-	72	23	-	-	Limonitic sandstone
5	17	26	57	tr	-	-	Limonitic sandstone
6	5	12	83	-	tr	-	Lt. green sandstone

Notes: K = kaolin, Ch = chlorite, M = montmorillonite, I = illite, I-M = illite-montmorillonite, Ch-M = chlorite-montmorillonite.

Ore Zones. One of the distinctive features of ore-zone alteration is the enrichment of chloritic minerals relative to montmorillonite. This feature was first reported in the Ambrosia Lake District by Granger (1962) who showed that chlorite enrichment is proportional to the magnesium, organic carbon and uranium contents. This trend has been confirmed by us in all primary ore suites studied in the Grants Mineral Belt (See Plate III). Chlorite is also found in the redistributed deposits, although the distribution is less conspicuous than in primary deposits.

Chlorite occurs as well-developed films on clasts (See Plate III) and intimately mixed with the OCM. In high-grade ore the chlorite is difficult to detect visually due to humic material, but in places where the ore material was leached away, it gives characteristic blue to greenish stains to the host sandstone. This type of chloritic structure often has sharp boundaries with the surrounding barren sandstone. In thin section, a few types of chlorite can be observed; patches of green coatings, and as fibrous, weakly pleochroic films. Both types are found in and near the ore zone and no differentiation can be made with regard to their specific occurrence.

Chemical analysis and microprobe study reveal that the chlorite is highly vanadiferous (See Table 7 and Plate V). In the vanadium-bearing sandstones of the Northern Colorado Plateau Foster (1959) has shown that the principal vanadium mineral is the mica-type roscoelite and that tetravalent vanadium is present in the octahedral sites. It was shown that the vanadium from mineralizing solutions replaced some of the octahedral aluminum with necessary charge adjustments occurring in the tetrahedral layer. Apparently roscoelite is only a minor phase in the Grants Mineral Belt where the U:V ratio is relatively high. Chlorite instead is the chief vanadium-bearing clay mineral. The V_2O_4 content ranges from 1.5 to 3.3% and the iron content is high as shown by weak

001 and 003 intensities. Much of the iron is in the ferrous state and comparable to ferric iron found in the Brushy Basin montmorillonite.

In addition to chlorite, variable amounts of kaolinite, montmorillonite and illitic clay minerals are present in the ore zone. Kaolinite, commonly in nests, is apparently unrelated to mineralization and is believed to have been formed later. The kaolinite is not coated either with OCM or hematite. Illitic clay minerals, although sparse, occur in and near the ore zones but are only minor constituents and bear no apparent significance to the uranium deposits.

TABLE 7
Analytical Data of the Ore Zone Chlorite, Westwater Canyon Member

	Analysis 1	Analysis 2
SiO ₂	40.68 %	48.55 %
Al ₂ O ₃	18.52	19.44
FeO	7.69	4.64
Fe ₂ O ₃	0.15	3.72
MgO	4.30	3.57
CaO	1.22	1.24
Na ₂ O	0.32	0.54
K ₂ O	1.31	2.61
TiO ₂	0.28	1.10
MnO	0.095	0.131
S	0.21	0.01
SrO	0.025	0.029
V ₂ O ₄	3.30	2.33
H ₂ O ⁻	4.70	3.77
H ₂ O ⁺ + CO ₂	14.36	8.13
P ₂ O ₅	0.092	0.15
<hr/> TOTAL	97.25 %	99.96 %

Note: Samples contained minor kaolinite and montmorillonite.

Remote bleached sandstone. Clay mineral analyses were also carried out for bleached or unoxidized Westwater sandstones from eight core holes farther north in the Ambrosia Lake District. Here the Westwater Canyon Member is mostly light gray and no mineralization has been reported. The nearest known mineralization is about 10 miles south. Some of the samples contained abundant titanomagnetite and thin layers of organic carbonaceous matter.

Two features are distinctive compared to the clay mineral assemblage in the outcrops; the presence of well-crystalline chlorite and regularly interstratified illite-montmorillonite. The chlorite is persistent in all sandstone samples studied whereas the mixed-layer illite-montmorillonite is somewhat sporadically distributed. In thin section, the chlorites often form worm-like patches on volcanic fragments, on interstitial montmorillonite or as thin, light green films around clastic grains. Petrographic study suggests that the chlorite was formed from both direct precipitation and solid state transformation of preexisting montmorillonite. The illite-montmorillonite commonly forms moderately birefringent coatings. The mixed-layer clays found in this area are commonly of the 1:1 type with regular interstratification and the textural relation suggest that it is later than montmorillonite but earlier than most chlorite.

The montmorillonite and kaolinite are again widespread and show non-diagnostic features. A few thin-sections showed possible montmorillonite-to-kaolinite and chlorite-to-kaolinite transitions. In many samples, kaolinite is being replaced by calcite cement.

Polytypism of Clay Minerals

Secondary, post-depositional chlorite is a common component in many sands (Weaver and Beck, 1971) and soils (Ball, 1966) where it commonly

forms from the alteration of volcanic material or montmorillonite. Brown and Bailey (1962) examined 300 chlorites from different localities and found that approximately 80% possess IIb structure, but they also found orthorhombic Ib and monoclinic Ib and Ia structural polytypes. The IIb chlorite is the stable polytype encountered in usual chlorite-grade metamorphism and in medium and high-temperature ore deposits. Brown and Bailey (1962) further found that the Ib polytypes were the ones most likely of diagenetic origin. Hayes (1970) also concluded that type-I chlorite in sedimentary rocks most likely represents authigenic chlorite and the IIb polytype generally indicates that the chlorite is detrital and reflects formation by igneous or metamorphic processes.

Random powder x-ray diffraction of about a dozen chlorite-rich samples reveal that the Ib structure is the only polytype in the Westwater Canyon Sandstones in both the ore zone and the remote barren and bleached zone. Thus it appears that the chloritic assemblage under study was formed after the host sandstones by a low-temperature process.

Theories concerning the illite polytypes have been well documented (Yoder and Eugster, 1955; Velde, 1965; Maxwell and Hower, 1967). It has been shown that the 2M polytype is stable at temperatures of 125°C or higher. The sequence of polytype transformation is $1\text{Md} \rightarrow 1\text{M} \rightarrow 2\text{M}$ with an increase of either time, temperature, or pressure. The present study indicates that illite is not a common mineral in the Morrison Formation, although some mixed-layered illites are present in the Jackpile and Westwater Canyon Sandstones. The mixed-layer varieties as well as a trace of illite in the ore zone, commonly possess 1Md structure. The sporadic occurrences of these minerals, however, probably exclude any possible correlation to uranium mineralization.

Keller (1962) reported occurrence of dickite in the Jackpile Sandstone which is better crystallized than kaolinite. Dickite is believed to be a common authigenic mineral in many sandstones where it has formed by alteration of detrital minerals and redistribution of their silica and alumina (See Bayliss and others, 1965; for example). Nash (1968) and our own observations, however, indicate that kaolinite instead of dickite occurs in the Jackpile Sandstone as well as in other sandstone units of the Morrison Formation.

Activity Relations

The stability relations of the clay minerals are best explained by the ion activity diagrams assuming that the minerals were formed in equilibrium with the surrounding water at a fixed temperature and pressure. The relative sequences and slopes of the boundaries are drawn using the logarithms of the ion activity ratios as variables. In actual systems, if the mineralogy of a given sediment is known, the measurement of the ionic activities in the pure solutions can be used to test for chemical equilibrium. The method has been utilized by Garrels and Christ (1965), Hess (1966) and Helgeson and others (1969) for many geologic systems.

In actual construction of the diagrams reliable ΔG_f° values of the component minerals are an absolute necessity. Recently Tardy and Garrels (1974) have demonstrated that the Gibbs free energy of formation of layer silicates can be determined by their oxide and hydroxide components. Following their method, calculated ΔG_f° values are given in Table 8.

Balancing of an equation is done further by assuming that aluminum species are not important variables in naturally occurring reactions. This assumption may not be valid since some dissolved alumina could have played an important role in the presence of organic acid for the formation of either

TABLE 8

Mineral or Species	Formula	ΔG_f° in kcal/mole
Kaolinite	$\text{Al}_2\text{Si}_2\text{O}_5(\text{OH})_4$	- 910
K-spr	KAlSi_3O_8	- 896.3
Gibbsite	$\text{Al}(\text{OH})_3$	- 277.0
Illite	$\text{K}_{0.6}\text{Mg}_{0.25}\text{Al}_{2.3}\text{Si}_{3.5}\text{O}_{10}(\text{OH})_2$	-1307.5
K-montmorillonite	$\text{K}_{0.33}\text{Al}_{2.33}\text{Si}_{3.67}\text{O}_{10}(\text{OH})_2$	-1286.6
Montmorillonite	$\text{Mg}_{0.54}\text{Al}_{1.93}\text{Si}_{3.78}\text{O}_{10}(\text{OH})_2$	-1291.0
Mg-chlorite	$\text{Mg}_5\text{Al}_2\text{Si}_3\text{O}_{10}(\text{OH})_8$	-1960
Al-chlorite	$\text{Mg}_{2.3}\text{Al}_{3.4}\text{Si}_{3.3}\text{O}_{10}(\text{OH})_8$	-1893.5
K^+		- 67.7
Mg^{2+}		- 108.9
OH^-		- 37.6

kaolinite or Al-chlorite. However a general picture appears in the system Mg-Al-Si-O-H. Fig. 12 shows that montmorillonite can be transformed to chlorite in a dissolved-silica-rich environment by changing either the pH or the activity of Mg (or Al). It also shows that kaolinite can be formed from both chlorite and montmorillonite in an acidic, silica-leaching environment. At a fixed activity of Mg^{2+} , chlorite is stable in the alkaline condition when compared to montmorillonite and kaolinite.

Shown in Fig. 13 and 14 are the activity diagrams of the system Mg-K-Al-Si-C-H. The first diagram was drawn at 25°C with amorphous silica saturation, i.e., $a_{\text{H}_4\text{SiO}_4} = 10^{-3.08}$. It is seen that chlorite appears only as a metastable phase and does not represent an equilibrium assemblage. This difficulty can be resolved by increasing the temperature of the system as shown in Fig. 14. Since the layer silicates have similar structures the ΔG_R° at an elevated temperature will not vary greatly from that at 25°C . However,

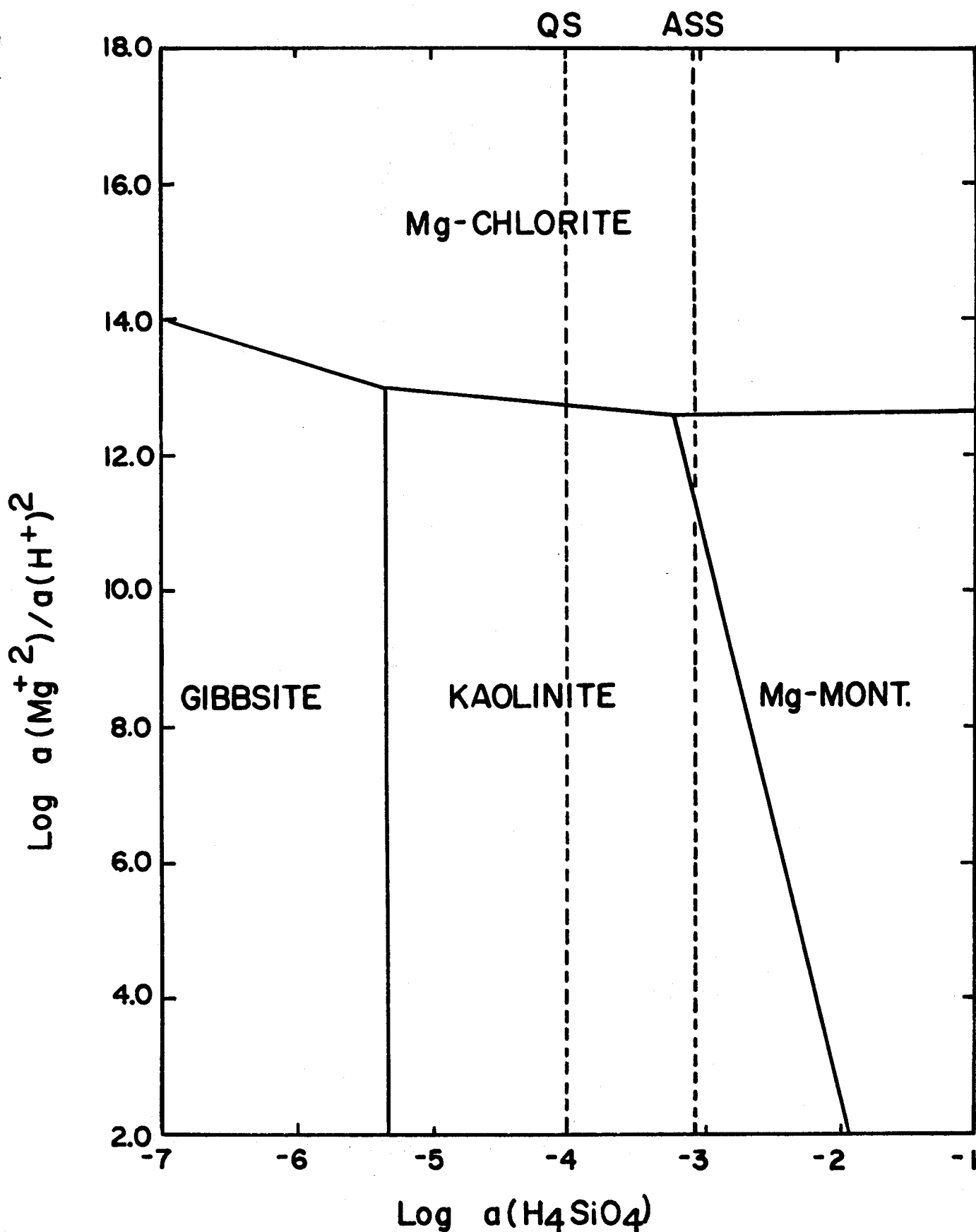
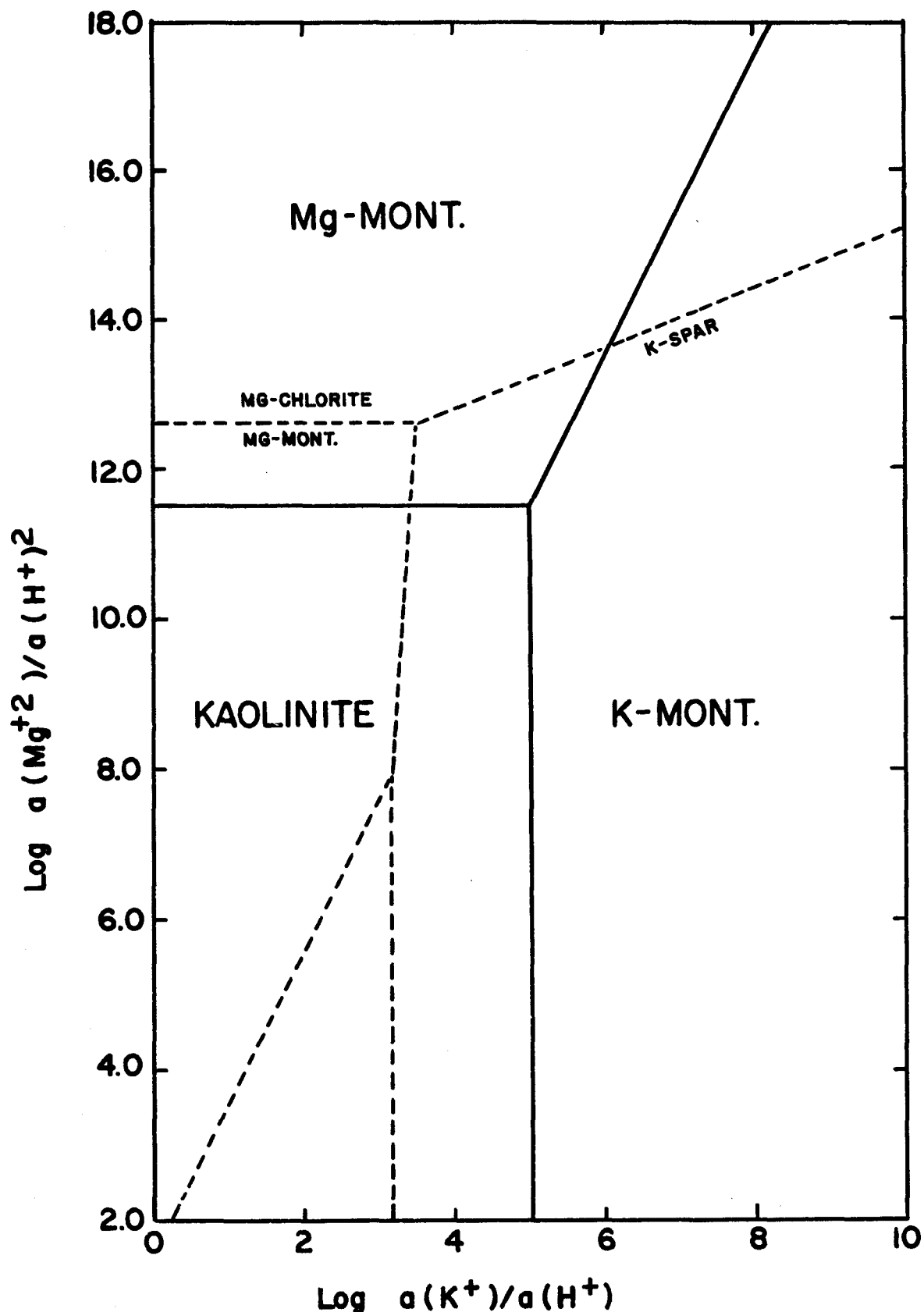


FIGURE 12. System Mg-Al-Si-O-H (25°C ; 1 atm.). QS=quartz saturation;
ASS = amorphous silica saturation.



$$25^{\circ} C \quad a(H_4SiO_4) = 10^{-3.08}$$

FIGURE 13. System Mg-K-Al-Si-O-H (1 atm.). Mg-Mont. = Mg-montmorillonite; K-Mont. = K-montmorillonite.

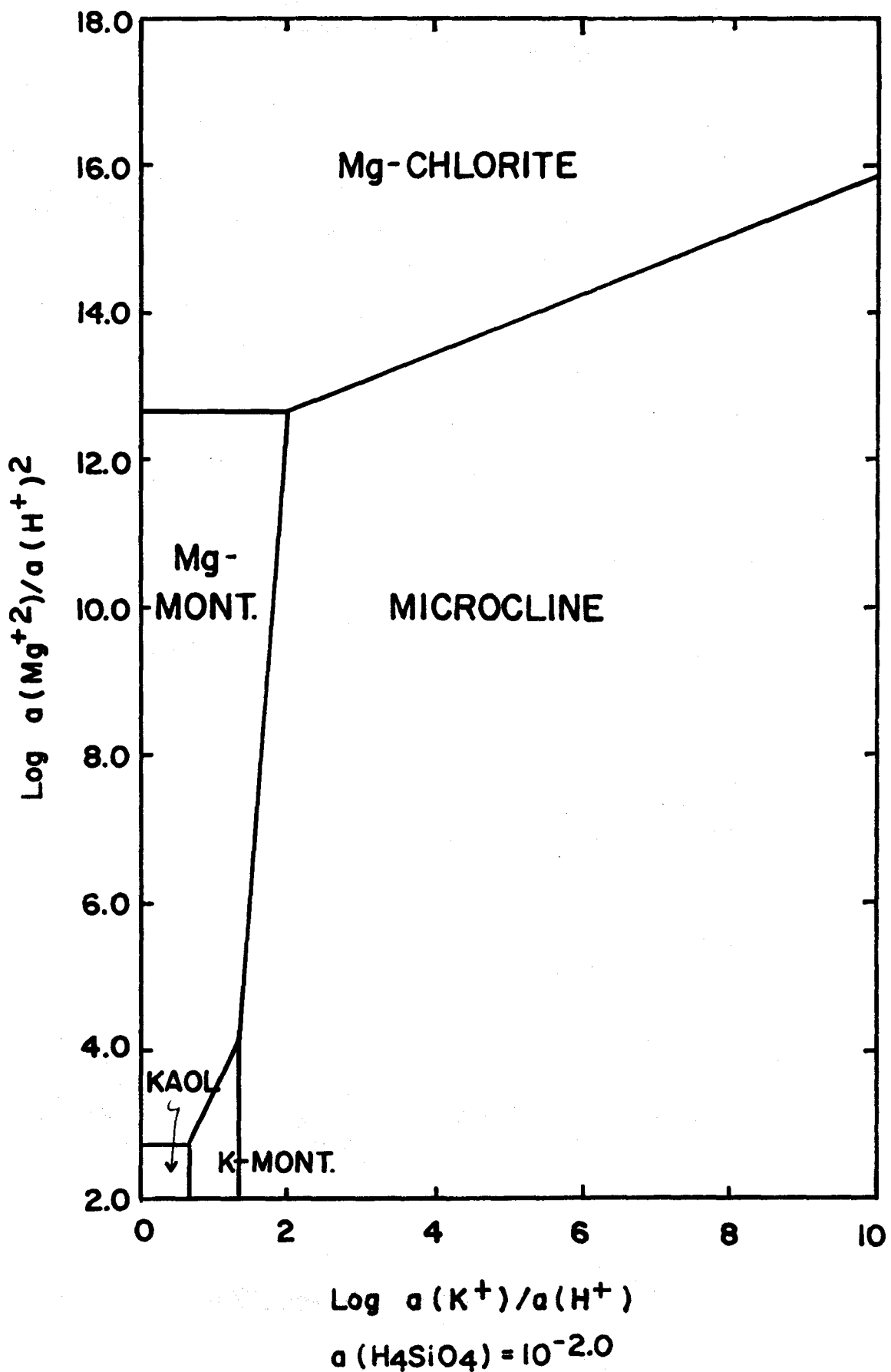


FIGURE 14. System Mg-K-Al-Si-O-H (1 atm.). Mont. = Montmorillonite; Kaol. = Kaolinite

by increasing the temperature, the activity of dissolved silica would increase and chlorite will become a stable phase. Thus at about 120°C the resulting diagram would be similar to Fig. 14.

We believe that this concept could be used as an indirect method for low-temperature geothermometry. For example, at a natural concentration of K^+ near neutral anaerobic water which corresponds to approximately 10^{-3} to 10^{-4} molal, the stability field of K-feldspar would be encountered. In the Morrison sandstones, however, authigenic microcline is only a minor phase; when reasonable activities are plotted, such as from Phoenix (1959), neither montmorillonite nor chlorite appears as a stable phase. This may imply that the ore-bearing solution, if such did exist, was never more than near 100°C. It is also interesting to note that the major uranium-bearing dissolved species, UDC, is unstable near 110°C.

Scanning Electron Microscopy

In a heterogeneous clay mineral assemblage, the sequence of mineral paragenesis cannot be identified satisfactorily by conventional petrographic or x-ray means. Recent development of the electron microscope, equipped with solid state detectors, has allowed study of the morphology of clay minerals and their compositions.

Several Westwater Canyon Member sandstone samples were analyzed; the electron photomicrographs were taken through the courtesy of the Cities Service Oil Company.

In general, well crystallized nest-type kaolinite in the Westwater Canyon Member forms well-developed pseudohexagonal booklets. These range in size from 5 to 20 microns. Poorly crystallized, reworked kaolinite

shows irregular hexagonal outlines and occurs as smaller and thinner particles.

Montmorillonite typically shows well-developed cellular or honeycomb patterns. Individual cells are smaller than the kaolinite booklets. Much of the well-crystalline montmorillonite coatings on sandstones possess interlocking textures suggesting that a high proportion of the mineral was formed in situ. Mixed-layer illite-montmorillonite coatings are sheet-like in character.

Typical authigenic chlorite is shown on Plate III. The chlorite usually developed rosette-like aggregates ranging from 2 to 5 microns in size. Individual rosettes are formed as pseudohexagonal booklets. Plate III shows clearly that the chlorite has been formed at the expense of preexisting montmorillonite. Size-wise, the authigenic chlorite is much smaller than ordinary detrital chlorites.

Organic-clay Mineral Reactions

Much has been written about clay mineral-organic reactions and an excellent summary can be found in Theng (1972). Of particular interest is the effect of various organic acids on the dissolution of clay minerals documented by the work of Huang and Keller (1971, 1972a and b). They have shown that in the presence of dilute aspartic, citric, salicylic, tartaric and tannic acids; common clay minerals yield much higher solubilities than in water. These acids may be considered as representative components of naturally occurring humic acid (Hem, 1960) and the experimental results bear some significance for the Morrison clay minerals. The results show that in the presence of organic acids clay minerals dissolve incongruently releasing significant quantities of Al, Fe and Si from their structures.

The dissolution effect is much greater for illite and montmorillonite than other clay minerals. Another point of interest is that the Al and Fe so released can be complexed by the organic acids.

Such organic-complexed Al and Fe appears to have been responsible for the clay mineral transformations in the Morrison sediments. In montmorillonites and vermiculites hydroxides and hydroxy species are precipitated in the interlayer positions to form a chlorite-like mineral (Jackson, 1963; Rich, 1968). Al(OH)_3 and Fe(OH)_3 tend to be precipitated in an acid to mildly alkaline environments and Mg(OH)_2 in a basic environment. Likewise, both Millot (1970) and Linares and Huertas (1971) recognized that kaolinite can be formed from a solution where hexacoordinated aluminum is in the form of an organic complex. Therefore, although Al is believed to be inactive in the common inorganic environment, in the presence of natural humic acid, it seems to have an important role in the alteration of clay minerals.

Discussion

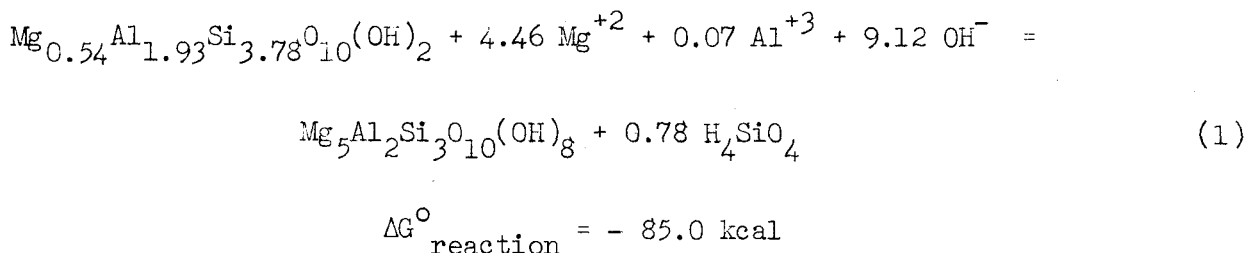
The overall clay mineral paragenesis in the Morrison Formation can now be discussed based on several lines of evidences. Major inferences are made from the mineral assemblages in the Westwater Canyon Member Sandstones. Similar interpretations can be made for the Jackpile Sandstone although much of the original clay minerals in this unit may represent reworked upper Morrison Formation sediments.

As Keller (1962) indicated, the concept of a terrigenous and fluvial origin for the Morrison Formation is sustained by the clay mineralogy. Many of the upper Morrison Formation sediments in the Grants Mineral Belt are believed to be first-cycle (Green, 1975) and during periods of prolific volcanic activity the amount of ash far exceeded the detrital clay minerals.

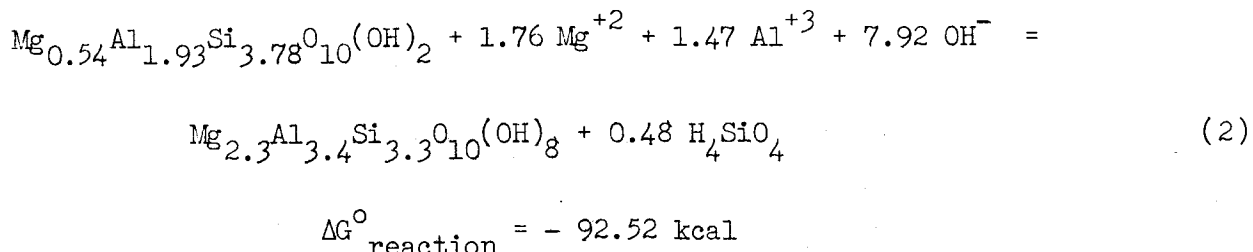
This can be evidenced by generally sparse illite in the Morrison Formation. The hydrolysis of volcanic ash instead developed an abundant montmorillonitic assemblage shortly after the deposition. Thus during the early diagenesis, the activity of dissolved silica was probably high as indicated by the activity diagrams. Some illite-montmorillonite could have been formed at this stage.

Coagulation of humic acid in the sediment, regardless of its source, caused local dissolution of previously-formed montmorillonite releasing much Al, Mg, Fe and to a lesser degree Si. Since other detrital silicates were also affected by the humic acid; the water present must have been enriched in dissolved silica. Much of the silica was probably consumed later in the formation of coffinite or precipitated in the form of quartz overgrowths outside the ore body.

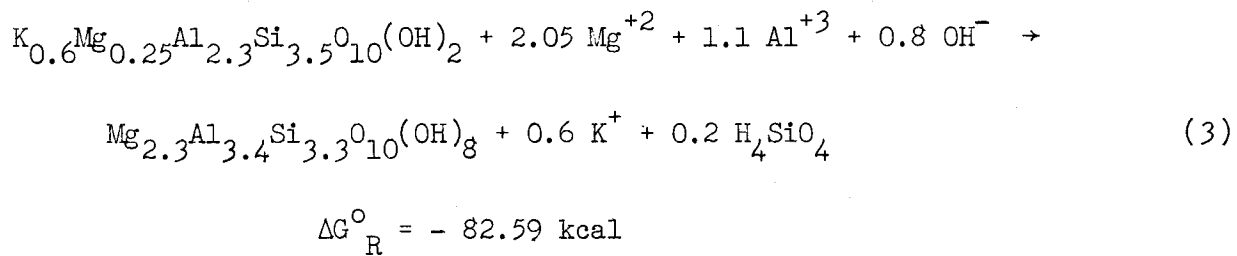
The close spatial relationship of chlorite with the humate-rich ore body suggest that the former mineral was developed at the time of encroachment of humic acid. This is further evident since chlorite is also enriched in the barren and bleached reduced sandstones in the northern Ambrosia Lake district. The following reactions are considered to be important for the formation of chlorite from montmorillonite; first if we consider end-member Mg-chlorite:



and, when a dioctahedral chlorite is involved,



Despite the uncertainties introduced by the lack of exact knowledge of the formulas for the clay minerals, the large negative ΔG°_R values in the above reactions indicate that chlorite should form from montmorillonite. Further any detrital illite in the sediment may have been converted to chlorite by the following reaction:



If we now substitute reasonable activities to the above reactions, some approximation can be made about the pH conditions which may have existed at the time of mineral alterations. The following activities were assumed based on several analyses of anaerobic pore waters of modern and ancient sediments. One such analysis for the Morrison Formation can be found in Phoenix (1959).

$$\begin{aligned}
 \{ \text{H}_4 \text{SiO}_4 \} &= 10^{-4}; \text{quartz saturation} \\
 \{ \text{Al}^{+3} \}, \{ \text{K}^+ \}, \text{ and } \{ \text{Mg}^{+2} \} &= 10^{-3}
 \end{aligned}$$

Substituting these values to the reactions (1) to (3), the pH obtained are as follows:

$$\text{pH} = 8.3 \text{ (1)}, \text{pH} = 6.4 \text{ (2)} \text{ and } \text{pH} = 6.1 \text{ (3)}$$

Assuming quartz saturation, these reactions can be easily related to the activity diagram shown in Fig. 15.

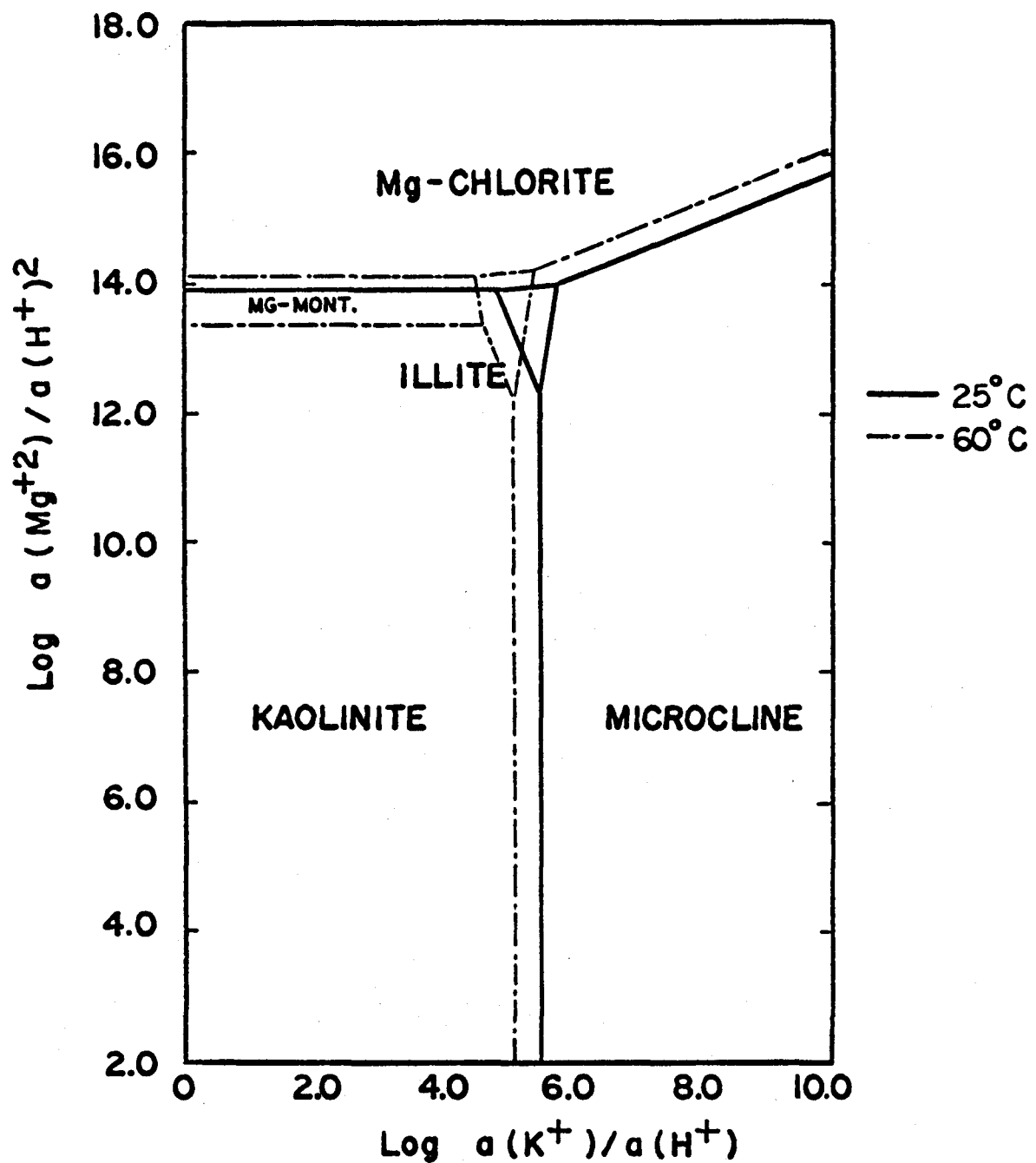


FIGURE 15. System Mg-K-Al-Si-O-H (1 atm.) for quartz saturation. Mont. = Montmorillonite.

Since the chlorite found in the Morrison Formation is not believed to be pure end-member Mg-chlorite, the pH estimation from the reaction (1) is probably too high and unreliable. However, intermediate dioctahedral chlorite in reactions (2) and (3) result in close agreement and the approximate pH values for the chlorite formation may be within the true range. The slightly acidic conditions postulated here (i.e., pH near 6) could also be applicable to the uranium mineralization. The pH estimation may not be valid if one considers the uncertain activities of the major dissolved species. However, changing the activities by an order of a magnitude or so does not affect pH estimation to a great extent. For example, in reaction (2), increasing the activity of silica from 10^{-4} to 10^{-3} , the pH change is only 0.1. Likewise, increase of Al-activity from 10^{-3} to 10^{-2} causes a pH shift of only 0.4. Geologic observations such as humate coagulation and the calcite halo around ore body, also suggest that, at the initial stage of uranium mineralization, conditions could have been slightly acidic (see Brookins, 1973).

Most kaolinite is formed by acidic leaching of alkaline rocks, primarily the feldspars and micas; however, any silicate rock or mineral will alter to kaolinite if leaching conditions are suitable for a sufficient geologic time. Two types of kaolinite can be recognized in the Morrison Formation; residual kaolinite; such as in Jackpile Sandstone that was formed by weathering and remained in place; and the diagenetic variety that was formed from resilication of aluminum-rich materials such as the nest-type kaolinite commonly found in the Westwater Canyon Member sandstone.

The intense kaolinization in the Jackpile Sandstone has been discussed by Leopold (1943) and by Moench and Schlee (1967). It has been postulated that the kaolinite is a weathering product formed under moist conditions

that occurred prior to deposition of the Cretaceous Dakota Sandstone. Granger (1963) further considered that the kaolinization reflects downward percolation of corrosive solutions as the overlying Dakota swamp was being deposited. However, much of the feldspar in the Jackpile Sandstone is generally fresh even where it is overlain by Dakota black shale. When altered, plagioclase grains commonly show sericitization rather than kaolinization. Thus, though it appears that the kaolinite in this case was formed during weathering and reworking prior to Dakota deposition, much of it probably came from alteration of montmorillonite that was originally abundant in the host sediment. The possibility of this alteration has been indicated earlier by Nash (1968) in his study of uranium deposits in the Jackpile and Paguate Mines. The transformation has also been shown by Sand and Bauer (1959), and by Altschuler and others (1963) in other similar geologic environments. Once formed, the kaolinite is the least affected among other clay minerals by subsequent attack from organic acid solutions (Huang and Keller, 1971).

Compared to the disseminated matrix kaolinite, the "nest-type" kaolinite is definitely secondary and appears to represent a post-ore process since it occurs widely both in mineralized and barren sandstones. The mode of field occurrence alone indicates that it was precipitated from solution, possibly in a colloidal state. The formation of kaolinite certainly requires acid solutions depleted in silica and a low cation/ H^+ ratio. However, prior to its formation, Al and Si must have been dissolved from some source and moved in solution in the zone of precipitation. Because of its relative immobility and amphoteric nature, Al has been considered as non-reactive and it is not well understood what geochemical mechanisms are responsible for the dissolution, transport and deposition of aluminous-

minerals in inorganic environments. However, when an organic acid solution is involved, such as the components of humic and fulvic acids, Al is easily dissolved and forms an Al-organic complex. The complex is stable until either the organic-ligand is destroyed by oxidation, or a strongly precipitating anion, such as $(OH)^-$, $(PO_4)^{3-}$ or $(SiO_4)^{4-}$, is encountered (Eberl, 1970; Linares and Huertas, 1971; Huang and Keller, 1972). The Al-minerals bauxites, latertic phosphates and flint clays, formed by this process typically show sponge-like, pisolithic and oolitic structures being precipitated as gel. A similar mechanism could have been operative for the formation of nest-type kaolinite in the Westwater Canyon Member Sandstone. After the emplacement of the primary ore bodies under reducing conditions, excess aluminous-humic acid complexes and dissolved silica must have been left. Acidic conditions were probably provided by the oxidation of ore-stage pyrite. Thus it is presumed that minor overlap is possible in the ages of formation of nest-type kaolinite and the primary ore as Kendall (1971) has indicated. The bulk of the kaolinite however, is believed to be post-primary ore. It is also suggested that oxidation and kaolinization were actually coincident with the formation of much of the redistributed ore. In the Section 23 Mine, for example, where redistribution is apparent, the kaolinite nests are much less abundant in ore than in the surrounding hematitic sandstone.

Preliminary Study of Drill Core Samples
from Northeast of the Ambrosia Lake District

Personnel of the U.S. Energy Research and Development Administration in Grand Junction, Colorado (especially S. R. Austin and W. L. Chenoweth) advised us of samples of drill cores in storage in Grand Junction and kindly retrieved these samples for our use. These cores, taken in the 1950's were from barren, reduced ground in the Westwater Canyon Member northeast of the redox front in the Ambrosia Lake District. The locations of these holes are plotted in Figure 16. Our initial attempt has been to study the clay mineralogy of these samples in detail and to study their trace element contents as well. The clay mineralogic data are essentially complete and are presented in Table 8. Forty two samples have been studied, of which eight have been selected so far for trace element study by NAA (work in progress; see Trace Element Studies section.). Both the whole rock and clay size (minus-two micron) fraction are being analyzed. The relative abundance of the various clay minerals from these drill holes is shown in Figure 17.

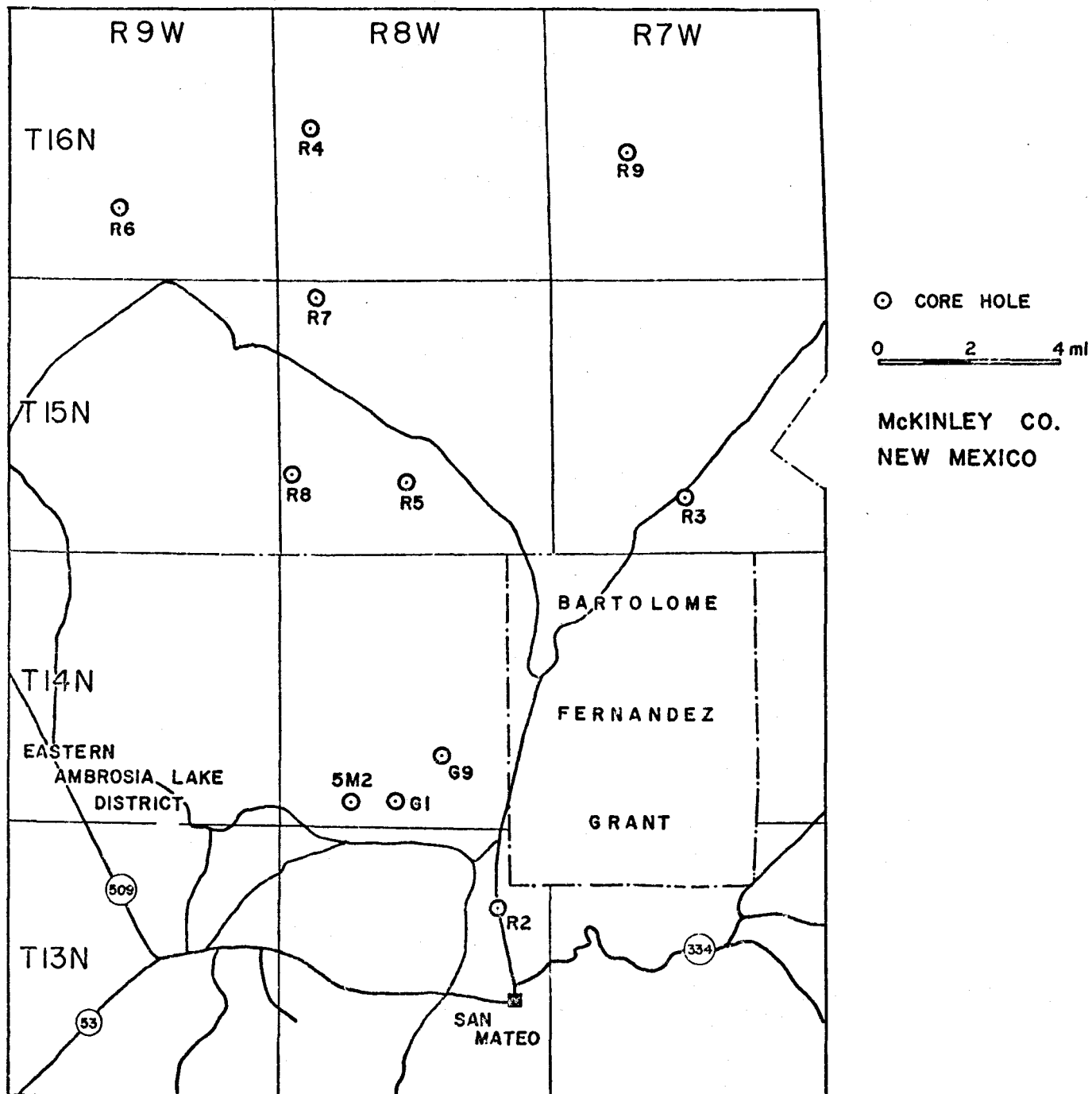


FIGURE 16. Drill hole locations in the area north of the Ambrosia Lake District

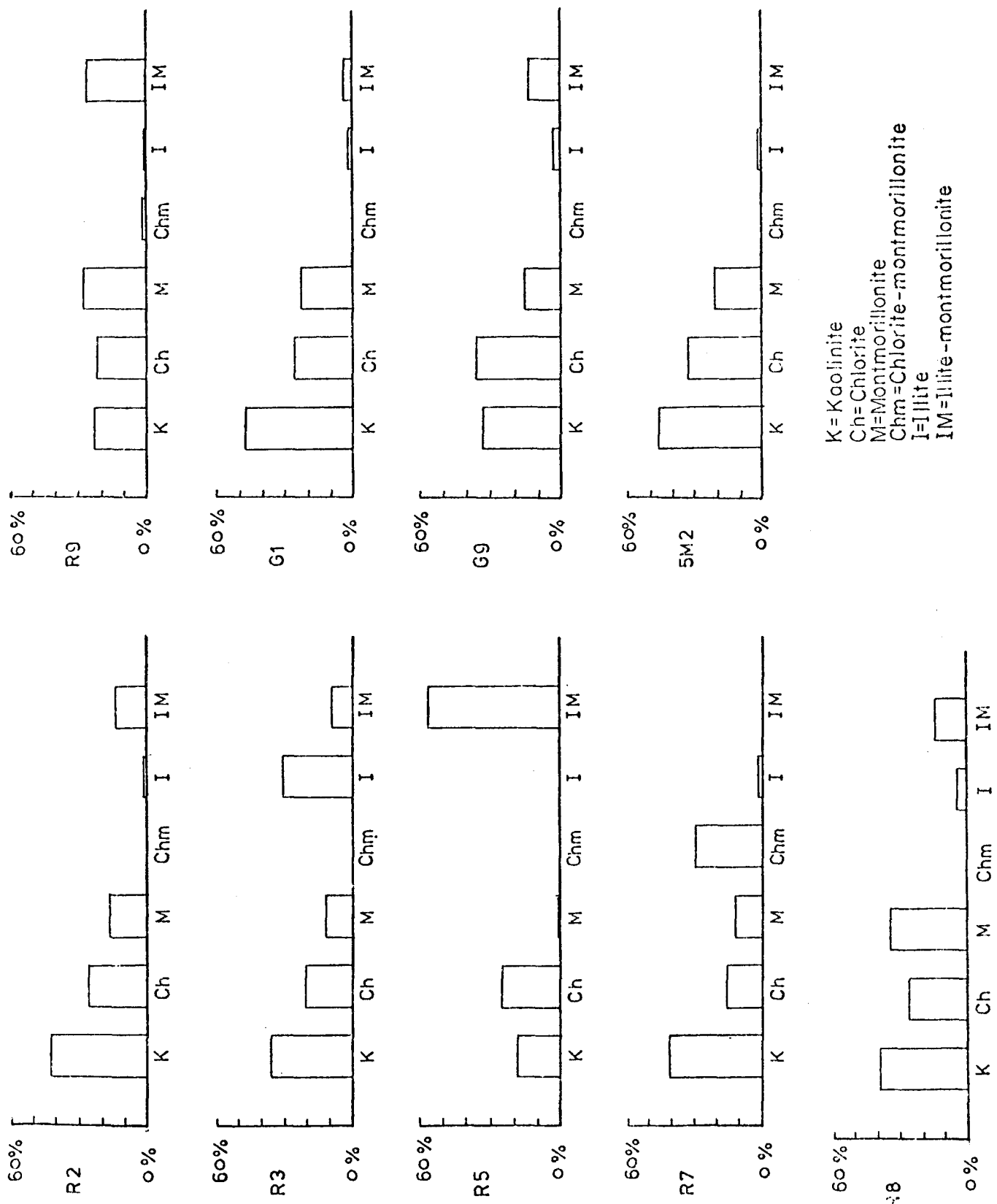


FIGURE 17. Relative Abundance of Clay Minerals for Locations Plotted in Figure 16.

TABLE 9
Clay Mineral Distribution in Sandstones North
of the Ambrosia Lake District

	K	Ch	M	Ch-M	I	I-M	Lithology
R-2							
3906-F	45	20	20	-	-	15	Greenish sandstone; reduced with disseminated OCM and magnetite
3906-J	17	20	24	-	tr	39	Greenish sandstone reduced with green clay galls
2660	51	27	17	-	5	tr	Bleached sandstone; limonitic
3906-C	57	36	7	tr	tr	tr	Greenish sandstone; reduced with disseminated OCM
Average	42.5	25.8	17	-	1.25	13.5	
R-3							
3907-D	40	34	20	-	5	tr	Greenish sandstone; reduced with disseminated OCM
3907-E	52	30	18	-	-	tr	Greenish sandstone; reduced with disseminated OCM
2661-B	15	-	-	-	56	29	Arkosic sandstone; hematitic cement
Average	35.7	21.3	12.7	-	30.5	9.7	
R-5							
3826-J	12	16	tr	-	-	72	Greenish sandstone; reduced with thin layers of OCM
3826-M	5	tr	tr	-	-	95	Greenish sandstone; reduced with sparse magnetite grains
3826-A	63	33	5	-	-	-	Greenish sandstone; reduced with disseminated magnetite
3826-N	5	13	tr	tr	tr	82	Greenish sandstone; reduced with thin layers of OCM

TABLE 9 (continued)

	K	Ch	M	Ch-M	I	I-M	Lithology
R-5 (cont.)							
2663-C	7	62	tr	-	-	31	Greenish grey sandstone; reduced
Average	18.2	24.8	1	-	-	56	
R-7							
2665-B	49	26	25	-	-	tr	Arkosic sandstone; bleached
3824-E	69	22	9	tr	tr	tr	Greenish sandstone; reduced with disseminated OCM
3824-A	5	tr	-	90	5	-	Greenish sandstone; reduced with disseminated OCM
Average	41	16	11.3	30	1.7	-	
R-8							
3823-B	61	31	8	-	-	-	Arkosic sandstone; hematite stained
3823-D	40	24	36	-	-	tr	Arkosic sandstone; reduced
3823-H	41	30	29	-	tr	tr	Arkosic sandstone, reduced with thin layers of OCM
3823-L	34	26	20	-	20	-	Greenish sandstone; reduced with OCM layers
2666-B	17	15	tr	-	tr	68	Greenish grey sandstone; reduced
Average	38.6	25.2	18.6	-	4	13.6	
R-9							
3825-E	44	33	23	-	-	-	Greenish sandstone; reduced
3825-P	12	14	tr	-	-	74	Greenish sandstone reduced with thin layers of OCM
3825-S	5	5	tr	-	-	90	Arkosic sandstone with thin layers of OCM; hematitic stains
3825-H	18	12	70	-	-	-	Greenish sandstone; reduced with sparse thin OCM layers

TABLE 9 (continued)

	K	Ch	M	Ch-M	I	I-M	Lithology
R-9 (cont.)							
3825-N	21	-	66	13	-	-	Greyish sandstone; bleached
3825-M	13	41	-	-	5	41	Greyish sandstone; bleached
3825-K	28	28	44	-	tr	-	Greenish sandstone; reduced
3825-L	43	40	17	-	tr	-	Greenish sandstone; reduced
Average	23	21.6	27.5	1.6	0.6	25.6	
G-1							
2670-J	50	11	39	-	-	-	Arkosic sandstone; hematitic stain
2670-A	51	35	14	-	-	-	Arkosic sandstone; reduced with disseminated magnetite
2670-M	47	15	38	tr	-	-	Greenish sandstone with thin OCM; reduced
2670-G	42	39	-	-	5	14	Greenish sandstone with thin OCM layers; reduced
Average	47.5	25	22.8	-	1.25	3.5	
G-9							
2668-X	49	36	-	-	-	15	Greenish sandstone; reduced
2668-I	38	31	13	-	-	18	Arkosic sandstone with thin OCM layer and magnetite; limonitic
2668-O	48	28	13	-	-	11	Arkosic sandstone; limonitic with disseminated magnetite
2668-E	25	36	34	-	5	-	Greenish sandstone with magnetite; reduced
2668-V	28	31	32	-	9	-	Arkosic sandstone; bleached
2668-C	13	51	tr	tr	tr	36	Greenish grey sandstone; reduced
Average	33.5	35.5	15.3	-	2.3	13.3	

TABLE 9 (continued)

	K	Ch	M	Ch-M	I	I-M	Lithology
5M-2							
2669-B	60	30	10	-	-	tr	Arkosic sandstone; limonitic with disseminated magnetite
2669-A	43	30	27	tr	tr	tr	Arkosic sandstone; limonitic with disseminated magnetite
2669-K	27	31	37	-	5	-	Arkosic sandstone; limonitic with disseminated magnetite
2669-E	52	40	8	-	-	tr	Greenish sandstone, reduced
Average	45.5	32.8	20.5	-	1.25	-	

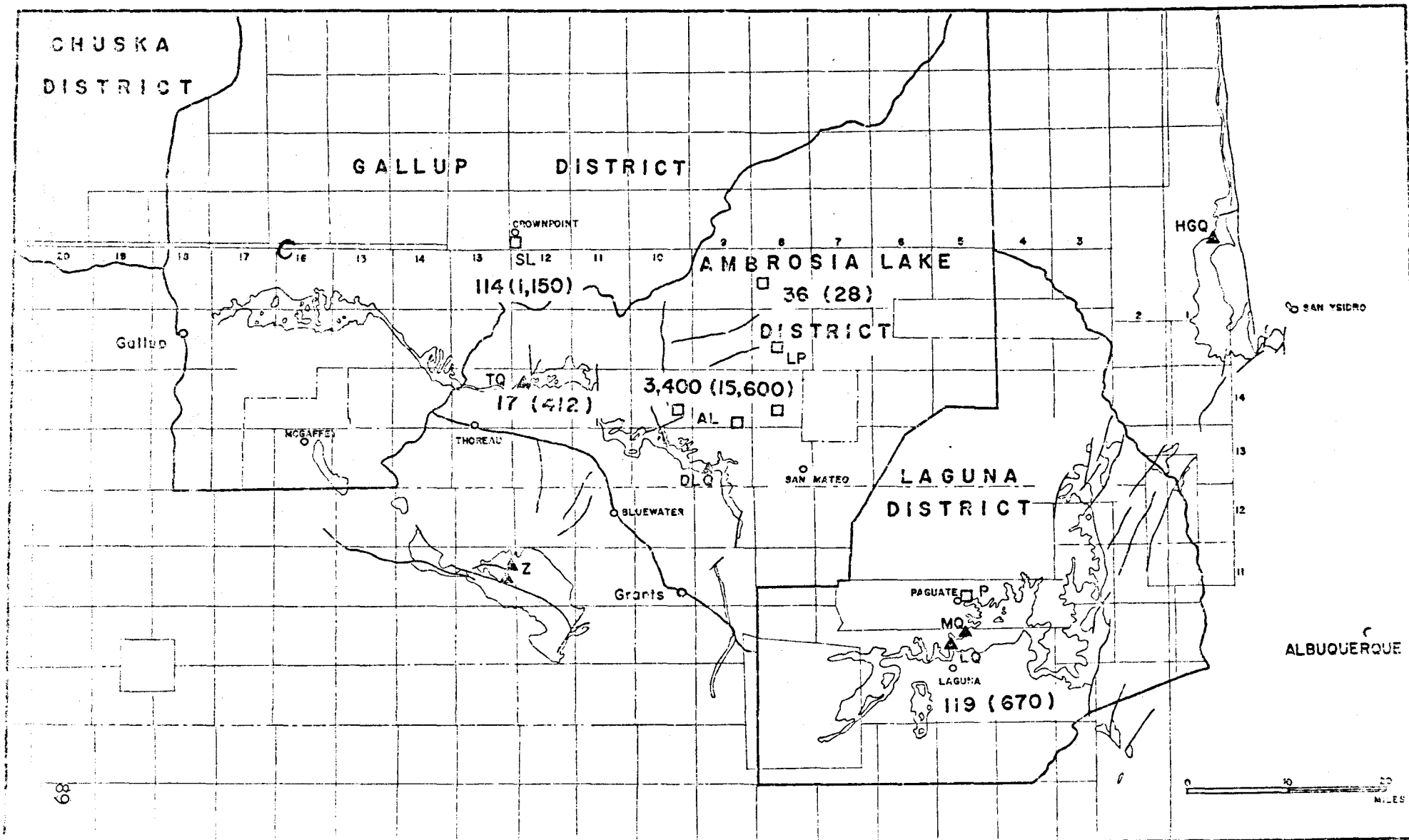
TRACE ELEMENT GEOCHEMISTRY

Introduction

Approximately one hundred samples of whole-rock sandstones, mudstones, and clay-sized fractions from them have been analyzed for their trace element contents. The analyses were done at Los Alamos Scientific Laboratory (LASL) by Instrumental Neutron Activation Analysis (INAA), using the Laboratory's 8MW Omega West Reactor as the neutron source. By using a combination of long and short irradiations in three different parts of the reactor, it was possible to analyze 23 elements listed in Tables 10 and 11. The INAA technique was described by Gordon and others (1968). For selected samples, uranium content was determined by Delayed Neutron Activation Analysis (DNAA). This method is particularly suitable for very low ranges of uranium concentration. Gale (1967) and Cumming (1974) have discussed the technique and demonstrated its application to a variety of geologic materials.

The objective of this study is to not only obtain hitherto unreported trace element data for ore versus barren samples, but to attempt to interpret the data such that some elements may, if transported into an ore-bearing site, not only be concentrated in the ore zone but left behind in lesser amounts, thus can be used as true pathfinder elements. The advantage of analyzing both the whole-rock and clay-sized fractions is that whole-rock data alone often give biased results due to effect of dilution with resistate minerals, whereas the latter, owing to the cation exchange and absorption capacities of clay minerals, has a better chance of enriching mobile trace elements. Further, any organo-metallic complexes present would be enriched in the fine fraction.

FIGURE 18. Vanadium distribution in whole rocks (no parentheses) and constituent clay minerals (in parentheses).



NOTE: SL=Smith Lake District; C=Churchrock District (both in Gallup District)

Results

The summary of trace element analysis is given in Tables 10 and 11. The analytical error for most of the elements is in the range of ± 5 to 10 percent. For Sb and Rb a somewhat higher range is expected. For high-grade ore samples the irradiation results are hindered by fission interferences so that La, Sm, Ce, Lu, Ni, Ba and occasionally Hf could not be determined. However, the overall REE distribution pattern can still be inferred from Eu and Tb.

The sample suites are divided into three different groups: outcrop, bleached barren zone and ore zone. This grouping is based on sample availability and is intended only to establish background factors not related to any predetermined concept on ore genesis.

It is evident from the data that the clay-sized fraction is preferentially enriched in most of the elements investigated except for Hf and Rb. This observation is more pronounced for rare earth elements, Fe, Cr, Ta, Co and Sb than for others. The same trend for V was also confirmed by Lee and others (1975). Whole-rock enrichment of Hf and Rb probably represents concentration of these elements in resistate heavy minerals and feldspars.

Rare Earth Elements (REE)

The REE enrichment in the sandstone-type uranium deposits has not been reported, although Shoemaker and others (1954) found some La and Y in the Salt Wash deposits of the northern Colorado Plateau. The scarcity of data is believed to be due to analytical difficulty. The REE, including Y and the lanthanides, have a strong tendency of geochemical coherence due to the "lanthanide contraction". In igneous rock, REE are mainly associated with major rock-forming minerals, whereas in sedimentary environments they enter into clay mineral structures or are associated with organic materials. These elements are lithophile in their behavior and all exist in the +3 oxidation state except Ce (+4 and +5) and Eu (+3 and +2). Due to this, Ce and Eu often show anomalous distribution patterns.

Table 10A

Trace Element Data of Whole-Rock Samples, Units in ppm

	Ore Zone		Bleached Zone		Outcrop	
	Range	Mean	Range	Mean	Range	Mean
Sm	3.2 - 7.78	5.49	1.96 - 5.8	3.79	1.84 - 10.83	6.37
Ce	27.9 - 69.6	51.15	16.9 - 48.2	31.81	4.86 - 60.7	37.22
Lu	0.15 - 0.34	0.25	0.1 - 0.26	0.16	0.10 - 0.59	0.29
Th	3.5 - 7.1	5.10	1.9 - 8.32	4.28	1.19 - 16.89	6.32
Cr	29.9 - 88.4	61.8	3.4 - 91.7	19.31	14.04 - 81.6	32.14
Hf	3.0 - 13.54	5.94	1.0 - 10.6	3.23	1.36 - 12.03	5.27
Ba	46 - 479	211	329 - 982	611	96 - 719	362
Nd	15.3 - 27.9	21.6	7.9 - 25.5	17.73	5.4 - 38	23.68
Cs	1.04 - 3.33	2.47	1.0 - 2.0	1.32	0.32 - 4.73	1.85
Tb	0.3 - 9.4	2.43	0.22 - 0.57	0.34	0.12 - 0.76	0.47
Sc	0.93 - 5.78	2.40	1.2 - 2.8	1.56	0.44 - 10.18	3.85
Rb	3.66 - 238	92.9	45 - 100	68.6	10.9 - 117	58.2
Fe	0.79 - 1.88%	1.32%	0.56 - 1.4%	0.93%	0.3 - 4.6%	1.50%
Ta	0.90 - 3.05	2.24	0.3 - 5.0	0.82	0.19 - 2.20	0.79
Co	1.5 - 11.4	6.88	1.4 - 3.1	2.10	0.81 - 5.88	2.59
Eu	0.97 - 8.18	3.10	0.3 - 1.3	0.76	0.10 - 0.91	0.67
La	15.71 - 59.3	27.5	10.0 - 28.5	19.55	12.13 - 42.94	31.95
Sb	0.15 - 9.77	2.29	0.1 - 0.3	0.23	0.18 - 1.71	0.55
Ni	14.6 - 24	18.0	9.2 - 24	16.1	-----n.a.-----	

Table 10B

Trace Element Data of Clay-Sized Fraction, Units in ppm

	Ore Zone		Bleached Zone		Outcrop	
	Range	Mean	Range	Mean	Range	Mean
Sm	15.3 - 22.9	19.75	3.4 - 15.1	9.78	7.1 - 18.3	11.23
Ce	143 - 149	146.4	14.2 - 107.1	52.79	62.2 - 96.1	77.02
Lu	1.12 - 1.16	1.14	0.11 - 0.74	0.432	0.25 - 0.66	0.46
Th	9.2 - 41	19.9	2.94 - 20.2	9.31	10.1 - 16.4	14.16
Cr	26 - 138	86.6	12 - 66	32.2	11.3 - 119.7	47.0
Hf	1.85 - 9.41	3.44	0.62 - 3.55	1.87	1.96 - 6.49	4.17
Ba	268 - 1998	826	162 - 2365	806	183 - 1214	459
Nd	78.1 - 91.7	84.89	36.9 - 48.6	41.5	53.7 - 54.8	54.25
Ba	9.3 - 35.0	26.3	21 - 43	29.3	18 - 40	30.67
As	105 - 454	254	3.6 - 11.9	8.02	11.7 - 13.8	12.91
Cs	0.89 - 8.74	4.54	0.96 - 6.61	2.63	1.75 - 8.33	4.21
Ni	332 - 756	493	166 - 194	180	171 - 428	300
Tb	0.87 - 32.67	3.66	0.47 - 1.41	0.92	0.68 - 0.98	0.83
Sc	3.08 - 21.9	10.39	5.16 - 16.0	10.81	7.8 - 17.5	13.03
Br	9.03 - 31.6	17.8	6.3 - 10.7	7.9	3.9 - 7.2	5.5
Rb	16 - 253	101.5	26 - 105	64.5	39 - 139	92.4
Fe	1.16 - 21.99%	7.46	3.17 - 15.63%	8.19%	0.88 - 10.28%	4.75%
Ta	0.44 - 10.95	3.59	0.68 - 2.91	1.44	0.94 - 2.18	1.44
Co	5.5 - 46	24.4	3.39 - 41.5	19.31	2.12 - 30.26	12.53
Eu	0.19 - 29.3	4.92	0.25 - 2.66	1.13	0.73 - 1.48	1.16
La	68.9 - 102	85.48	16.3 - 60.9	38.22	37.8 - 70.2	56.2
Sb	0.63 - 30.9	4.88	0.21 - 1.16	0.47	0.33 - 0.86	0.51
Mn	740 - 970	833	106 - 360	269	82 - 228	179

TABLE 11

TRACE ELEMENT DATA** (Plus Iron), Units in ppm

A. Oxidized Samples, Outcrop and Core

	1) TQ Kd *WR	2) TQ Kd-1 WR	3) TQ Jmw-4 WR	<2u
Sm	1.83	10.8	10.63	7.08
Ce	4.85	32.1	26.64	33.07
Lu	0.09	0.43	0.60	0.15
Th	1.19	53.48	58.47	3.21
Cr	115.9	24.97	27.52	81.60
Hf	3.4	15.82	12.63	1.82
Ba	118.2			719.2
Nd	5.4			31.45
Cs	0.31			1.48
Mn				
Tb	0.12	0.63	0.86	0.33
Sc	0.43	22.95	27.0	1.50
Rb	11.62	10.86	13.04	88.16
Fe	3486.0	4102.0	6742.0	7910.0
Ta	0.19	4.54	4.48	0.39
Co	0.80	1.70	2.20	1.55
Eu	0.07	0.57	0.52	0.76
La	12.1	38.51	32.04	34.8
Sb	0.24	1.71	1.63	0.17
Ni			324.0	
As			13.27	
Ga			13.92	
Br			3.85	

*WR = whole rock

*<2u = Less than 2 micron fraction

- 1) Dakota Sandstone
- 2) Dakota Black Shale
- 3) Westwater Canyon Ss, Goethitic

**Where no data are shown in Table 11 this indicates interference from fission products; absence of data does not indicate that the particular element(s) are below detection level.

TABLE 11 (continued)

4) TQ Jmw-9		5) DLQ Jmw-6		6) DLQ Jmr-1	
WR	<2u	WR	<2u	WR	<2u
Sn	4.85	7.10	8.49	18.29	8.29
Ce	46.47	93.13	32.15	62.17	60.64
Lu	0.32	0.30	0.13	0.62	0.58
Th	6.05	10.12	2.86	10.59	16.89
Cr	24.44	46.45	18.04	119.67	17.39
Hf	7.67	2.44	1.36	3.80	7.97
Ba	392.2	364.2	598.6	361.7	348.9
Nd	27.21		15.94		407.0
Cs	1.98	2.97	1.48	5.55	4.73
Mn		760.0		225.9	
Tb	0.44		0.31	0.67	0.76
Sc	4.87	13.79	2.04	17.54	10.17
Rb	67.95	67.10	76.62	134.2	117.2
Fe	28353.	102759.	7445.0	38046.0	45910.
Ta	0.76	0.94	0.35	1.55	2.19
Co	5.87	30.25	1.84	11.44	9.41
Eu	0.86	1.20	0.70	1.20	0.90
La	31.12	30.35	40.37	68.35	42.93
Sb	0.36	0.36	0.22	0.46	0.94
Ni		170.8		427.9	
As		12.8			
Ga		40.61			
Br		4.63			

4) Westwater Canyon Ss, Goethitic

5) Westwater Canyon Ss, Hematitic

6) Recapture Siltstone, Hematitic

TABLE 11 (continued)

	7) LQ Jmb-3 WR	<2u	8) MQ Jmj-5 WR	<2u	9) LQ Jmw-7 WR	<2u
Sm	5.48	8.98	4.75	12.59	5.69	8.66
Ce	45.77	53.82	47.12	129.85	32.77	65.82
Lu	0.41	0.64	0.23	0.45	0.26	0.25
Th	6.48	15.09	6.77	15.09	7.04	16.43
Cr	14.04	16.92	15.67	11.32	61.01	99.06
Hf	5.14	6.23	2.73	2.92	12.03	1.95
Ba	278.16	319.44	95.9	182.6	342.8	1214.0
Nd	30.52		37.58	53.65	17.67	
Cs	2.55	4.09	0.98	1.75	1.23	1.75
Mn		227.9				
Tb	0.65	0.87	0.48	0.93	0.45	
Sc	5.13	14.43	3.95	9.75	2.68	7.80
Rb	78.9	101.6	26.1	36.2	46.8	51.6
Fe	9825.0	27051.0	4193.0	8835.0	24528.0	92987.0
Ta	0.69	1.74	0.53	1.17	1.18	1.39
Co	2.55	6.52	0.90	2.11	5.49	23.87
Eu	0.73	0.77	0.80	2.16	0.53	0.73
La	36.21	59.14	25.73	66.04	25.70	37.77
Sb	0.66	0.86	0.34	0.42	0.30	0.65
Ni						
As		13.8				
Ga		17.70				
Br		7.19				

7) Brushy Basin, Green Mudstone

8) Jackpile Ss, Kaolinitic

9) Westwater Canyon, Goethitic Magnetite

TABLE 11 (continued)

B. Bleached Barren Samples, Core and Mine Workings

	1) 2665-B	2) 2666-B	3) 2668-E/I			
	WR	<2u	WR	<2u	WR	<2u
Sm	3.16	5.99	4.11	3.99	5.80	13.10
Ce	35.33	86.94	30.55		39.83	22.26
Lu	0.12	0.59	0.12		0.15	0.43
Th	2.98	12.14	3.59	3.50	4.10	9.43
Cr	3.80	26.59	11.94	14.38	6.11	50.46
Hf	1.56	2.36	1.74	1.24	1.64	2.10
Ba	586.0	804.0	532.0	162.6	981.0	515.4
Nd	13.78	38.94	21.76		22.86	
Cs	1.74	2.40	1.50	1.37	1.90	2.28
Mn				338.1		
Tb	0.37	0.83	0.28		0.39	
Sc	1.76	10.70	1.92	9.47	1.50	14.96
Rb	87.6	79.8	76.7	38.2	100.4	49.0
Fe	6865.0	62931.0	10213.0	63914.0	7805.0	119755.0
Ta	0.33	1.54	0.28	0.67	0.31	1.73
Co	2.17	18.74	2.82	13.47	2.39	41.50
Eu	0.81	1.36	0.63	0.37	0.96	1.26
La	21.01	49.15	23.03	18.30		34.60
Sb	0.20	0.52	0.15	0.20	0.28	0.58
Ni	13.61		24.04		14.72	
As						11.89
Ga				24.16		42.68
Br						6.84

- 1) Westwater Canyon, bleached
- 2) Westwater Canyon, bleached and light green
- 3) Westwater Canyon, bleached

TABLE 11 (continued)

	4) 2670-A		5) 3823-D		6) 3825-L	
	WR	<2u	WR	<2u	WR	<2u
Sm	3.36		3.89	14.27	2.90	10.46
Ce	38.10	97.8	39.91	107.14	24.89	42.16
Lu	0.13	0.47	0.18	0.12	0.24	0.74
Th	4.56	15.92	4.94	20.16	4.13	8.82
Cr	17.04	43.77	5.91	45.86	11.76	32.43
Hf	1.19	1.90	2.10	3.55	9.94	1.80
Ba	519.0	496.0	981.9	986.8	455.1	829.3
Nd	18.44	36.86	25.1	48.62	13.62	
Cs	1.31	3.13	1.96	6.61	1.02	3.01
Mn			363.3			
Tb	0.40		0.40	0.97	0.36	
Sc	1.41	10.98	1.69	13.63	2.16	11.27
Rb	73.5	75.1	98.7	104.6	50.24	56.4
Fe	7170.0	93066.0	5608.0	50315.0	13997.0	123296.0
Ta	0.42	1.59	4.96	2.19	0.80	1.62
Co	1.53	25.13	1.61	14.42	2.80	23.43
Eu	0.87	1.25	0.97	1.52	0.59	0.83
La	23.40	50.74	25.15	60.94	13.03	44.83
Sb	0.16	1.15	0.22	0.63	0.27	0.56
Ni	16.19			166.0		
As				20.70		
Ga				6.12		
Br						

TABLE 11 (continued)

7) 3826-A		8) 3826-M		9) 3907-D	
	WR		WR		WR
	<2u		<2u		<2u
Sm	5.62	7.44	1.95	15.06	2.35
Ce	48.17	36.94	15.85	14.16	21.70
Lu	0.25	0.64	0.10	0.32	0.11
Th	8.32	12.30	2.67	2.94	3.08
Cr	15.39	65.77	3.41	13.39	7.02
Hf	10.56	1.76	0.97	0.62	2.77
Ba	488.0	755.0	329.0	340.9	552.94
Nd	25.45		22.75		13.46
Cs	1.30		1.02	0.96	
Mn					2.70
Tb	0.56		0.22		0.31
Sc	2.74	15.99	1.16	6.14	1.97
Rb	54.2	65.2	44.8	26.6	53.1
Fe	16551.0	156281.0	4992.0	31688.0	7180.0
Ta	0.98	2.90	0.48	0.69	0.32
Co	3.11	33.72	1.35	6.55	1.86
Eu	1.02	1.26	0.40	1.24	0.48
La	28.51	46.06	9.97	16.33	13.27
Sb	0.22	0.45	0.24	0.16	0.21
Ni			11.64		16.14
As				8.55	
Ga				16.94	
Br				10.69	

TABLE 11 (continued)

10) P. 163		11) P. 164		12) 2661-A		13) 2666-C	
WR	<2u	WR	<2u	WR		WR	
Sm			4.90		2.74		4.64
Ce			16.96		24.79		45.6
Lu			0.12		0.13		0.17
Th	3.16	5.01	1.91	4.77	2.32		5.60
Cr	91.73	25.10	8.84	12.76	32.75		16.00
Hf	1.71	1.39	1.50	1.83	1.19		1.79
Ba			673.2		904.0		331.3
Nd			7.987		18.46		9.07
Cs	1.60	1.62	1.249	2.15	1.25		0.96
Mn		106.0					
Tb	0.45	1.41	0.22	0.47	0.40		0.50
Sc	1.25	5.16	1.41	6.98	1.22		1.65
Rb	85.0	52.4	51.9	95.8	72.9		43.0
Fe	8168.0	35599.0	8875.0	45881.0	6529.0		11815.0
Ta	0.32	0.89	0.30	0.94	0.28		0.81
Co	1.67	3.38	1.61	5.86	2.16		2.21
Eu	1.29	2.65	0.31	0.88	0.76		0.80
La			17.56		14.94		25.10
Sb	0.29	0.22	0.19	0.46	0.14		0.36
Ni	14.42	194.3	18.83		22.09		9.18
As							
Ga		7.65					
Br							

10) Jackpile Ss, pyritic, bleached
 11) Jackpile Ss, light green
 12) Westwater Canyon Ss, bleached
 13) Westwater Canyon Ss, green, magnetite

TABLE 11 (continued)

C. Ore Zone Samples, Mine Workings and Core

1)	23-302	WR	<2u	2)	23-301	<2u	3)	SL 171	WR	<2u
----	--------	----	-----	----	--------	-----	----	--------	----	-----

Sm										
Ce										
Lu										
Th	3.60			24.56			7.08			
Cr	29.94		106.02		25.89		22.10		112.18	
Hf	3.02						0.85			
Ba										
Nd										
Cs	1.27			4.87			1.67		6.84	
Mn		965.6								
Tb	0.92		4.56		1.12		0.33		4.58	
Sc	1.33		3.34		12.06		2.51		21.90	
Rb	80.3			42.3			27.5			
Fe	16706.0		79754.0		62901.0		12785.0		92385.0	
Ta	2.51		8.54		2.65		0.62		10.94	
Co	9.96			16.31			4.23		45.50	
Eu	2.67		4.89		3.10		1.41		6.72	
La										
Sb	2.27		24.51		27.06		4.32		20.76	
Ni				352.3						
As				454.0						
Ga				24.8						
Br				18.0						

1) High-grade Ore, Section 23 Mine

2) High-grade Ore, Section 23 Mine

3) High-grade Ore, Smith Lake

TABLE 11 (continued)

	4) P. 142 WR	<2u	5) P. 107 WR	<2u	6) 35-208 WR	<2u
Sm						
Ce						
Lu						
Th						
Cr	88.37	138.46	83.63	102.86	16.29	78.05
Hf						
Ba						
Nd						
Cs	3.32		2.77	6.47	2.60	7.31
Mn						
Tb	1.51	5.20	2.87	3.78	0.48	
Sc	1.85	5.48	0.92	8.00	1.68	9.33
Rb	238.0	32.0			135.8	
Fe	18796.0	71113.0	9036.0	77458.0	9615.0	53182.0
Ta	3.04	7.52	2.21	3.68	2.54	7.46
Co	11.07	23.52	4.18	36.71	11.36	45.72
Eu	2.66	7.60	5.45	7.52	1.38	8.11
La						
Sb	5.86	9.70	9.76	16.75	2.13	30.90
Ni						
As		208.0				
Ga						
Br		31.6				

4) High-grade Ore, Pagnate Mine

5) High-grade Ore, Pagnate Mine

6) High-grade Ore, Section 35 Mine

TABLE 11 (continued)

	7) 35-301	WR	<2u	8) 35-201	WR	<2u	9) SL 271	WR	<2u
Sm							3.16		15.29
Ce							27.90		143.3
Lu							0.15		0.56
Th	3.95		30.17		3.51	15.60	3.72		15.4
Cr	54.73		45.22		13.09	20.44	14.01		33.30
Hf	3.01		2.36		1.56	4.35	3.78		2.39
Ba							45.84		382.3
Nd							15.30		78.07
Cs	1.36		2.34		1.68	4.33	1.04		2.90
Mn									
Tb	0.43		1.47		0.34	1.47	0.26		1.01
Sc	1.74		9.37		1.55	21.06	1.31		15.67
Rb	84.5		59.9		99.4	139.0	57.9		68.3
Fe	7339.0		45893.0		5301.0	30173.0	7854		147917.0
Ta	0.56		4.93		0.63	1.20	0.52		2.83
Co	1.86		15.10		2.16	5.96	3.47		32.81
Eu	0.43		2.87		0.85	2.99	0.62		2.52
La							15.71		68.93
Sb	0.30		1.41		0.35	0.75	0.15		0.63
Ni	23.64								
As									
Ga									
Br									

7) Near Ore Zone, low-grade, Section 35 Mine

8) Near Ore Zone, low-grade, Section 35 Mine

9) Near Ore Zone, low-grade, Smith Lake

TABLE 11 (continued)

10) MQ Jmj-1		11) MQ Jmj-3		12) 35-51	
	WR		WR		WR
	<2u		<2u		<2u
Sm	7.78	22.94			
Ce	55.96	149.5			
Lu	0.33	1.15			
Th	6.95	37.64	5.91	9.35	5.94
Cr	13.56	22.46	21.82	32.40	34.00
Hf	6.87	9.41	3.09	1.84	3.65
Ba	108.3	267.7			
Nd	27.88	91.70			
Cs	0.36	1.18	2.91	2.42	3.17
Mn				82.2	4.40
Tb	0.96	2.49	9.38	32.66	1.25
Sc	2.04	12.94	2.83	9.32	5.78
Rb	3.66	16.00	94.4	68.5	86.1
Fe	3534.0	11633.0	13348.0	47099.0	17606.0
Ta	0.89	3.89	0.62	2.08	0.84
Co	0.35	1.11	2.75	11.05	9.26
Ru	0.97	2.78	8.18	29.2	2.04
La	39.29	102.03			
Sb	0.64	2.11	5.49	23.58	0.94
Ni	14.60				1.97
As				11.72	157.0
Ga				32.72	18.4
Br				6.33	9.30
					6.26

10) Near Ore Zone, Paguate Mine

11) Near Ore Zone, Paguate Mine

12) Low-grade, Mudstone, Section 35 Mine

TABLE 11 (continued)

	13) 2037 <2u	14) 23-307 <2u	15) 23-308 <2u	16) 23-211 <2u	17) 23-315 <2u
Sm	5.47			21.00	
Ce	152.93		59.56	179.4	
Lu					
Th	9.97	9.20	31.34	41.02	12.18
Cr	13.04	33.49	27.15	20.03	11.95
Hf		2.26	2.29	4.45	2.29
Ba		661.4	559.4	1087.0	
Nd	119.1	60.20	69.14	102.04	
Cs	2.70	4.055	1.37	7.41	4.27
Mn					
Tb	1.03	1.19	0.86	0.96	1.16
Sc	9.94	7.62	7.63	9.97	10.45
Rb	77.20	41.3	49.4	116.9	104.7
Fe	32021.0	147240.0	115955.0	219865.0	59122.0
Ta	1.02	1.41	4.12	1.57	0.44
Co	20.53	18.23	5.52	41.21	15.18
Eu	1.12	1.07	1.18	1.62	1.76
La	42.42	10.37	22.61	38.32	
Sb	3.02	9.23	7.71	1.89	3.15
Ni					
As				247.0	
Ga				27.66	
Br				12.57	

13) Low-grade, Mudgall, Section 23 Mine
 14) Low-grade, Hematitic Ss, Section 23 Mine
 15) Low-grade, Goethitic Ss, Section 23 Mine
 16) Low-grade, Goethitic Ss, Section 23 Mine
 17) Low-grade, Goethitic Ss, Section 23 Mine

TABLE 11 (continued)

	18) 23-316 <2u	19) 23-317 <2u	20) 35-211 <2u	21) P. 112 <2u	22) P. 151 <2u
Sm					
Ce			59.78		
Lu			1.12		
Th	20.74	11.80	10.05		17.48
Cr	36.03	26.42	18.52	74.02	24.35
Hf		2.89	4.30		
Ba			1997.9		
Nd			74.83		
Cs	5.91	6.22	8.74		0.89
Mn					
Tb	1.69	0.87		4.04	1.05
Sc	8.76	14.35	16.17	5.29	3.07
Rb	252.7	110.7	217.4	98.0	99.2
Fe	25052.0	65828.0	44098.0	100927.0	95267.0
Ta		2.42	1.01	4.46	4.98
Co	19.66	31.70	21.59	16.49	22.96
Eu	2.43	2.10	0.18	10.33	2.65
La					
Sb	7.92	6.93	7.38	10.45	6.30
Ni		389.5		756.0	
As		105.0		254.0	
Ga		24.8		34.58	
Br		9.03			

18) High-grade, pyritic Ss. with Mudstone pebbles, Section 23 Mine.
 19) Low-grade, Hematitic Ss, Section 23 Mine.
 20) Near Ore Zone, Mudstone, Section 35 Mine.
 21) High-grade, Paguate Mine.
 22) High-grade, Paguate Mine.

TABLE 11 (continued)

	23) P. 121 <2u	24) P. 104 WR	25) P. 147-A WR	26) P. 147-B WR	27) P. 158 WR
Sm			2.20		
Ce		69.6			
Lu		0.20	0.10		
Th	25.43	2.84	2.00	2.93	6.03
Cr	56.19	21.60	79.99	21.24	37.33
Hf		1.69	1.63	13.54	4.73
Ba			479.1		
Nd					
Cs	6.17	1.72	1.69	1.21	2.33
Mn					
Tb	2.80	0.27	1.13	0.23	0.33
Sc	3.88	1.33	1.36	1.29	4.10
Rb	211.9	94.0	71.4	59.6	97.4
Fe	59633.0	7847.0	30123.0	6770.0	24131.0
Ta	3.76	0.33	0.44	0.66	0.71
Co	28.60	1.46	1.03	7.21	5.60
Eu	5.15	0.69	0.20	0.44	0.79
La			7.06		
Sb	3.10	0.26	0.64	0.55	0.67
Ni		14.61			
As					
Ga					
Br					

23) High-grade, Paguate Mine
 24) Near Ore Zone, Paguate Mine
 25) Original (?) Goethitic Ss, Paguate Mine
 26) Bleached Ss near Location 25
 27) Original (?) Red Mudstone pellets, Paguate Mine

TABLE 11 (continued)

D. Trace Element Data of Volcanic and Granitic Rocks, Whole-Rock

	1) Qbt	2) Qbo	3) Qubb-1	4) Z-111	5) Z-115A	6) 3001-S
Sm	11.59	14.63	5.50	7.60	6.16	12.94
Ce	96.65	93.94	67.28	77.54	70.81	133.26
Lu	0.84	1.30	0.46	0.74	0.35	0.87
Th	20.56	44.93	20.89	22.07	10.41	17.17
Cr	4.64	3.07	12.73	12.06	70.98	36.90
Hf	7.65	11.49	4.15	4.94	4.94	6.10
Ba	173.0	101.1	542.53	207.77	727.36	847.56
Nd	41.52	39.6	22.33	48.93	39.40	74.27
Cs	5.02	9.83	4.32	10.79	9.47	9.14
Fe	10716.0	9340.0	12238.0	9282.0	29820.0	23026.0
Tb	2.0	2.72	0.70	1.26	0.53	1.53
Sc	1.55	0.59	3.87	5.01	12.48	11.27
Rb	174.66	318.6	137.17	259.65	116.14	204.83
Ta	5.69	13.58	3.21	1.87	0.99	2.40
Co	1.21	0.49	3.48	0.94	1.35	5.42
Eu	0.17	0.06	0.58	0.52	1.20	2.27
La	56.23	52.05	42.09	29.41	37.73	65.05
Sb	0.33	0.54	0.271	3.20	0.32	0.36

- 1) Bandelier Tuff, Jemez Mountains
- 2) Obsidian, Jemez Mountains
- 3) Pumice, Jemez Mountains
- 4) Metarhyolite from Zuni Mountains
- 5) Mafic intrusive rock, Zuni Mountains
- 6) Sandia granite

The results of the present study are shown in Figure 19. The average REE concentration of each sample group is compared to the North American Shale Composite (NAS) using the method of Haskin and others (1968). The whole-rock fractions of the three groups of samples have similar distribution patterns except for the enrichment of Eu and Tb in ore zone samples. Except for these two elements, the absolute REE content of the ore zone samples is not pronounced. Both the bleached and outcrop samples have slightly negative Ce anomalies whereas the negative Eu anomaly is limited to oxidized outcrop samples.

Compared to this, the clay-sized fraction of the ore zone samples is different in both the absolute REE abundances and the distribution pattern compared to the rest. There is only a slight Ce anomaly but the Ce content is higher than in other samples. The bleached zone samples have the least amount of REE and the distribution pattern is similar to the outcrop sample. For comparative purposes, the REE contents in some volcanic rocks of the Jemez Mountains were also analyzed and are shown in Figure 20 along with the data of the Brushy Basin mudstones and Dakota swamp deposits. All volcanic samples have strongly negative Eu anomalies whereas the latter group of samples show both negative Ce and Eu anomalies.

Chromium

Both the whole-rock and clay-sized fractions of the ore zone samples show chromium enrichment. The enrichment is by a factor of about two. Anomalous Cr concentrations in epigenetic sandstone uranium deposits have been noted previously (ie: see Fischer, 1970). According to Shoemaker and others (1959) chromium is an intrinsic element in sandstone and independent of any enrichment due to uranium mineralization. It is recalled here that the magnetite separates from the Westwater Canyon Member contain quite high chromium contents. Along with other unstable detrital minerals, the dis-

FIGURE 19

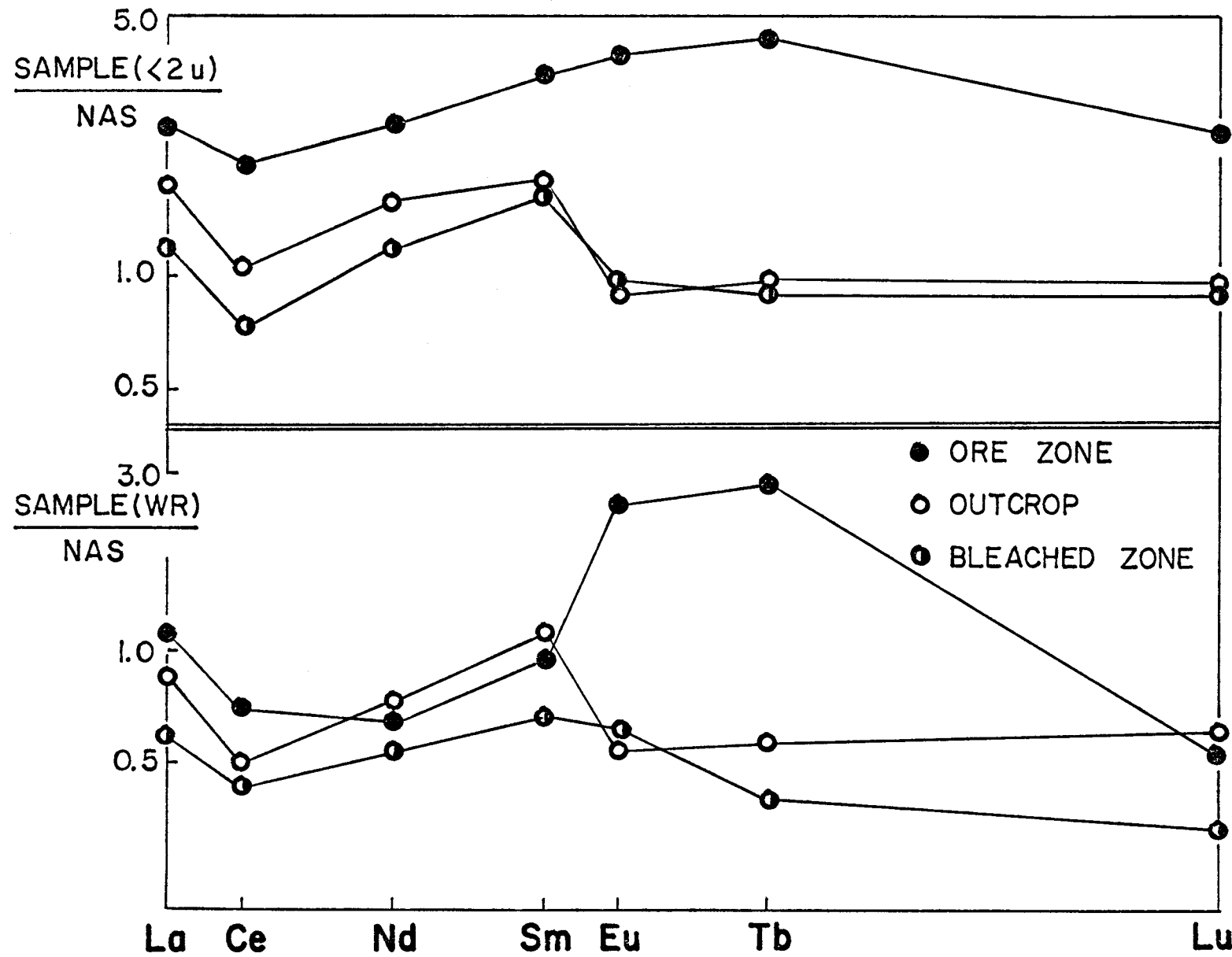
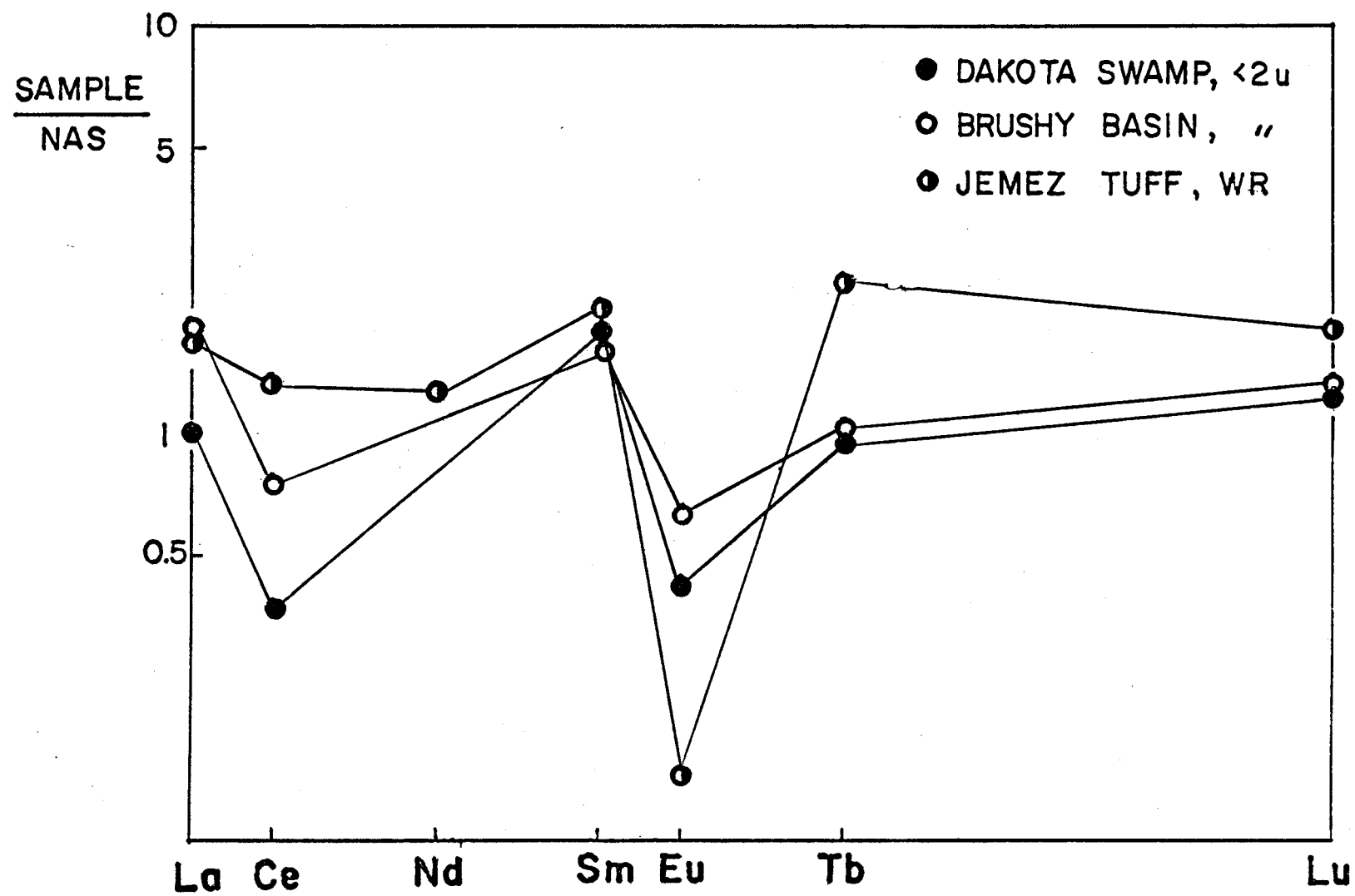


FIGURE 20



solution of these magnetites (see Plate IIB) would have provided enough chromium for the enrichments noted.

Tantalum

Although Wood (1968) reported occasional anomalies of niobium in uranium deposits, the occurrence of tantalum has not been reported. Due to similar chemical behavior under oxidizing conditions, both niobium and tantalum could occur together. The amount of Nb and Ta that go into solution as oxy-metal complexes is believed to be proportional to vanadium. Since vanadium has almost phenomenal association with the uranium deposits, Ta (and Nb) enrichment would be expected under approximately the same Eh-ph conditions as vanadium.

The data indicate that Ta is indeed enriched in the ore zone samples. The enrichment in the clay-sized fraction is as high as ten fold. Thus along with vanadium Ta could serve as a pathfinder element for uranium. Barren samples generally have very low background concentrations ranging up to a few ppm. Nb is subject to interferences during the INAA and cannot be determined.

Cobalt and Nickel

The presence of cobalt and nickel has been reported previously (Wood, 1968; Fischer, 1970). Cobalt and nickel are estimated to be about twenty times as abundant in ores as in unmineralized sandstones of the Salt Wash Member (Shoemaker and others, 1959). Cobalt enrichment is not as high as reported in the above studies in the present samples, although the estimated ratios of abundance between ores and barren sandstones are about 2 to 3. Nickel enrichment is more pronounced in the clay-sized fraction than in whole-rock samples. The somewhat high Ne content in the outcrop samples is probably due to small number of samples analyzed.

Scandium

Although the clay-sized fraction contains more scandium than the whole-rock, ore-zone enrichment was not detected. The overall scandium content appears to be correlated with the iron content. Shoemaker and others (1959) reported a moderate tendency of scandium to accompany high-aluminum ores, and postulated a probable relation to the initial mudstone content of the ores.

Manganese

Manganese analyses were determined for the representative samples of the clay-sized fraction. The limited data indicate that the manganese is somewhat enriched in the ore zone clay minerals. The maximum content found was 970 ppm and, although enriched relative to barren samples, this is believed to be similar to the average crustal abundance.

Manganese enrichment in the whole-rock fractions would also be expected since calcite haloes are abundant in the ore zone.

Arsenic

Arsenic enrichment in the deposits has been noted by many investigators. Concentrations as high as 300 ppm As have been found (Squyres, 1969) compared to a crustal abundance of about 2 ppm. According to Shoemaker and others, arsenic, in terms of abundance ratios, may be the third or fourth most important extrinsic element in sandstone-type uranium deposits.

The phase with which the arsenic is associated in the deposits is not well understood. The presence of native arsenic is possible and even organo-arsenic compound is possible. Nevertheless, the clay fractions from the ore zone contain up to about 450 ppm As in this study, and the overall background concentration in barren rocks appears quite high.

Bromine

Analytical data for halogens are virtually absent. The elements Cl, Br and I would be expected to be geochemically similar to a marked degree, while their compounds are sufficiently abundant in volcanic rocks so as to provide tests concerning the origin of uranium deposits. Limited data indicate that the Br contents in barren samples are fairly uniform, ranging from 3 to 10 ppm, but that ore zone samples have slightly higher concentrations, averaging about 18 ppm. However, reliable conclusions cannot be made due to only a few analyses of ore zone samples. This element is thought to be intrinsic, probably from volcanic materials in the sediments. Its association with organic matter has been reported (Goldschmidt, 1958), although inorganic Br compounds are believed to be mostly insoluble during the weathering process.

Rb, Cs and Ba

The distribution of group IA and IIA elements appears to be controlled by lithology and bears no specific relation to the uranium deposits. However, occasional enrichment of Ba and Ca is possible near the ore zones due to the presence of radiobarite and calcite. Cs and Ba are slightly enriched in the clay fraction although their distribution is uniform in all sample groups. Their average contents are similar to the crustal average, 300 and 400 ppm respectively, in the whole-rock fraction.

Antimony

In both hydrolysate and exidate sediments, antimony occurrence is associated with arsenic in amounts roughly one-fifth by weight (Goldschmidt, 1958). It is also concentrated in some sulphidic sediments. Due to similar ionic radius, trivalent antimony can substitute for Nb and Ta. Since both As and Ta are enriched in the ore zones, one would expect Sb enrichment as well. The scarcity

of data in uranium deposits is probably due to analytical difficulty and lack of suitable standards.

The present analyses were carried out using Spex. standard and the error is presumably large, up to about $\pm 50\%$. Nevertheless, enrichment of this element can be inferred in both the whole-rock and the clay-sized fractions. The average concentrations in the barren rocks is fairly close to the crustal average of 0.5 to 1.0 ppm.

Hafnium

Hafnium, as well as Zirconium and Titanium, appears to be intrinsic and bears no specific relation to uranium deposits. The whole-rock fractions contain more Hafnium, indicating that the element is contained in the resistate minerals.

Thorium

Data for thorium in sandstone-type uranium deposits are generally absent. In sandstones it is mainly concentrated in the resistate heavy minerals. In the sedimentary cycle, Th behaves similar to Sc; and because of the very high ionic potential of Th^{+4} , only very small amounts of Th can be kept in ionic solution in near neutral waters due to precipitation of highly insoluble Th hydroxide. However, some shales and coal ashes do contain appreciable amounts of Th indicating certain circulation of the element in aqueous solutions.

The present study also indicates that whole-rock sandstones show normal Th content, ie. with an average of about 5 ppm, while the clay fractions have 2 or 3 times this amount. However, its distribution in all sample groups is rather uniform indicating no specific relation to the uranium deposits.

Uranium

Uranium analysis by DNAA was carried only for barren samples and the results are summarized below.

Table 12

Uranium Content in Barren Whole-rock Samples, in ppm			
Sample Group	No. Samples	Range	Mean
Westwater Canyon			
Goethitic Ss.	10	0.9 - 3.8	2.1
Hematitic Ss.	5	6.9 - 10.3	9.1
Bleached Ss.	10	1.3 - 4.3	2.5
Upper Recapture	5	4.0 - 21.1	10.3
Middle Recapture	3	0.6 - 3.2	1.8
Brushy Basin	5	8.1 - 20.1	11.7
Poison Canyon Ss.	3	7.0 - 30.7	17.7
Jackpile Ss.	5	3.5 - 30.0	13.7
Dakota Black Shale	3	10.2 - 14.5	12.3
Dakota Ss.	3	0.3 - 0.6	0.5

Some important inferences can be made from the results. First of all, uranium is certainly extrinsic as far as the best sandstones are concerned as seen by low concentration both in bleached and oxidized samples. However, mudstone units in the Westwater Canyon and the Brushy Basin Members contain as much as five times the concentration observed in the sandstones. Thus, the volcanic leaching theory appears to be very attractive.

The higher uranium content in the Poison Canyon and the Jackpile sandstones are attributed to the proximity of samples collected to known deposits. A systematic increase in uranium concentration was noted along the northeast trending Jackpile outcrops from near Laguna to near the Paguate Mine. This suggests that if accurate measurement of uranium is possible for low ranges of concentration such as by DNAA, uranium is certainly the best pathfinder element for uranium deposits.

The few hematitic sandstones analyzed were collected from an outcrop exposed northwest of Grants. The outcrop there is somewhat peculiar in that

oxidation is stronger than at other outcrops along the margin of the San Jan Basin. The uranium content in these sandstones is much higher than in other sandstones. The above observations suggest that at this particular location before oxidation, the sandstone units had abundant pyrite and possibly were part of a low-grade deposit. This interpretation is also based on high uranium contents in the uppermost recapture siltstones at this location.

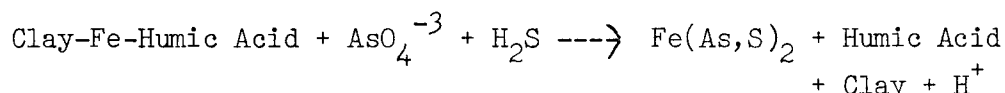
The average uranium in the Dakota Swamp deposit is similar to that in the Brushy Basin even though the former contains abundant OGM. Uranium was presumably unavailable for enrichment, but the Dakota-source-theory of the Morrison humate is very unlikely.

Discussion

The enrichment of various elements in the fine fraction of the ore zone samples tells us that adsorption, fixation or cation exchange of colloidal particles were mainly responsible. The role of clay-rich sediments in the formation of primary deposits has been discussed in the previous chapter. It was postulated that humic acid--and/or fulvic acid--clay complexes were significantly responsible for the precipitation of uranium.

It is only natural to suggest here that a similar mechanism was operative for the concentration of other elements. The strong affinity between a cation and the clay bound organic matter can be considered as an attraction between a positive ion and a negative surface of the organic molecule. According to Ong and Swanson (1966), this type of electrokinetic adsorption actually depends upon ionic potential; as the ionic potential increases, the amount of metal cation adsorbed increases proportionally. Thus cations with large ionic potentials are preferentially adsorbed replacing the ones with lower ionic potential. Similarly, Szalay (1964) explained such accumulation as cation exchange of humic acids, which he postulated depends on the valence

and atomic weight of cations. The results of the present study strongly confirm these theories as seen by enrichment of REE and most of the transition metal groups investigated. Elements in anionic migrating form, such as As, Sb, and Br, can also be enriched by similar mechanism once they are reduced to their cationic forms in the presence of H_2S . Or, if the clay-organo complex was formed by an iron-ligand during the bleaching of the sediments, the following generalized reaction could also happen:



The iron released from the clay-organo complex may well be replaced by cations such as Ca, Mg or Al. The enrichment of As and/or Se would thus be found in the ore-stage pyrite.

Some important interpretations can be made from the results of present study that may be used in uranium exploration. First of all, since clay minerals, especially montmorillonite, possess a high electrokinetic force, there is a good chance that they have competed with UDC or other soluble uranyl complexes for the uranyl ion and preferentially enriched it. This has been suggested before and can be seen in Figures 19 and 20. The implication here is that by looking at trace of uranium content in the argillaceous sediments, such as the Morrison Formation, one can possibly differentiate passage of ore solution. The overall background in sedimentary host rocks is generally low so that a reliable analytical method is an utmost necessity. DNAA meets this requirement and has a bright future for commercial application. It is the writer's opinion that uranium is still the best pathfinder element for sandstone-type uranium deposits barring analytical difficulty.

Secondly, since both humic and fulvic acids are known to complex with 2:1 type clay minerals (Schmidt-Collerus, 1967), organic carbon content in the clay-sized fraction must be examined. This may have limited application

on a local scale but a basin analysis on a regional scale should include this aspect to locate large humate masses.

The writer feels that, when the above analyses result in location of a favorable trend, analyses of accessory elements must be followed. Elements which appear to be particularly promising are REE, Ta, Sb, Br, As, V and a few other transitional group metals.

The suggestions made above may be of limited applicability for actual exploration at present time due to economics, analytical difficulty and other factors. However, as the drilling will certainly continue into deeper parts of the basin in the Grants Mineral Belt and elsewhere, the suggestions made here may actually lead to a saving of exploration cost.

Uranium Content of Various Rocks from the Grants Mineral Belt and Other
Selected Areas

Introduction

One of the problems that faces any investigator in dealing with the evolution of the Grants Mineral Belt (or any uranium deposit for that matter) is that of provenance. The general problem of provenance for the Grants Mineral Belt has been described earlier in this report; here I shall attempt to summarize recently determined uranium values for barren* (*used in the sense of subeconomic, i.e. some samples are in close proximity to known ore deposits whereas others are well removed from deposits) rocks from both the Grants Mineral Belt area and nearby Zuni Mountains and from the Precambrian granites and associated rocks of the Sandia Mountains and Pedernal Hills and from the Madera Formation (Late Pennsylvanian). The data were determined by the delayed neutron activation analysis (DNAA) technique at the Omega West Reactor Site at the Los Alamos Scientific Laboratory. This system was only recently completed and calibration of USGS standards completed with satisfactory precision in February 1976. The data for approximately 120 samples are presented in Table 13. The errors are as follows: for samples with greater than 10 ppm uranium the precision is $\pm 2-5$ percent; for 3 to 10 ppm, the precision is $\pm 5-10$ percent; and for less than 1 ppm, the precision is approximately ± 25 percent; and approximately ± 50 percent near 0.4 ppm. The reasons for this are as follows: (a) During initial calibration, standards in the 1.5 to higher concentrations were used with the exception of one dunite-diluted sample of USGS standard BCR-1 to 0.05 ppm; hence the calibration curves are heavily weighted by standards with more than 1 ppm uranium. (b) As samples to date have been chosen for near uniform weight (i.e. 1 to 1.5 grams) the counting statistics have been found to be poor in the 0.2 to 1 ppm range and background, reactor power drift and other factors prevent determinations below the 0.2 ppm level (even at ± 50 percent precision) at this time (note: this problem will be investigated in future work).

Results

The uranium analyses for the samples from the Jurassic Poison Canyon and Jackpile Sandstones and the Brushy Basin, Westwater Canyon and Recapture Members (Table 13; Sections V. A-E) have been discussed earlier (p.115) as have the samples from the Cretaceous Dakota Formation (Table 13; Section IV.).

The Jurassic Todilto Formation (Table 13; Section VI.) yields a mean of 1.39 ppm uranium for twelve samples, including both gypsiferous and carbonate rocks. Twelve additional samples (marked by an asterisk) contain less than about 0.2 ppm uranium and are not included in the mean. We suspect that, relative to other units, the Todilto Formation is in general low in uranium content even though mineralization has been reported from some areas. If the overall low content was due to removal of uranium by leaching, then other similar formations (i.e. see data for Madera Limestone; Table 13; Section VII.) might be similarly affected, and this is evidently not the case.

The rocks from the Precambrian Sandia granite and associated rocks (Table 13; Section I. A.-C.) are few in number but probably sufficient to indicate that, as might be expected, the granite contains more uranium than metamorphic rocks (Juan Tabo Series and Cibola Gneiss). The Juan Tabo Series contain numerous pegmatites presumably related to the Sandia Granite, but these have not yet been investigated. The Cibola Gneiss contains both meta-arkoses and quartzites; only sample 3014 is a quartzite and it is significantly lower in uranium content than the meta-arkoses.

We have examined nineteen Precambrian rocks from the Zuni Mountains (Table 13; Section II. A.-C.). Seven granite and/or aplite samples yield a mean of 3.71 ppm whereas seven metarhyolite samples yield an identical mean of 3.70 ppm. This is not surprising as the initial Rb-Sr systematics for these rocks (D.G. Brookins; unpublished data) indicate them to be coeval. Five Precambrian basic rocks from the Zuni Mountains yield a mean of 2.70 ppm uranium. It is perhaps

significant that the ruanium content for all the Precambrian Zuni Mountain rocks is in excess of 3 ppm as the ancestral Zuni Mountains must have provided abundant uranium during their destruction to the San Juan Basin.

Precambrian rocks from the Pedernal Hills are of interest as the Pedernals have fed detritus to the Estancia Basin since the latest Precambrian. Despite the low uranium content of the schists and quartzites and somewhat lower uranium content of the eleven granite samples (Table 13; Section III. A.), abundant uranium has been provided for incorporation into Phanerozoic rocks and may account for the relatively high values noted in the samples of the Madera Formation (Table 13; Section VII.).

The data for 17 samples of the Madera Formation and 2 samples of the Sandia Formation (see Mukhopadhyay, 1974, for locations and descriptions) yield a mean uranium content of 5.65 ppm. As these rocks are commonly referred to as 'barren' then the argument can be made that the relatively high means for the Brushy Basin and Recapture Members of the Morrison Formation (Table 13; Section V. C. and V. E. are not due to their proximity to the ore deposits of the Grants Mineral Belt. To resolve these and related questions, it is obvious that many more data from the so-called 'barren' rocks will be necessary; and this has been proposed for future studies.

Table 13

I. Sandia Mountains		II. C. <u>Basic rocks</u>		<u>ppm U</u>
A. <u>Granites</u>		Z115A		2.28
3001S	ppm U	Z115B		2.40
3002S	3.83	Z115C		2.64
3003S	6.45	Z115D		3.42
	3.09	Z115E		2.95
	mean = 4.46			
B. <u>Juan Tabo Series</u>				mean = 2.70
3004 a100	1.64	III. Pedernal Hills		
3004 a40	0.59	A. <u>Granites</u>		
3005 JT _s	1.42	4A		3.05
	mean = 1.22	4B		2.00
C. <u>Cibola Gneiss</u>		4C		1.77
3012A	2.62	4D		2.25
3013A	2.48	4E		2.02
3014	0.39	4F		2.08
3015	2.18	5A		3.60
	mean = 1.92	5B		3.10
II. Zuni Mountains		5C		2.73
A. <u>Granites and Aplites</u>		5D		2.76
Z101	3.35	5E		2.84
Z103	3.35			
Z105	3.24	mean = 2.56		
Z108	1.82	B. <u>Schists (greenstone)</u>		
Z112	3.77	1A		0.59
Z114	3.22	1B		0.30
Z104	7.23	1C		0.28
	mean = 3.71	1D		0.98
B. <u>Metarhyolite</u>				mean = 0.54
Z106	5.28	C. <u>Metaquartzites & Volcanics</u>		
Z109	2.61	2A		0.52
Z110	4.74	2B		1.86
Z111	3.19	2C		2.66
Z116	3.94	2D		2.08
Z117	3.62			mean = 1.78
Z118	2.54	D. <u>Schists (non-greenstones)</u>		
	mean = 3.70	3A		0.69
		3B		0.63
				mean = 0.66

Table 13 (continued)

IV. Dakota Formation	ppm U	V. E. Recapture Member	ppm U
TQKdl	0.63	TQJmr-1	4.0
TQKdb	0.51	TQJmr-2	5.42
MQKd	0.36	TQJmr-4	3.17
mean = 0.50		DLQJmr-1	10.5
		DLQJmr-2	21.1
V. Morrison Formation		DLQJmr-4	0.63
A. <u>Jackpile Sandstone</u>		DLQJmr-5	1.63
MQKd:Jmj	12.3	mean = 6.64	
LQJmj-5	4.87		
MQJmj-2	29.6	VI. Todilto Formation	
MQJmj-4	16.7	Jt-504L	2.98
MQJmj-1	3.5	Jt-302L	*
mean = 13.39		Jt-511G	1.29
B. <u>Poison Canyon Sandstone</u>		Jt-406G	*
TQJmpc-1	14.5	Jt-403G	*
TQJmpc-2	7.0	Jt-401G	*
DLQJmpc-1	7.1	Jt-204L	1.12
DLQJmpc-3	15.1	Jt-507G	1.03
DLQJmpc-4	31.3	Jt-402G	*
mean = 15.0		Jt-203L	0.73
C. <u>Brushy Basin Member</u>		Jt-301G	*
DLQ-Jmb-4	3.77	Jt-202L	0.87
DLQ-Jmb-1	10.8	Jt-108L	*
DLQ-Jmb-2	20.1	Jt-404G	*
LQ-Jmb-1	8.07	Jt-106G	*
LQ-Jmb-5	2.65	Jt-105L	*
mean = 9.08		Jt-303L	3.45
D. <u>Westwater Canyon Member</u>		Jt-103L	1.25
TQJmw-1	1.35	Jt-204L	1.18
TQJmw-3	2.25	Jt-201L	0.57
TQJmw-7	1.22	Jt-501G	1.47
TQJmw-9	2.46	Jt-508G	1.01
TQJmw-12	2.88	Jt-102L	*
TQJmw-11	1.87	Jt-407G	*
DLQJmw-4a	2.01	mean = 1.39	
DLQJmw-4b	10.2	(all samples except those	
DLQJmw-5	6.93	marked with an *)	
DLQJmw-6	10.3		
LQJmw-1	1.13		
LQJmw-5	0.91	(* = less than 0.2 ppm)	
LQJmw-7	3.62		
mean = 3.63		L = Limestone, G = Gypsum	

Table 13 (continued)

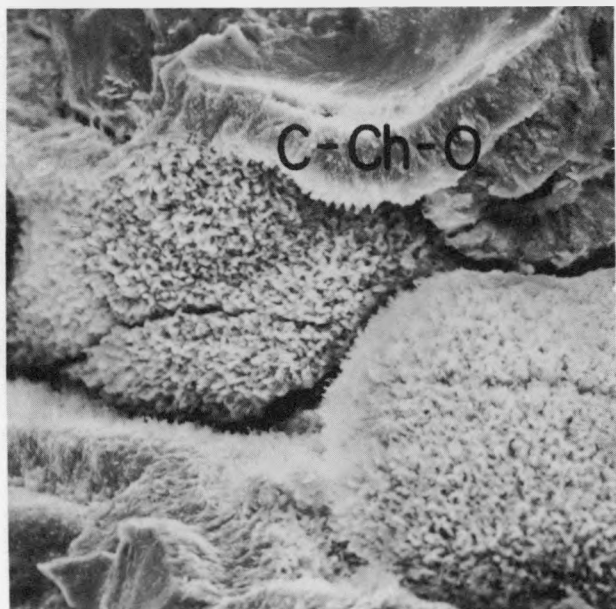
VII. Madera Formation (17) & Sandia Formation (2)

	<u>ppm U</u>	<u>Rock Type</u>
SNP4-1	2.05	coarse ss
SNP7-1	3.06	bedded ls
SNP6-2	3.53	mudstone
7SP1-2	8.05	sandstone (Sandia Formation)
7SP1-8	4.47	shaly ss (Sandia Formation)
7SP10-1	2.78	shale
SH-7	4.94	calcareous shale
SH2-3	16.9	sandy shale
SH3-4	6.17	shaly ls
SH4-3	5.87	shale with coal lenses
SH5-6	7.26	nodular ls
SH8-3	8.79	nodular ls
KQ4-1	4.77	bedded ls
KQ5-1	1.68	bedded ls
KQ7-1	1.77	bedded ls
KQ8-1	3.28	bedded ls
TRS1-A	15.5	bedded ls
TRS8	2.26	bedded ls
TRS2-3	4.19	bedded ls

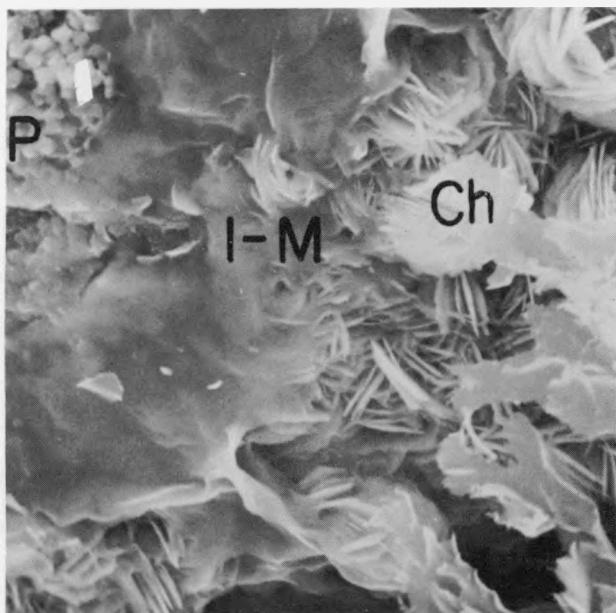
mean = 5.65

Explanation for Plate IA. Electron photomicrograph showing coatings of coffinite-chlorite-OCM mixture of high grade ore.

Explanation for Plate IB. Electron photomicrograph showing close spatial relationship of pyrite (P), illite-montmorillonite (I-M), and chlorite (Ch); the formation of chlorite from illite-montmorillonite is obvious.



— 25 Microns



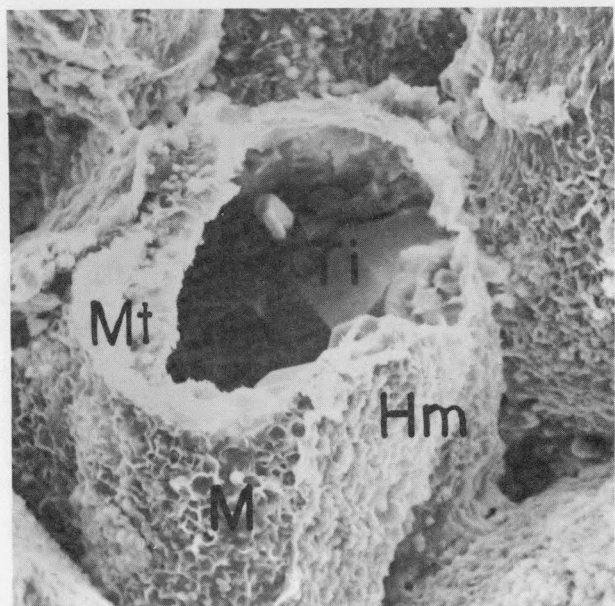
— 25 Microns

PLATE I

Explanation for Plate IIA. Electron photomicrograph of corroded magnetite (Mt) coated with montmorillonite (M) and hematite (Hm). Authigenic Ti-oxides (Ti) have been formed inside the corroded magnetite grain.

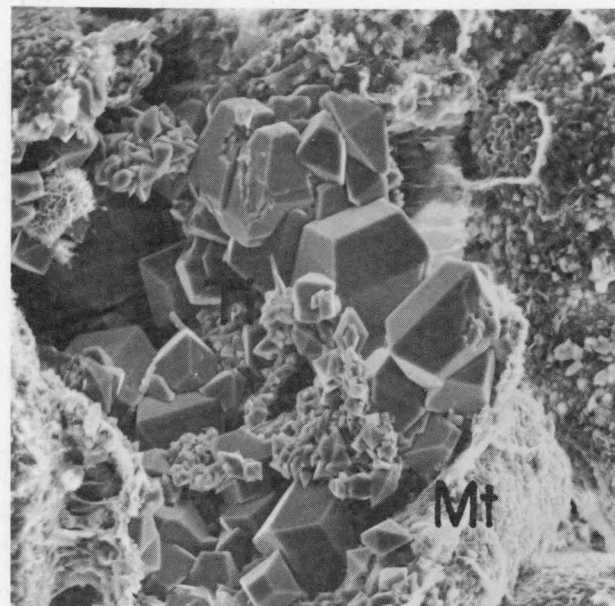
Explanation for Plate IIB. Electron photomicrograph of the authigenic Ti-oxides (Ti) shown in Plate IIA. The smaller octahedrons are probably anatase whereas the longer, prismatic crystals are thought to be rutile. The magnetite (Mt) here is almost entirely corroded.

A



— 20 Microns

B



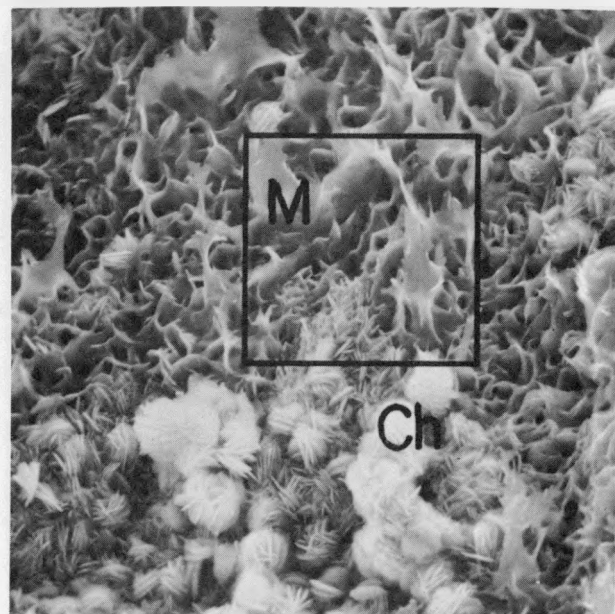
— 25 Microns

PLATE II

Explanation for Plate IIIA. Electron photomicrograph showing cellular montmorillonite (M) and rosettes of chlorite (Ch). The chlorite is forming from the montmorillonite.

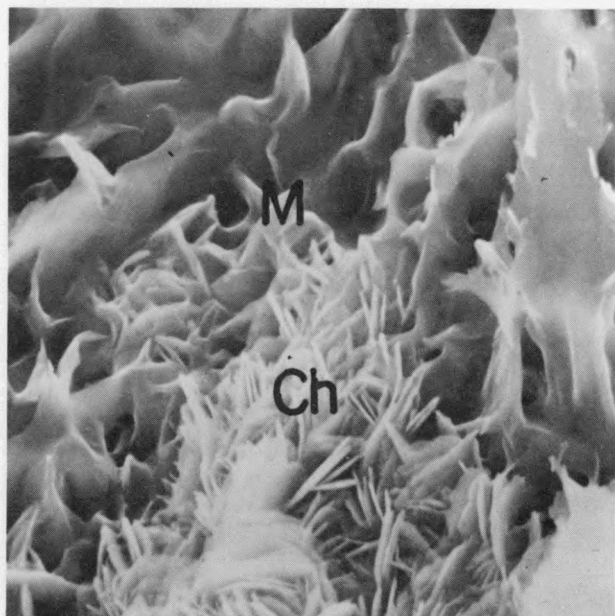
Explanation for Plate IIIB. A higher magnification of Plate IIIA. The montmorillonite to chlorite transformation is apparent.

A



— 6 Microns

B



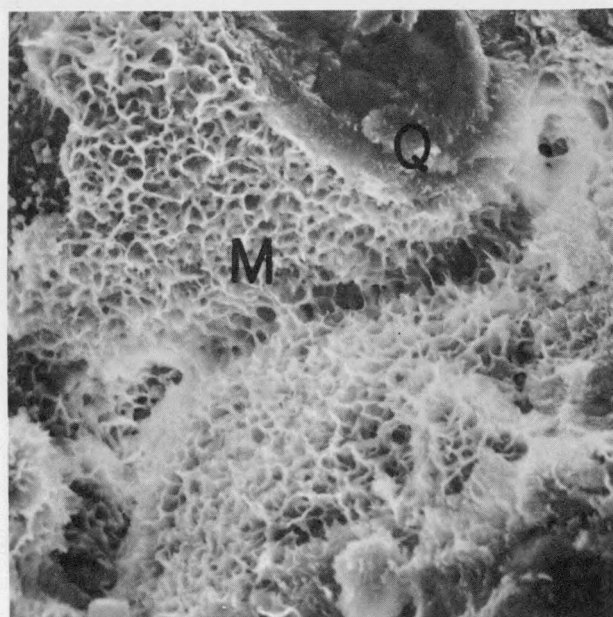
— 2 Microns

PLATE III

Explanation for Plate IVA. Electron photomicrograph of well crystallized montmorillonite (M); its interlocking texture is indicative of authigenic formation. The detrital grain is quartz (Q).

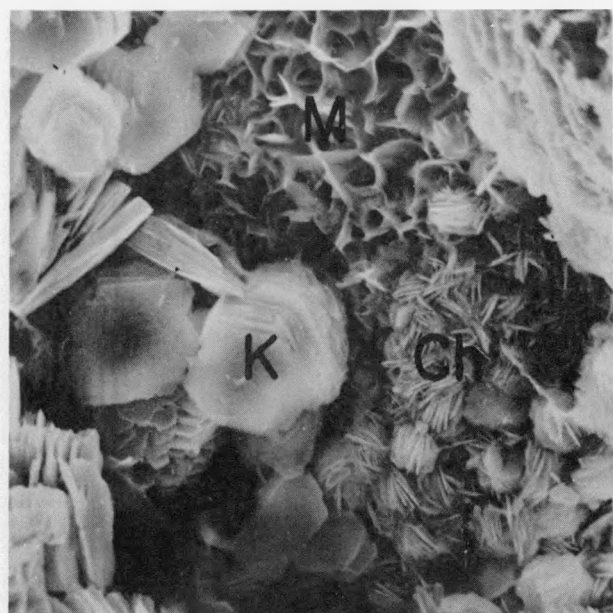
Explanation for Plate IVB. Electron photomicrograph showing some of the major varieties of clay minerals from the Westwater Canyon Member. The montmorillonite (M) is authigenic and in the process of being transformed into chlorite (Ch); the pseudo-hexagonal booklets of kaolinite (K) are the last to form.

A



— 15 Microns

B



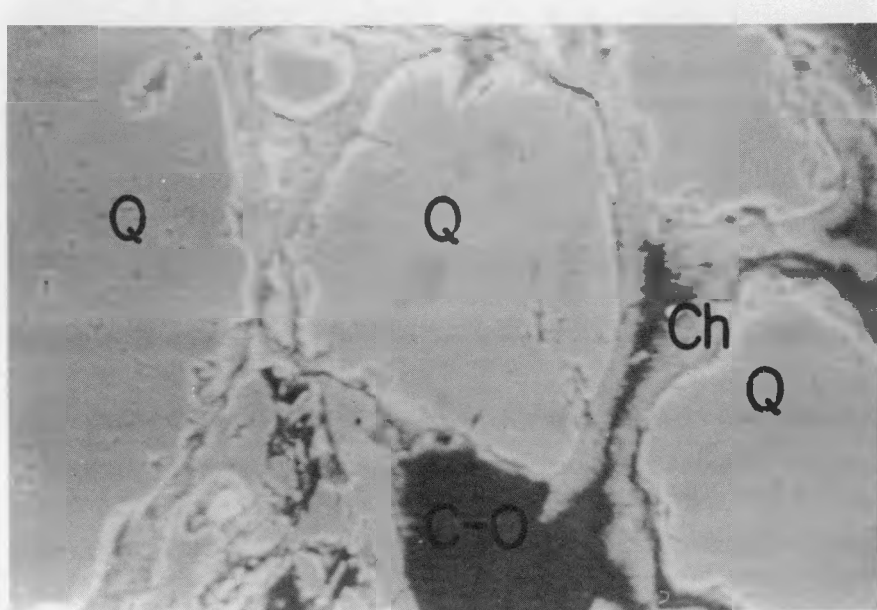
— 5 Microns

PLATE IV

Explanation for Plate VA. Electron microprobe photomicrograph of a polished section showing detrital quartz (Q), chlorite (Ch) rimming grains, and a coiffinite-OCM (C-O) mixture.

Explanation for Plate VB. 'Vanadium' x-ray photomicrograph of the section shown in Plate VA; The vanadium distribution is shown by the "light" intensity; this plate demonstrates that the chlorite is a vanadiferous variety.

A



30 Microns

B

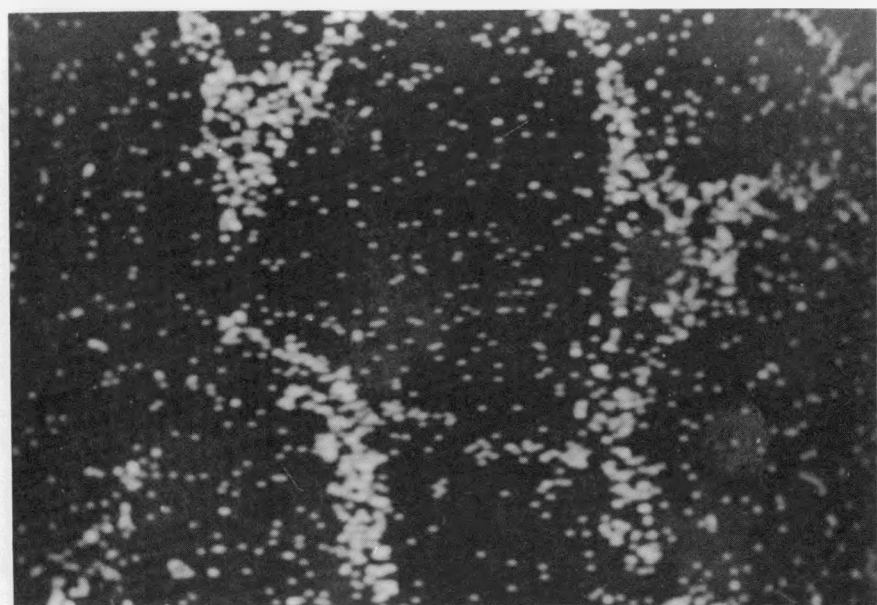


PLATE V

REFERENCES CITED

Adams, S. S., Hafen, P. L., and Salek-Nejad, H., 1975, Aspects of detrital and authigenic mineralogy of the Jackpile Sandstone, northwestern New Mexico; (abs.) Am. Assoc. Petrol. Geologists, Rocky Mtn. Section, 24th Annual Meeting, p. 8.

Altschuler, Z. S., Dwornick, E. J., and Kramer, H., 1963, Transformation of montmorillonite to kaolinite during weathering; Science, v. 141, p. 148-152.

Andreyev, P. F., and Chumachenko, A. P., 1964, Reduction of uranium by natural organic substances; Geochem. International, v. 1, p. 3-7.

Austin, S. R., 1963, Alteration of Morrison Sandstone; in op cit, New Mexico Bur. Mines and Min. Res., Memoir 15, p. 38-44.

Baker, A. A., Dane, C. H., and Reeside, J. B., Jr., 1936, Correlation of Jurassic formations of parts of Utah, Arizona, New Mexico, and Colorado; U. S. Geol. Survey Prof. Paper 183, 66p.

Bassett, W. A., Kerr, P. F., Schaffer, O. A., and Stoener, R. W., 1963, Potassium-argon ages of volcanic rocks near Grants, New Mexico; Geol. Soc. America Bull., v. 74, p. 221-226.

, 1963b, Potassium-argon ages of volcanic rocks north of Grants; in Geology and Technology of the Grants Uranium Region, Kelley, V. C., ed., New Mexico Bur. Mines and Min. Res., Memoir 15, p. 214-216.

Bayliss, P., Loughnan, F. C., and Standard, J. C., 1965, Dickite in the Hawkesbury Sandstone of the Sydney Basin; Am. Mineralogists, v. 50, p. 418-426.

Brookins, D. G., 1973, Grants, New Mexico, U deposits: Revised Eh-pH constraints for primary minerals; Trans. Amer. Geophys. Union, v. 54, p. 1228.

, 1975, Coffinite-uraninite stability relations in the Grants Mineral Belt; Am. Assoc. Petrol. Geol. Bull., v. 59, p. 905.

Brown, B. E., and Bailey, S. W., 1962, Chlorite polytypism, Pt. I, Regular and semi-random one-layer structures; Am. Mineralogists, v. 47, p. 819-850.

Cadigan, R. A., 1967, Petrology of the Morrison Formation in the Colorado Plateau Region; U. S. Geol. Survey, Prof. Paper 556, 113p.

Carroll, D., 1970, Clay Minerals: A guide to their x-ray identification; Geol. Soc. America, Special Paper 126, 80p.

Clark, D. S., and Havenstrite, S. R., 1963, Geology and ore deposits of the Cliffside Mine, Ambrosia Lake Area; in op cit, New Mexico Bur. Mines and Min. Res., Memoir 15, p. 108-116.

Cooley, M. E., and Davidson, E. S., 1963, The Mogollon Highlands - Their influence on Mesozoic and Cenozoic erosion and sedimentation; Arizona Geol. Soc. Digest, v. 6, p. 7-36.

Craig, L. C., Holmes, C. N., Cadigan, R. A., Freeman, V. L., Mullens, T. E., and Weir, G. W., 1955, Stratigraphy of the Morrison and related formations: Colorado Plateau region - A preliminary report; U. S. Geol. Survey Bull., v. 1009E, p. 125-168.

_____, 1959, Measured sections of the Morrison Formation and adjacent formations; U. S. Geol. Survey Open-file Report, 700p.

Demolin, A., and Barbier, G., 1929, Conditions de formation et constitution du complexe argilohumique des sols; Compt. Rend., v. 188, p. 654-656.

Dodge, C. N., Pebbles from the Chinle and Morrison Formations; New Mexico Geol. Soc., 24th Field Conf. Guidebook, p. 114-121.

Dooley, J. R., Jr., Granger, H. C., and Rosholt, J. H., Jr., 1966, Uranium-234 fractionation in the sandstone-type uranium deposits of the Ambrosia Lake District, New Mexico; Econ. Geology, v. 61, p. 1362-1382.

Eberl, D. D., 1970, Low temperature synthesis of kaolinite from amorphous material at neutral pH; (abs.) 19th Annual Clay Min. Conference, Miami Beach, Florida.

Emmons, S. F., Cross, W., and Eldridge, G. H., 1896, Geology of the Denver Basin in Colorado; U. S. Geol. Survey Mon. 27, 556p.

Fitch, R., 1961, Let's look at Lance's uranium mines; Mining World, v. 23, p. 23-27.

Flesch, G. A., 1974, Stratigraphy and Sedimentology of the Morrison Formation (Jurassic), Ojito Spring Quadrangle, Sandoval County New Mexico: A preliminary discussion; New Mexico Geol. Society, 25th Field Conf. Guidebook, p. 185-195.

Folk, R. L., 1968, Petrology of sedimentary rocks; Hemphill's, Austin, Texas, 170p.

Foster, M. D., 1959, Chemical study of the mineralized clays; U. S. Geol. Survey, Prof. Paper 320, p. 121-132.

Freeman, V. L., and Hilpert, L. S., 1956, Stratigraphy of the Morrison Formation in part of northeastern New Mexico; U. S. Geol. Survey Bull., v. 1030-J, p. 309-334.

Fuchs, L. H., and Hoekstra, H. R., 1959, The preparation and properties of uranium (IV) silicate; Am. Mineralogist, v. 44, p. 1057-1063.

Garrels, R. M., and Pommer, A. M., 1959, Some quantitative aspects of the oxidation and reduction of the ores; U. S. Geol. Survey Prof. Paper 320, p. 157-164.

Garrels, R. M., and Christ, C. L., 1965, Solutions, Minerals, and Equilibria; Harper and Row, New York, 450p.

Granger, H. C., 1962, Clays in the Morrison Formation and their spatial relationship to the uranium deposits at Ambrosia Lake, New Mexico; U. S. Geol. Survey, Prof. Paper 450-D, p. 15-20.

_____, 1963a, Mineralogy, in op cit, New Mexico Bur. Mines, Memoir 15, p. 21-37.

_____, 1963b, Radium migration and its effect on the apparent age of uranium deposits at Ambrosia Lake, New Mexico; U. S. Geol. Survey Prof. Paper 475B, p. B60-63.

_____, 1966, Ferroselite in a roll-type uranium deposit, Powder River Basin, Wyoming; U. S. Geol. Survey Prof. Paper 550-C, p. 133-137.

_____, 1968, Localization and control of uranium deposits in the southern San Juan Basin Mineral Belt, New Mexico - An hypothesis; U. S. Geol. Survey Prof. Paper 600B, p. B60-70.

_____, Santos, E. S., Dean, B. G., and Moore, F. B., 1961, Sandstone-type uranium deposits at Ambrosia Lake, New Mexico--An interim report; Econ. Geology, v. 56, p. 1179-1210.

_____, and Ingram, B. L., 1966, Occurrence and identification of jordisite at Ambrosia Lake, New Mexico; U. S. Geol. Survey Prof. Paper 550B, p. 120-124.

_____, and Santos, E. S., 1963, An ore-bearing cylindrical collapse structure in the Ambrosia Lake uranium district, New Mexico; U. S. Geol. Survey Prof. Paper 475-C, p. 156-161.

Green, M. W., 1975, Paleodepositional units in Upper Jurassic rocks in Gallup-Laguna area, N. M.; Am. Assoc. Petrol. Geol. Bull., v. 59, p. 910.

Grim, R. E., 1968, Clay Mineralogy (2nd Ed.), McGraw-Hill, NY, 596p.

Gruner, J. W., 1959, The decomposition of ilmenite; Econ. Geology, v. 54, p. 1315-1316.

_____, Rosenzweig, A., and Smith, D. K., 1955, The problem of coffinite; U. S. Atomic Energy Comm., RME 3020, p. 16-24.

Haji-Vassiliou, A., and Kerr, P. F., 1973, Analytical data on nature of urano-organic deposits; Am. Assoc. Petrol. Geologists, Bull., v. 57, p. 1291-1296.

Harshbarger, J. W., Repenning, C. A., and Irwin, J. M., 1957, Stratigraphy of the uppermost Triassic and the Jurassic rocks of the Navajo Country; U. S. Geol. Survey, Prof. Paper 291, 74p.

Harshman, E. N., 1972, Geology and uranium deposits, Shirley Basin Area, Wyom.; U. S. Geol. Surv. Prof. Paper 745, 82p.

Hayes, J. B., 1970, Polytypism of chlorite in sedimentary rocks; Clays and Clay Minerals, v. 18, p. 285-306.

Hazlett, G. W., and Greek, J., 1963, Geology and ore deposits of the south-eastern part of the Ambrosia Lake Area; in op cit, New Mexico Bur. Mines and Min. Res., Memoir 15, p. 82-89.

Helgeson, H. E., Brown, T. H., and Leeper, R. H., 1969, Handbook of theoretical activity diagrams depicting chemical equilibria in geologic systems involving an aqueous phase at one atm. and 0 to 300°C; Freeman, Cooper and Co., San Francisco, 253p.

Hem, J. D., 1960, Complexes of ferrous iron with tannic acid; U. S. Geol. Survey, Water Supply Paper 1459-D, p. 75-94.

Hess, P. C., 1966, Phase equilibria of some minerals in the $K_2O-Na_2O-Al_2O_3-SiO_2-H_2O$ system at 25°C and 1 atmosphere; Am. Jour. Sci., v. 264, p. 289-309.

Hilpert, L. S., 1963, Regional and local stratigraphy of uranium-bearing rocks; in op cit New Mexico Bur. Mines and Min. Res., Memoir 15, p. 6-18.

, and Corey, A. F., 1957, Regional synthesis studies - north-west New Mexico; U. S. Geol. Survey TEI 690, p. 365-381.

Hoekstra, H. R., and Fuchs, L. H., 1956, Synthesis of coffinite- USiO_4 ; Science, v. 123, p. 105.

Hoskins, W. G., 1963, Geology of the Black Jack No. 2 Mine, Smith Lake Area; in op cit New Mexico Bur. Mines and Min. Res., Memoir 15, p. 49-52.

Hostetler, P. B., and Garrels, R. M., 1962, Transportation and precipitation of uranium and vanadium at low temperatures with special reference to sandstone-type uranium deposits: Econ. Geology, v. 57, p. 137-167.

Hower, J., and Mowatt, T. C., 1966, The mineralogy of illites and mixed-layer illite/montmorillonite: *Am. Mineralogist*, v. 51, p. 825-853.

Hunt, C. B., 1956, Igneous geology and structure of the Mount Taylor volcanic field, New Mexico: U. S. Geol. Survey, Prof. Paper 189-B, 80p.

Huang, W. H., and Keller, W. D., 1970, Dissolution of rock-forming silicate minerals in organic acids: Simulated first-stage weathering of fresh minerals surfaces: *Am. Mineralogist* v. 55, p. 2076-2094.

Huang, W. H., and Keller, W. D., 1971, Dissolution of clay minerals in dilute organic acids at room temperature; *Am. Mineralogist*, v. 56, p. 1082-1095.

_____, 1972a, Organic acids as agents of chemical weathering of silicate minerals; *Nature*, v. 239, p. 149-151.

_____, 1972b, Geochemical mechanics for the dissolution, transport and deposition of aluminium in the zone of weathering; *Clays and Clay Minerals*, v. 20, p. 69-74.

Imlay, R. W., 1952, Correlation of the Jurassic Formations of North America, exclusive of Canada; *Geol. Soc. America Bull.*, v. 63, p. 953-992.

Jackson, M. L., Interlayering of expandible layer silicates in soils by chemical weathering; *Clays and Clay Minerals*, v. 11, p. 29-56.

Jacobs, M. L., Warren, C. G., and Granger, H. C., 1970, Chemical extraction of an organic material from uranium ore; *U. S. Geol. Survey Prof. Paper 700B*, p. 184-186.

Keller, W. D., 1962, Clay minerals in the Morrison Formation of the Colorado Plateau; *U. S. Geol. Survey Bull.* 1150, 90p.

Kelley, V. C., 1955, Regional tectonics of the Colorado Plateau and relationships to the origin and distribution of uranium; *Univ. New Mexico Publications in Geology*, No. 5, Albuquerque, New Mexico, 120p.

_____, Ed., 1963, Geology and technology of the Grants uranium region; *New Mexico Bur. Mines and Min. Res.*, Memoir 15, 277p.

_____, and Clinton, N. J., 1958, Fracture systems and tectonic elements of the Colorado Plateau; *U. S. Atomic Energy Comm.*, RME-108, 107p.

Kendall, E. W., 1971, Trend ore bodies of the Section 27 Mine, Ambrosia Lake uranium district, New Mexico; *Unpub. Ph. D. Thesis*, Univ. of California, Berkeley, 167p.

Kittel, D. F., 1963, Geology of the Jackpile Mine Area; *in New Mexico Bur. Mines*, Memoir 15, p. 167-176.

Konigsmark, T. A., 1955, Color changes and uranium deposits of the upper Morrison Formation northeast flank of the Zuni Uplift, New Mexico; *U. S. Atomic Energy Comm.*, RME-76, 15p.

Lee, W. T., 1902, The Morrison Shales of southern Colorado and northern New Mexico; *Jour. Geology*, v. 10, p. 36-58.

_____, 1917, Geology of the Raton Mesa and other regions in Colorado and New Mexico; *U. S. Geol. Survey Prof. Paper 101*, p. 9-221.

Linares, J., and Huertas, F., 1971, Kaolinite synthesis at room temperature; *Science*, v. 171, p. 896-897.

Ludwig, K. R., 1975, Uranium-lead apparent isotope ages of pitchblendes, Shirley Basin, Wyo.; Am. Assoc. Petrol. Geol. Bull., v. 59, p. 915.

MacEwan, D. M. C., 1961, Montmorillonite minerals; in The x-ray identification and crystal structures of clay minerals, Brown, G., Ed., Min. Soc. London, p. 143-207.

MacRae, M. E., 1963, Geology of the Black Jack No. 1 Mine, Smith Lake Area; in New Mexico Bur. Mines, Memoir 15, p. 45-48.

Maxwell, G. T., and Hower, J., 1967, High-grade diagenesis and low-grade metamorphism of illite in the Precambrian Belt; Am. Mineralogist, v. 52, p. 843-857.

Millot, G., 1970, Geology of clays; Springer Verlag, New York, 388p.

Moench, R. H., 1963, Geologic limitations on the age of uranium deposits in the Laguna District; in op cit New Mexico Bur. Mines, Memoir 15, p. 157-166.

_____, and Schlee, J. S., 1967, Geology and uranium deposits of the Laguna District, New Mexico; U. S. Geol. Survey Prof. Paper 519, 117p.

Nash, J. T., 1968, Uranium deposits in the Jackpile Sandstone, New Mexico; Econ. Geology, v. 63, p. 737-750.

_____, and Kerr, P. F., 1966, Geologic limitations on the age of uranium deposits in the Jackpile Sandstone, New Mexico; Econ. Geology, v. 61, p. 1283-1287.

O'Sullivan, R. B., and Craig, L. C., 1973, Jurassic rocks of northeast Arizona and adjacent areas; New Mexico Geol. Soc., 24th Field Conf. Guidebook, p. 79-85.

Phoenix, D. A., 1959, Occurrence and chemical character of groundwater in the Morrison Formation; U. S. Geol. Survey Prof. Paper 320, p. 55-64.

Pierce, J. W., and Siegel, F. R., 1969, Quantification in clay mineral studies of sediments and sedimentary rocks; Jour. Sed. Petrology, v. 39, p. 187-193.

Pommer, A. M., 1957, Reduction of quinquevalent vanadium solutions by wood and lignite; Geochim. Cosmochim. Acta, v. 13, p. 20-27.

Rapaport, I., 1963, Uranium deposits of the Poison Canyon ore trend Grants District; in op cit New Mexico Bur. Mines, Memoir 15, p. 122-135.

_____, Hadfield, J. P., and Olson, R. H., 1952, Jurassic rocks of the Zuni Uplift, New Mexico; U. S. Atomic Energy Comm., RMO 642.

Renick, B. C., 1931, Geology and ground-water resources of western Sandoval County, New Mexico; U. S. Geol. Survey Water-Supply Paper 620, 117p.

Repennig, C. A., Cooley, M. E., and Akers, J. P., 1969, Stratigraphy of the Chinle and Moenkopi Formations, Navajo and Hopi Indian Reservations, Arizona, New Mexico, and Utah; U. S. Geol. Survey Prof. Paper 521-B, 34p.

Rich, C. I., 1968, Hydroxy interlayers in expandible layer silicates; *Clays and Clay Minerals*, v. 16, p. 15-30.

Robie, R. A., and Waldbaum, D. R., 1968, Thermodynamic properties of minerals and related substances at 298.15°K (25.00°C) and one atmosphere (1.013 bars) pressure and at higher temperatures; *U. S. Geol. Survey Bull.* 1259, 256p.

Rubin, B., 1970, Uranium roll front zonation in the southern Powder River Basin, Wyoming; *Wyoming Geol. Assoc., Earth Sci. Bull.*, v. 5, p. 5-12.

Sand, L. B., and Baur, G. S., 1959, Genesis of kaolinite in Cretaceous shales of central Colorado; *Clay and Clay Min.*, v. 6, p. 188-196.

Santos, E. S., 1963, Relation of ore deposits to the stratigraphy of host rocks in the Ambrosia Lake Area; in op cit *New Mexico Bur. Mines Memoir 15*, p. 53-59.

_____, 1970, Stratigraphy of the Morrison Formation and structure of the Ambrosia Lake District, New Mexico; *U. S. Geol. Survey Bull.*, v. 1272E, 27p.

_____, 1975, Lithology and uranium potential of Jurassic formations in San Ysidro - Cuba and major ranch areas, northwestern New Mexico; *U. S. Geol. Survey Bull.* 1329, 22p.

Saucier, A. E., 1974, Stratigraphy and uranium potential of the Burro Canyon Formation in the southern Chama Basin, New Mexico; *N. M. Geol. Soc. Gdbk.*, No. 25, p. 211-218.

Schlee, J. S., and Moench, R. H., 1961, Properties and genesis of Jackpile Sandstone, Laguna New Mexico; *Am. Assoc. Petrol. Geologists Bull.*, v. 62, p. 134-160.

Schmidt-Collerus, J. J., 1969, Investigations of the relationship between organic matter and uranium deposits, Part II - Experimental investigations; Univ. Denver, Denver Res. Institute, Report 2513, 192p.

Sharp, J. V. A., 1955, Uranium deposits in the Morrison Formation, Churchrock Area, McKinley County, New Mexico; *U. S. Atomic Energy Comm.*, RME-79, 19p.

Shawe, D. R., Archbold, N. L., and Simmons, G. D., 1959, Geology and uranium-vanadium deposits of the Slick Rock District, San Miguel and Dolores Counties, Colorado; *Econ. Geology*, v. 54, p. 395-415.

Smith, C. T., 1959, Jurassic rocks of the Zuni Mountains; *New Mexico Geol. Soc. 10th Field Conf.*, Guidebook, p. 74-80.

Smith, J. V., and Yoder, H. S., 1956, Experimental and theoretical studies of the mica polymorphs; *Min. Magazine*, v. 31, p. 209-235.

Squyres, J. B., 1969, Origin and depositional environment of uranium deposits of the Grants Region, New Mexico; Unpub. Ph. D. Thesis, Stanford University, 228p.

Stevenson, F. J., and Butler, J. H. A., 1969, Chemistry of humic acids and related pigments; in Organic geochemistry, methods and results, Eglington, G., and Murphy, J. T. J., Eds., Springer Verlag, New York, p. 535-557.

Stewart, J. H., Poole, F. G., and Wilson, R. F., 1972, Stratigraphy and origin of the Chinle Formation and related Upper Triassic strata in the Colorado Plateau region; U. S. Geol. Survey Prof. Paper 690, 336p.

Stieff, L. R., Stern, T. W., and Sherwood, A. M., 1956, Coffinite, a uranous silicate with hydroxyl substitution - A new mineral; Am. Mineralogist, v. 41, p. 675-688.

Strobell, J. D., 1956, Geology of the Carrizo Mountains area in northeastern Arizona and northwestern New Mexico; U. S. Geol. Survey Oil and Gas Inv. Map OM-160.

Swain, F. M., 1963, Geochemistry of humus; in Organic geochemistry, Breger, I. A., Ed., MacMillan and Co., p. 183-247.

Szalay, A., 1964, Sorption of uranium by humic acid; Geochim. Cosmochim. Acta, v. 28, p. 1605-1614.

_____, and Szilagyi, M., 1968, Accumulation of microelements in peat humic acids and coal; in Advances in organic geochemistry, Schenck, D. A., and Havenar, I., Ed., Pergamon Press, p. 567-578.

Tardy, Y., and Garrels, R. M., 1974, A method of estimating the Gibbs energies of formation of layer silicates; Geochim. Cosmochim. Acta., v. 38, p. 1101-1116.

Thaden, R. E., Santos, E. S., and Raup, O. B., 1967, Geologic map of the Grants Quadrangle Valencia County, New Mexico; U. S. Geol. Survey Geol. Quad. Map GQ-681.

Theng, B. K. G., 1974, The chemistry of clay-organic reactions; John-Wiley and Sons, New York, 343p.

Velde, B., 1965, Experimental determination of muscovite polymorphs stabilities; Am. Mineralogist, v. 50, p. 436-449.

_____, and Hower, J., 1963, Petrological significance of illite polymorphism in Paleozoic sedimentary rocks; Am. Mineralogist, v. 48, p. 1239-1254.

Vine, J. D., 1962, Geology of uranium in coaly carbonaceous rocks; U. S. Geol. Survey Prof. Paper 356-D, p. 113-170.

Warren, C. G., 1968, The synthesis of ferroselite from an aqueous solution at low temperature; Econ. Geology, v. 63, p. 418-419.

Weaver, C. E., 1958, The effects and geologic significance of potassium "fixation" by expandable clay minerals derived from muscovite, biotite, chlorite and volcanic material; Am. Mineral., v. 43, p. 839-861.

Weaver, C. E., and Ball, D. F., 1966, Chlorite minerals in ordovician pumice-tuff and derived soils in Snowdonia, North Wales; *Clay Miner.*, v. 6, p. 195-209.

Weaver, C. E., and Beck, K. C., 1971, Clay water diagenesis during burial: How much becomes gneiss; *Geol. Soc. America, Special Paper 134*, 96p.

Weege, R. J., 1963, Geologic of the Marquez Mine, Ambrosia Lake area; in op cit New Mexico Bur. Mines, Memoir 15, p. 117-121.

Weeks, A. D., Coleman, R. G., and Thompson, M. E., 1959, Summary of the ore mineralogy; *U. S. Geol. Survey Prof. Paper 320*, p. 65-79.

Weiss, A., 1969, Organic derivatives of clay minerals, zeolites and related minerals; in *Organic geochemistry*, op cit, 828p.

Yoder, H. S., and Eugster, H. D., 1955, Synthetic and natural muscovites; *Geochim. Cosmochim. Acta*, v. 8, p. 225-280.

York, D., 1966, Least squares fitting of a straight line; *Can. Jour. Phys.*, v. 44, p. 107-110.

Young, R. G., 1960, Dakota Group of the Colorado Plateau; *Am. Assoc. Petro1. Geologists*, v. 44, p. 156-184.

Zunino, H., Appelt, H., and Bernardi, C., 1974, Influence of extracted aluminum on organic matter fractionation in soils derived from volcanic ash; *Soil Science*, v. 115, p. 28-30.

ADDITIONAL REFERENCES

Gale, N. H., 1967, Development of delayed neutron technique as rapid and precise method for determination of uranium and thorium at trace levels in rocks and minerals, with applications to isotope geochronology. In: Radioactive Dating and Methods of Low-Level Counting. International Atomic Energy Agency, Vienna, p. 431-452.

Gordon, G. E., Randle, K., Goles, G. G., Corlis, J. B., Beeson, M. H. and Oxley, S. S., 1968, Instrumental activation analysis of standard rocks with high-resolution γ -ray detectors. *Geochim. Cosmochim. Acta*, v. 32, p. 369-396.

Cumming, G. L., 1974, Determination of uranium and thorium in meteorites by the delayed neutron method; *Chemical Geology*, v. 13, p. 257-267.

Goldschmidt, V. M., 1958, *Geochemistry*; Oxford Univ. Press, London, 730 p.

Shoemaker, E. M., Miesch, A. T., Newman, W. L., and Riley, L. B., 1959, Elemental composition of the sandstone-type deposits: in op. cit. U. S. Geol. Survey Prof. Paper 320, p. 25-54.

Wood, H. R., 1968, Geology and exploitation of uranium deposits in the Lisbon Valley area, Utah, Graton-Sales Volume, J. D. Ridge, ed., v. 1, p. 771-789.

APPENDIX A. Laboratory Procedure for Clay Mineral Analyses Size Fractionation of Clay Minerals

About 500 grams of air-dried sample were put in a beaker and covered with distilled water for 48 hours. The disaggregated material was wet-sieved through a 230-mesh screen and the finer fraction was repeatedly centrifuged until dispersion could be effected. No dispersing agent was used in this study. The washed slurry was put in 1000 ml cylinders for gravity settling. The length of time necessary for settling was calculated from the equation given by Folk (1968, p. 40). Fractions finer than 0.5 to 2 microns were siphoned off after proper length of settling time and the slurry was used for oriented slides, random powders and cation saturation. The bulk of the slurry was dried for geochemical and Rb-Sr isotopic analyses.

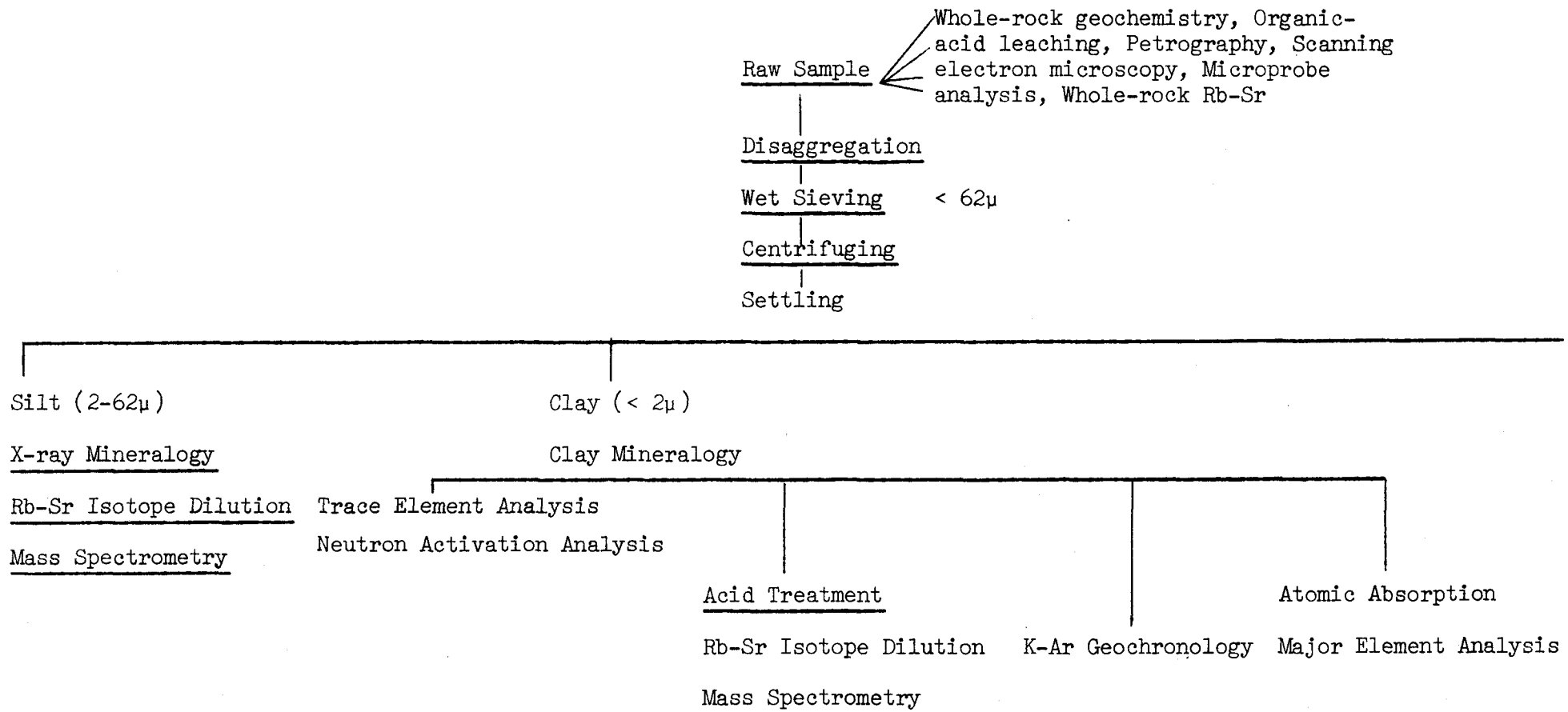
X-ray Diffraction

Identification of clay minerals was solely based on x-ray diffraction, using a Norelco wide range diffractometer. Untreated and random powders, as well as silt-sized fractions for other mineralogical studies, were scanned from 2 to 62 or 2 to 90 degrees two theta with Ni-filtered $\text{CuK}\alpha$ radiation. Additional diffractograms for glycolated and heated samples were run from 2 to 30 inch/hr., using a time constant of two seconds; a scintillation counter detector and pulse height analyzer. The goniometer slit system was composed of a divergent and anti-scatter slits of one degree and a 0.003 inch receiving slit.

Sample Treatment

Oriented slides were vapor-soaked with ethylene glycol and heated at 450°C and 600°C for proper clay mineral identification. When additional information was needed, the clay slurry was treated with 2N HCl for 10 hours at 60°C or it was saturated with 1N chloride or nitrate salt solutions of K^+ , Mg^{2+} and Ca^{2+} .

FLOW SHEET



APPENDIX B. Rb-Sr Data
 Montmorillonite-rich Samples, Ambrosia Lake District
 Section 23 and 35 (< 2 μ fraction)

Sample No.	Rb ppm	Sr ppm	Rb/Sr	$^{87}\text{Rb}/^{86}\text{Sr}$	$^{87}\text{Sr}/^{86}\text{Sr}$
2037(mudgall)	127.0	36.8	3.45	10.0306	0.7276
23-316	127.5	80.0	1.59	4.6168	0.7140
23-311	134.2	99.9	1.34	3.8911	0.7133
35-51	125.0	77.5	1.61	4.6744	0.7184
35-207	163.4	46.7	3.50	10.0516	0.7193
35-212	210.6	47.9	4.40	12.7565	0.7302
35-206	111.2	45.7	2.43	7.0518	0.7186
35-211	205.6	52.0	3.95	11.4737	0.7321
35-305	132.6	55.8	2.38	6.8869	0.7186
Jpc-1	97.4	51.0	1.91	5.5348	0.7221

Chlorite-rich Samples, Ambrosia Lake District
Sections 23 and 35 ($< 2\mu$ fraction)

Sample No.	Rb ppm	Sr ppm	Rb/Sr	$^{87}\text{Rb}/^{86}\text{Sr}$	$^{87}\text{Sr}/^{86}\text{Sr}$
AL 23-302	59.3	101.2	0.586	1.6972	0.7128
AL 23-303	34.6	75.7	0.457	1.3238	0.7118
AL 23-307	49.1	39.2	1.25	3.6295	0.7174
AL 23-313	26.4	59.8	0.441	1.2780	0.7103
AL 23-314	61.1	105.3	0.580	1.6805	0.7115
AL 2038	34.4	38.6	0.891	2.5817	0.7144
AL 35-208	109.8	42.1	2.61	7.5621	0.7235
AL 35-209	22.5	49.2	0.457	1.3245	0.7117
AL 23-304	89.9	228.8	0.393	1.1380	0.7119

Chlorite-rich, Smith Lake Core Samples
 < 2 μ fraction ore samples

Sample No.	Rb ppm	Sr ppm	Rb/Sr	$^{87}\text{Rb}/^{86}\text{Sr}$	$^{87}\text{Sr}/^{86}\text{Sr}$
SL 168	120.8	103.2	1.17	3.3920	0.7179
SL 166	74.7	18.9	3.95	11.4714	0.7337
SL 169-171	90.0	60.3	1.49	4.3254	0.7182
SL 165	103.3	30.6	3.38	9.7946	0.7303
SL 158	133.5	54.9	2.43	7.0492	0.7215
SL 159	81.7	38.6	2.12	6.1370	0.7234
SL 161	134.0	48.4	2.77	8.0298	0.7265
SL 167A2	86.0	53.8	1.60	4.6333	0.7199
SL 172	125.0	44.0	2.84	8.2384	0.7251

Non-clay Fraction, Ambrosia Lake District
(2-62 μ fraction size)

Sample No.	Rb ppm	Sr ppm	Rb/Sr	$^{87}\text{Rb}/^{86}\text{Sr}$	$^{87}\text{Sr}/^{86}\text{Sr}$
23-301	91.3	50.6	1.8043	5.2326	7256
23-303	37.8	88.6	0.4266	1.2359	7144
23-308	40.1	46.5	0.8624	2.4985	7154
23-313	39.8	67.6	0.5888	1.7063	7183
23-314	74.0	82.9	0.8926	2.5859	7146
35-201	163.0	119.4	1.3652	3.9565	7189
35-210	51.1	118.1	0.4327	1.2537	7161
35-204	60.3	84.3	0.7153	2.0742	7243
35-301	71.1	113.8	0.6248	1.8112	7215

Montmorillonite-rich Samples,
 ($< 2\mu$ and $< 0.5\mu$)

Sample No.	Rb ppm	Sr ppm	Rb/Sr	$^{87}\text{Rb}/^{86}\text{Sr}$	$^{87}\text{Sr}/^{86}\text{Sr}$
P-143	80.7	36.7	2.1989	6.3748	7225
P-145	18.9	49.7	0.3803	1.1017	7143
P-146	21.6	55.3	0.3906	1.1312	7114
P-163	78.7	85.5	0.9205	2.6667	7147
P-164	16.9	50.1	0.3373	0.9769	7119
P-104-0.5	14.0	81.7	0.1714	0.4963	7103
MQ JmJ-1	16.9	128.6	0.1314	0.3805	7096
MQ JmJ-2	30.7	33.5	0.9164	2.6555	7176
MQ JmJ-4	111.5	47.9	2.3278	6.7490	7232

Laguna District
($< 0.5\mu$ ore samples)

Sample No.	Rb ppm	Sr ppm	Rb/Sr	$^{87}\text{Rb}/^{86}\text{Sr}$	$^{87}\text{Sr}/^{86}\text{Sr}$
P-137	31.5	12.8	2.4609	7.1346	7224
P-121	39.2	9.3	4.2151	12.2280	7289
P-151	40.3	14.6	2.7603	8.0021	7214
P-135	48.3	68.5	0.7051	2.0422	7123
P-119	67.0	48.2	1.3900	4.0266	7141
P-128	46.5	24.6	1.8902	5.4767	7163
JP-201-2	90.5	19.0	4.7632	13.8209	7311
JP-203	67.9	16.0	4.2438	12.3070	7254

($< 2\mu$ ore samples)

P-121	43.0	32.4	1.3272	3.8460	7178
P-137	31.8	104.7	0.3037	0.8796	7116
P-151	39.9	27.3	1.4615	4.2357	7184
P-135	44.1	63.1	0.6989	2.0244	7134
P-144	57.9	15.8	3.6646	10.6303	7282
P-128	39.6	48.7	0.8131	2.3556	7145
P-140	41.7	24.0	1.7375	5.0365	7207
P-142	31.9	67.4	0.4733	1.3712	7150
P-141	45.5	39.6	1.1490	3.3291	7161
P-112	43.5	19.3	2.2539	6.5341	7216
JP-201	41.1	66.0	0.6227	1.8042	7157
JP-203	64.1	57.1	1.1226	3.2520	7145
JP-202	60.3	55.6	1.0845	3.1428	7175
P-107	62.0	35.7	1.7367	5.0338	7201
P-119	73.9	103.4	0.7147	2.0703	7137

Outcrop plus Mine Samples, Grants Mineral Belt

Sample No.	Rb ppm	Sr ppm	Rb/Sr	$^{87}\text{Rb}/^{86}\text{Sr}$	$^{87}\text{Sr}/^{86}\text{Sr}$
AL 35-201b	344.6	169.9	2.0283	5.9332	8156
AL 35-202	251.4	129.0	1.9486	5.6970	8091
MQ JmJ-2	383.0	244.7	1.5652	4.5668	7882
*Sec. 11-43.0 m (3.25 Ø)	190.1	174.3	1.0906	3.1755	7669
*Sec. 1-175 m (3.25 Ø)	458.3	190.3	2.4083	7.0587	8358
*Sec. 1-162 m (3.25 Ø)	434.5	208.0	2.0889	6.1181	8278
*Sec. 1-175 (RF)	118.6	242.0	0.4899	1.4187	7106

* Samples from R. Martinez, U. S. Geological Survey